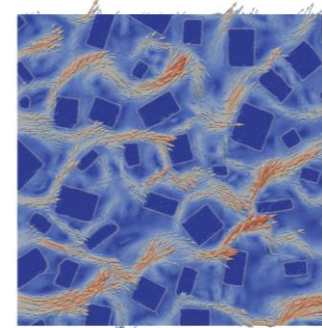
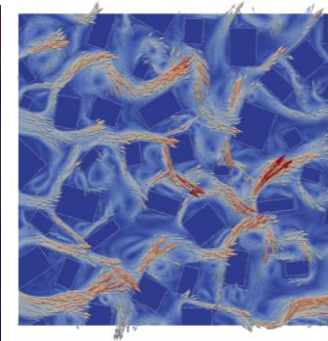
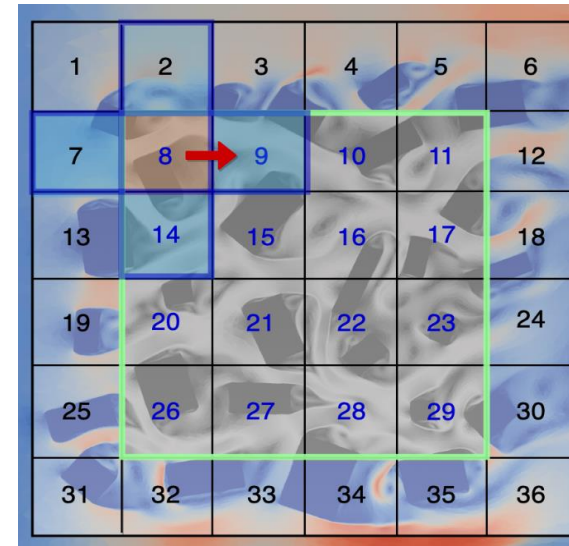
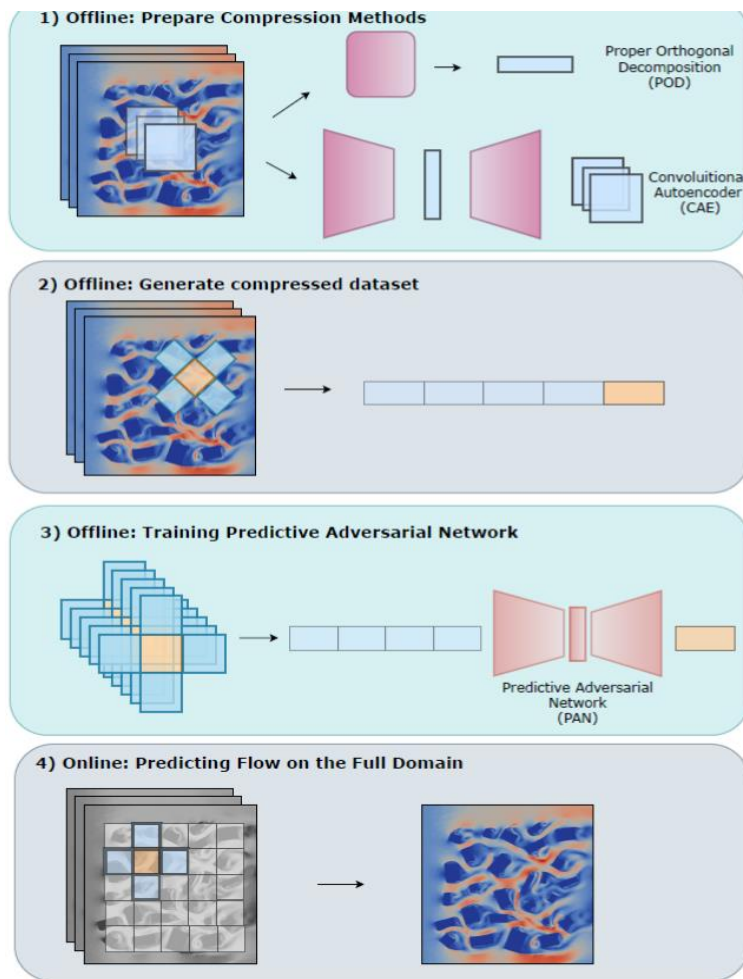


Modelling using AI from laptops to eXascale (MAtrIX):

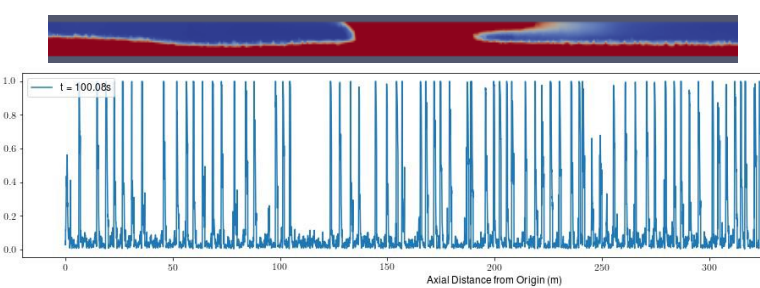
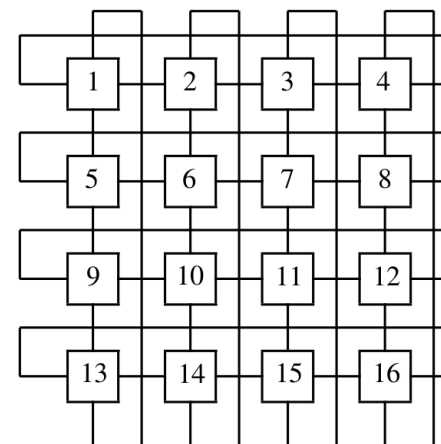
- 1) Programming CFD/Nuclear Models using AI software** which enables interoperability between GPUs, CPUs and AI computers (energy efficient exascale Cerebras CS2 ~1M node chip) & exploitation of community AI software;
- 2) AI-Physics modelling** to reduce the number of unknowns solved for which can be important for some computer architectures as well as speeding up models;
- 3) Hybrisation of AI Physics modelling and discretization** of the differential equations in order to construct; new sub-grid-scale (SGS) models, methods that force the equation residuals to zero (RDEIM) or physics informed methods - it's now accepted that future SGS methods will increasing be based on AI and they may need implicit coupling to CFD using AI programming (1 above);
- 4) Digital twins** that are able to assimilate data, perform uncertainty quantification and optimization using the optimization engine embedded in all AI software.

Building a detailed flow model of using AI modelling

– bottom middle grid architecture of an AI computer e.g. Cerebras CS-2 with 800,000 nodes on a chip



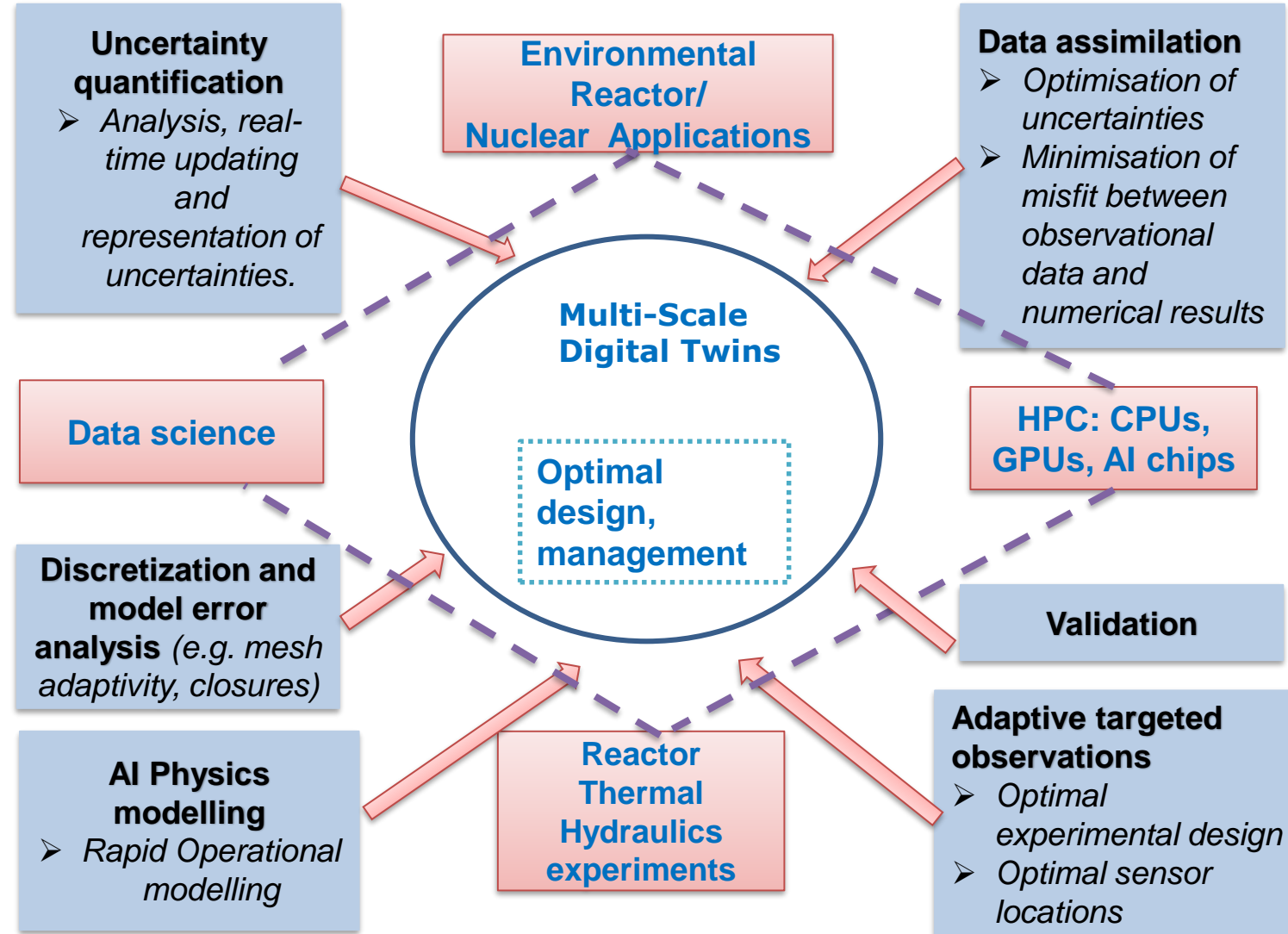
AI model of flow past buildings velocity vectors. Left: High Fidelity Model.
Right: Surrogate



AI model of multiphase slug flow in 1000m pipe from subdomains. Top: cross section of liquid in subdomain. Bottom: liquid along pipe fraction

Nuclear Modelling using AI at eXascale (MATRIX):

- AI-Physics modelling
- AI SGS CFD/TH/RT modelling
- Hierarchical modelling – from CFD/RT to AI Models - multiscale
- AI computers e.g. ~1M node Cerebras chip
- Digital Twins (Right) taking advantage of AI optimization
- Code in AI e.g. PyTorch, SymPy
- Summary speed: AI models 10^3 - 10^6 faster, AI computer 10^3 faster, Total 10^6 - 10^9 faster



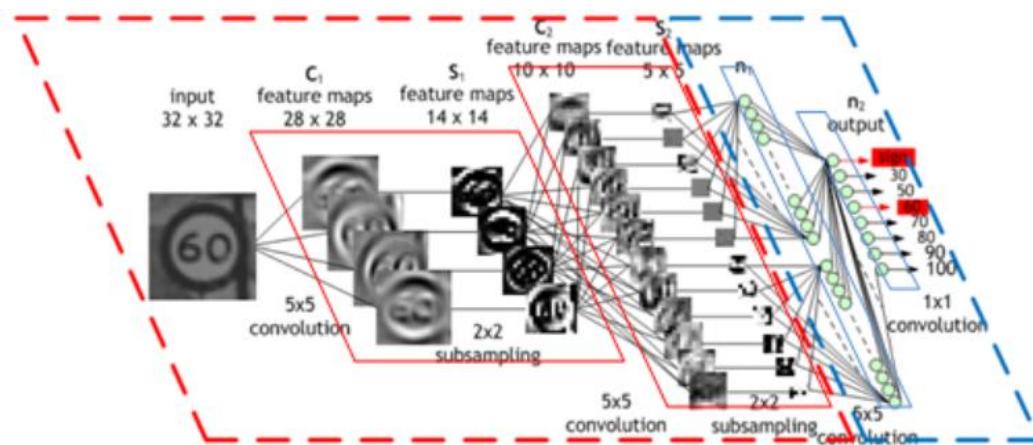
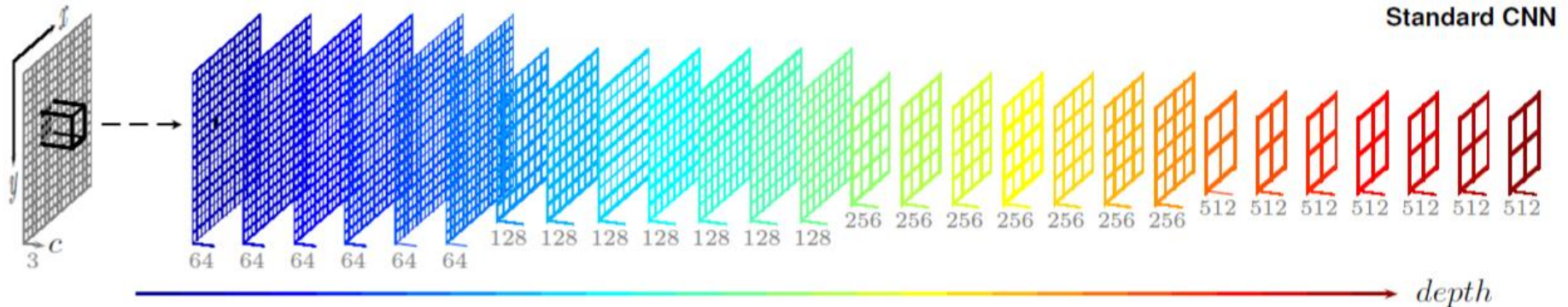
Advantages of programming CFD/Neutronics/Solids in AI:

- 1) Solvers:** Linear, non-linear multigrid methods using convolutional auto-encoders, Newton Raphson iteration. AI models can also be used as preconditions in CFD.
- 2) Hierarchical solvers:** From CFD to fine and coarse AI-Physics models and one catch switch between these locally or globally.
- 3) Embedded CFD and AI Physics modelling** in a single neural network – SGS modelling, PINN, RDEIM.
- 4) Automatic Adjoint Generation and Digital twins** that are able to assimilate data, perform uncertainty quantification and optimization using the optimization engine embedded in all AI software.
- 5) Realize new features in modelling:** reduced arithmetic speed; coupling different physics, finance, economic, language and/or social models; leverage AI code.
- 6) More accessible AI programming for modelers** - similar to AI applications.
- 7) Optimized code interoperability between computer architectures:** CPU, GPU and AI chips - exascale.
- 8) Long term model/code sustainability.**

Strategy Issues for CFD implementation using AI software:

- 1) Multi-grid solvers – through CNN autoencoder (done)
- 2) Adoints – through weights and activation functions (done)
- 3) Unstructured meshes e.g. Space Filling Curves CNN, MeshCNN (done)
- 4) Defining discretization e.g. **DEVITO**, **OpenSBLI**, **SymPy**, **Firedrake**
- 5) Parallel updating of halos e.g. **SciML**, **Lightning-Horovod**, **DeepSpeed**,
transformer methods (dense), **MPI** may be used for block unstructured
- 6) Large matrix/solution free methods e.g. radiation transport – use single
CNN filter for semi-structured discretization in each block (done)
- 7) GUIs linkage – keep flexible

Convolutional ANNs with linear activation functions and weights from discretization stencil can be Multi-Grid Solvers:

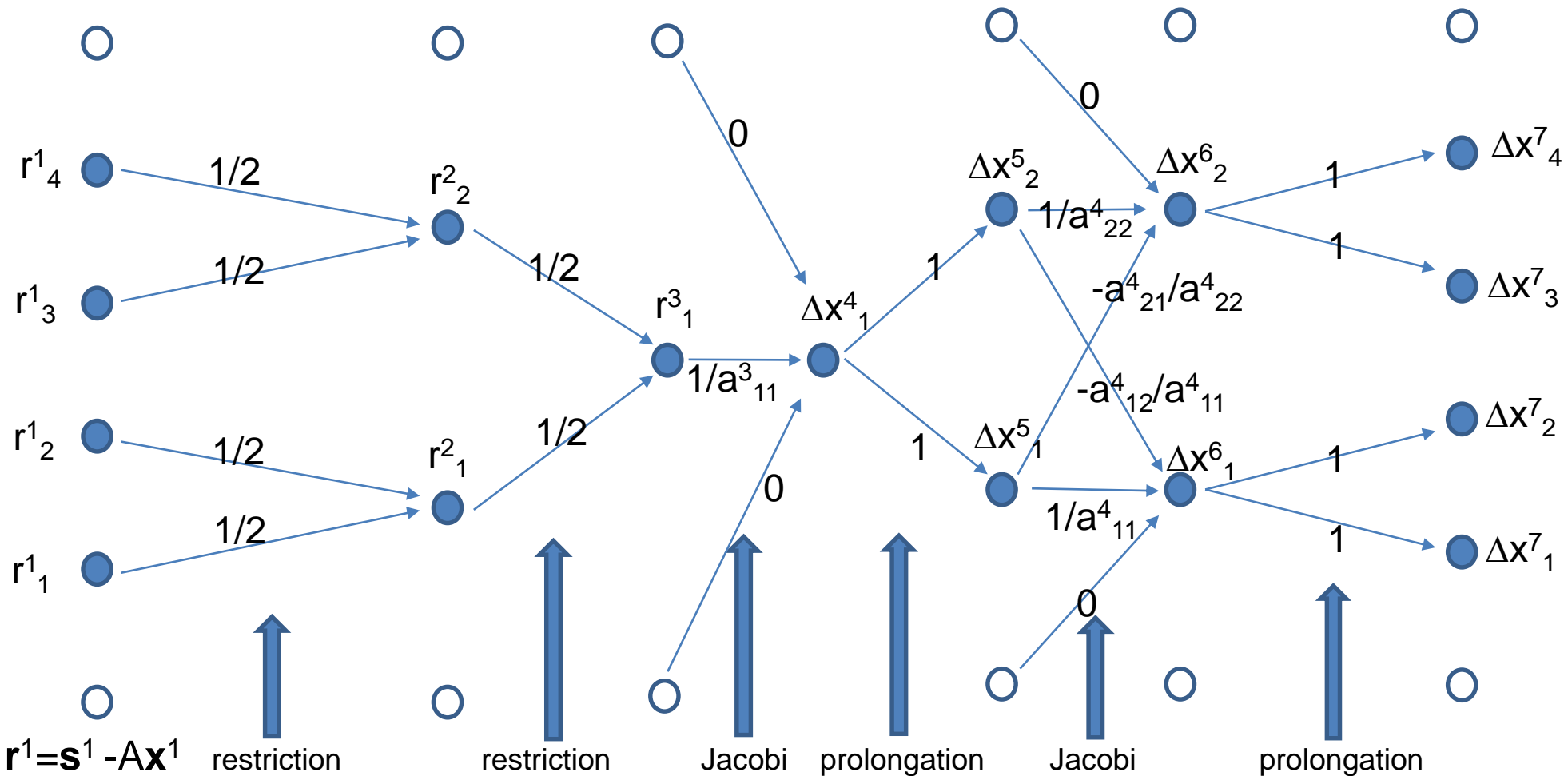


Input (+pad 1) (7x7x1)	Filter W_0 (3x3x1)	Output (3x3x1)
0 0 0 0 0 0 0	0 0 0	-1 3 -1
0 0 1 2 0 1 0	1 -1 0	-2 1 2
0 1 2 2 0 0 0	1 1 -1	0 -1 -2
0 0 1 2 1 0 0		
0 0 2 1 1 0 0		
0 0 0 1 0 2 0		
0 0 0 0 0 0 0		

The diagram shows a 7x7 input matrix with padding 1, a 3x3 filter W_0 , and a resulting 3x3 output matrix. The filter W_0 is highlighted with a blue border. The multiplication operation is shown as \ast , and the resulting output values are listed to the right.

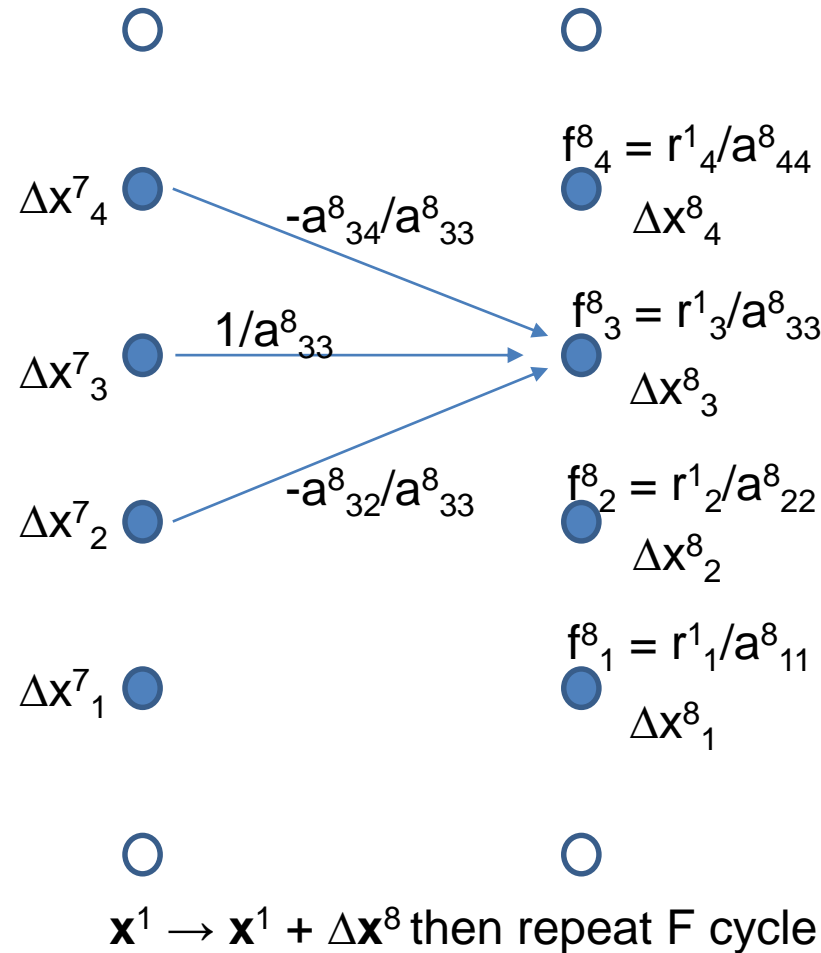
Solve $Ax=s$ using Simplest F-cycle Multi-Grid Method and Convolutional ANN in 1D – neural network shown:

Superscript ANN level, subscript ANN neuron; Jacobi smoother



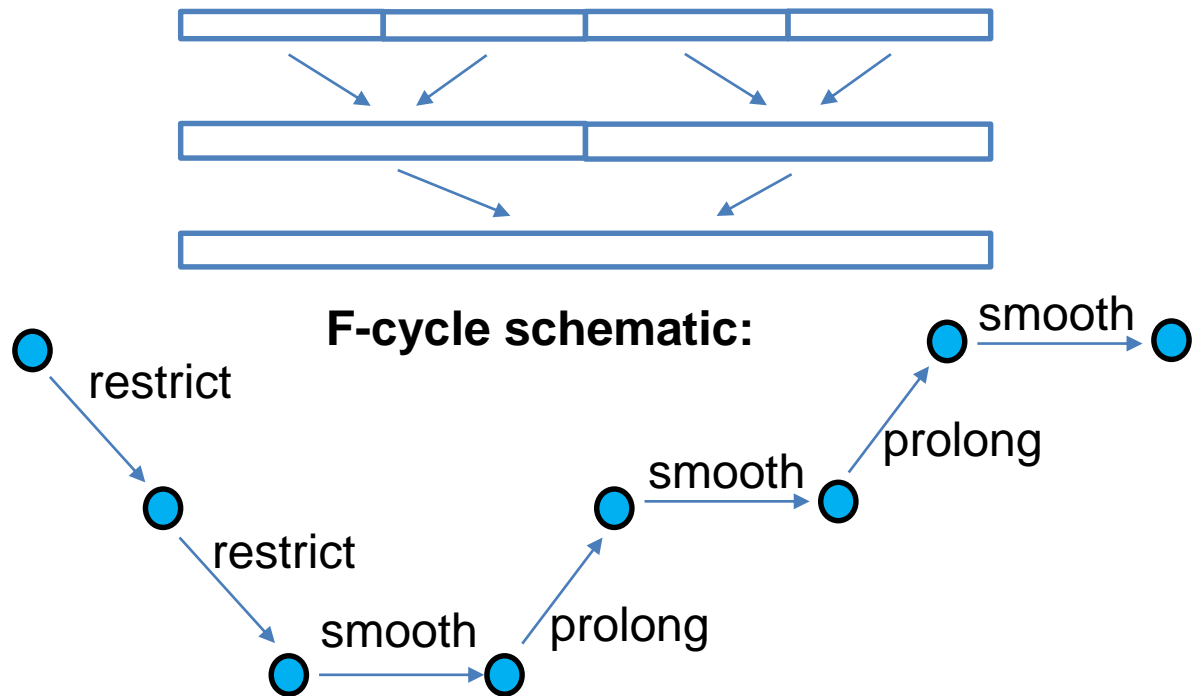
Final Layer – Jacobi iteration with bias

f is the bias



For 1D linear DG: Have 2 channels. One for each DG node and use the inverse of the 2×2 matrix rather than $1/a^8_{33}$ etc. **3D linear DG** has 8 channels for each DG node.

Cells/nodes/neurons:



Jacobi relaxation when solving $Ax=s$:

Jacobi iteration: $x_i^{\text{new}} = (1/a_{ii}) \left(-\sum_{j \neq i} a_{ij} x_j^{\text{old}} + s_i \right)$

Suppose $\alpha \in (0,1]$ is the relaxation coefficient (e.g. $\alpha=0.5$)
then

$$x_i = (1 - \alpha) x_i^{\text{old}} + \alpha (1/a_{ii}) \left(-\sum_{j \neq i} a_{ij} x_j^{\text{old}} + s_i \right).$$

Thus $x_i = \sum_j b_{ij} x_j^{\text{old}} + c_i$

in which $b_{ij} = -\alpha (1/a_{ii}) a_{ij}$ if $i \neq j$

and $b_{ii} = 1$

and $c_i = \alpha (1/a_{ii}) s_i$ (is the bias)

Thus $w_{ij} = b_{ij}$ are the weights of the convolutional filter

Time stepping of $\partial T / \partial t + u \partial T / \partial x + v \partial T / \partial y + \sigma T - \mu \nabla \cdot \nabla T = s$ (advection velocity (u, v)):

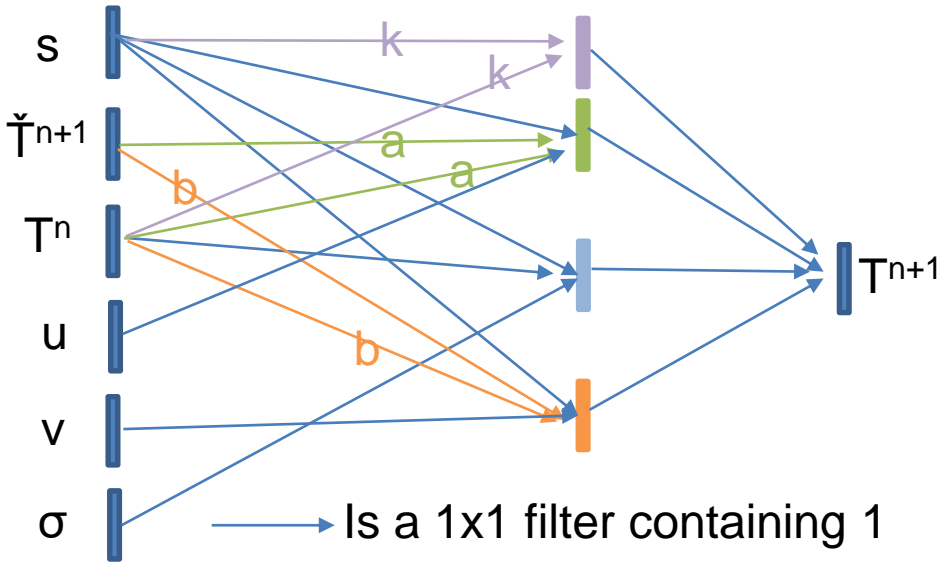
Two filters are needed a_{ij} and b_{ij} . The half in the bellow is used to obtain 2nd order accuracy in time, \check{T}^{n+1} is the best guess for T^{n+1} which might be T^n . Δt = time step size. α , β are advection/diffusion stencils/discretizations. Discretization becomes:

$$(T^{n+1}_i - T^n_i) / \Delta t + \sigma_i T^{n+1}_i + u_i \sum_j a_{ij} (1/2) (\check{T}^{n+1}_j + T^n_j) + v_i \sum_j b_{ij} (1/2) (\check{T}^{n+1}_j + T^n_j) + \sum_j k_{ij} (1/2) (\check{T}^{n+1}_j + T^n_j) = s_i$$

in which $a_{ij} = (1/2) \sum_j \alpha_{ij} \Delta t$, $b_{ij} = (1/2) \sum_j \beta_{ij} \Delta t$ and $k_{ij} = (1/2) \sum_j \mu_{ij} \Delta t$.

$$T^{n+1}_i = (1/(1 + \Delta t \sigma_i)) T^n_i + s_i + (u_i / (1 + \Delta t \sigma_i)) \sum_j a_{ij} (\check{T}^{n+1}_j + T^n_j) + (v_i / (1 + \Delta t \sigma_i)) \sum_j b_{ij} (\check{T}^{n+1}_j + T^n_j) + \sum_j k_{ij} (\check{T}^{n+1}_j + T^n_j) \quad (1)$$

This can be turned into a CNN as follows:



Change the activation functions

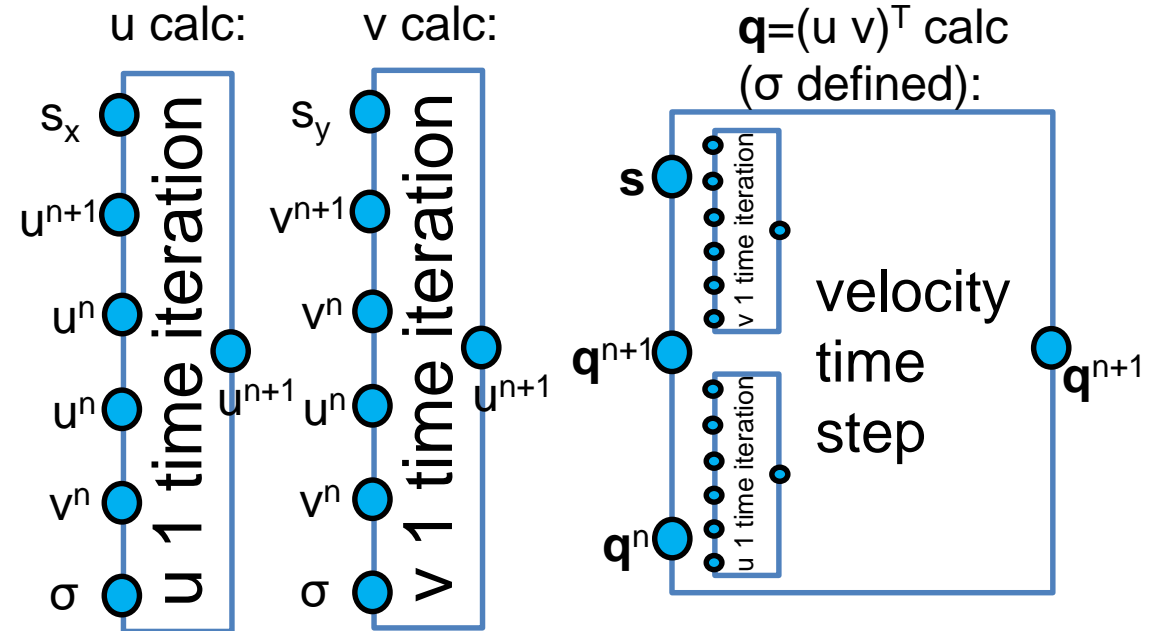
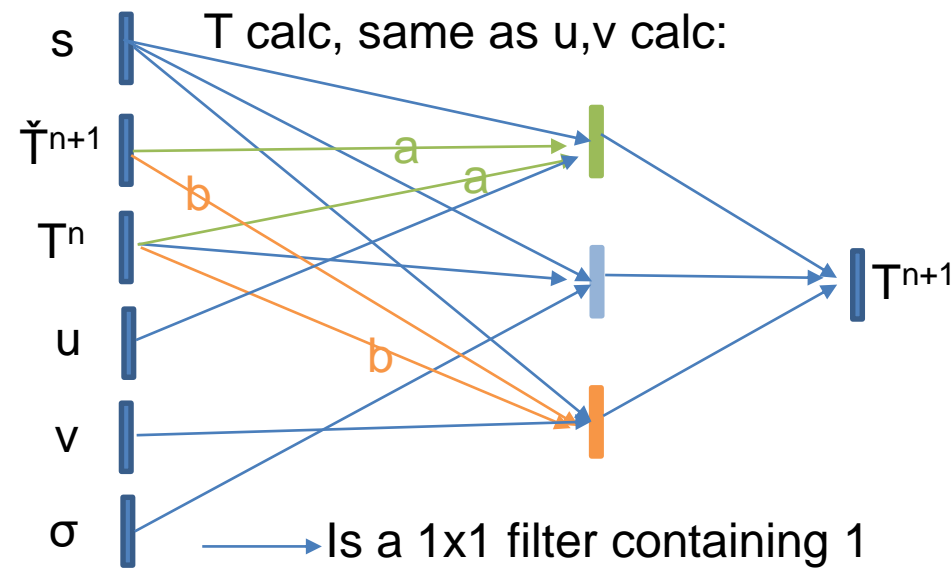
to implement equation (1) above.

The green and orange CNN layers have these tailored activation functions and the purple filter is for constant diffusion.

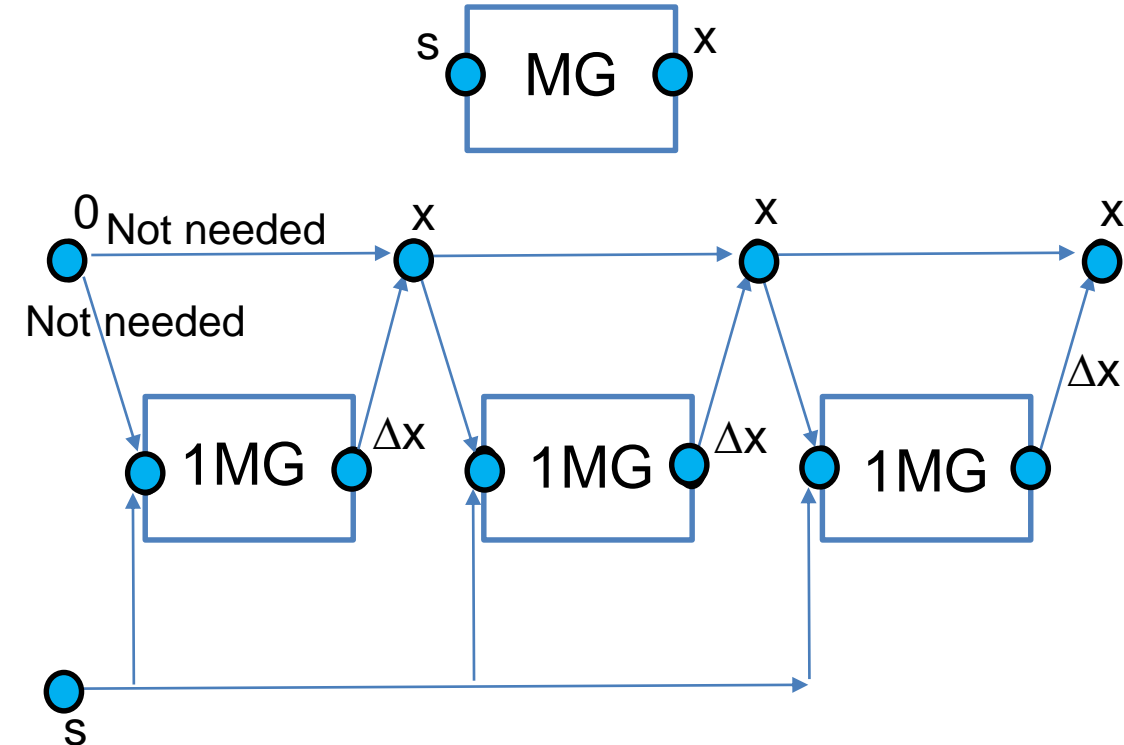
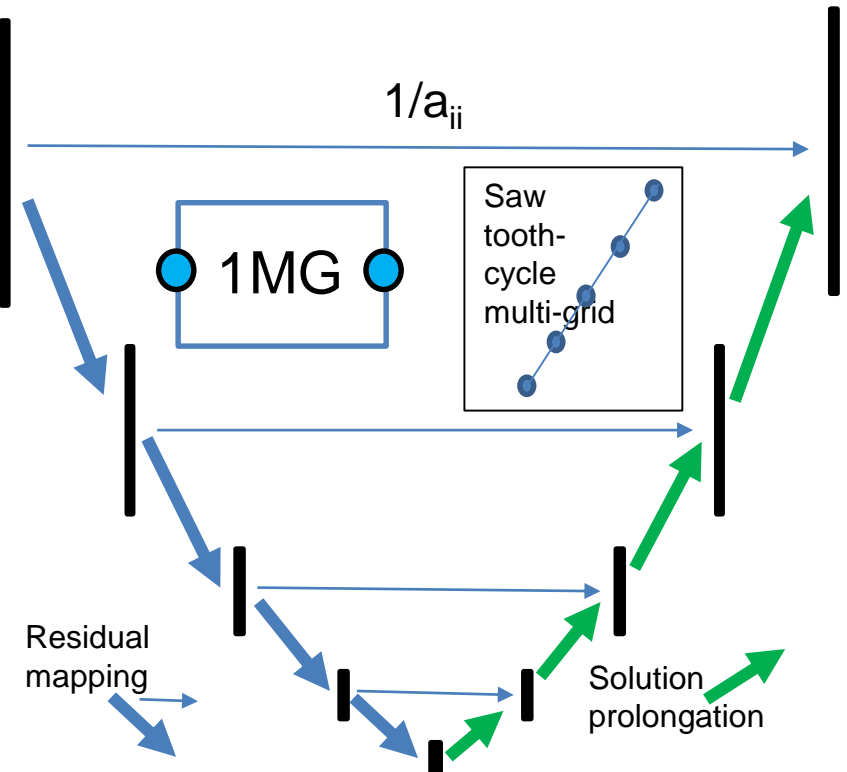
Use two steps of this CNN gives 2nd order in time.

Boundary conditions are applied through padding e.g. Dirichlet - put a value in the halo. For zero derivative apply same value or nearest neighbour padding

Time stepping of $\partial \mathbf{q} / \partial t + u \partial \mathbf{q} / \partial x + v \partial \mathbf{q} / \partial y + \sigma \mathbf{q} - \mu \nabla \cdot \nabla \mathbf{q} = \mathbf{s}$ (advection velocity $\mathbf{q} = (u \ v)^T$ & source $\mathbf{s} = (s_x \ s_y)^T$):

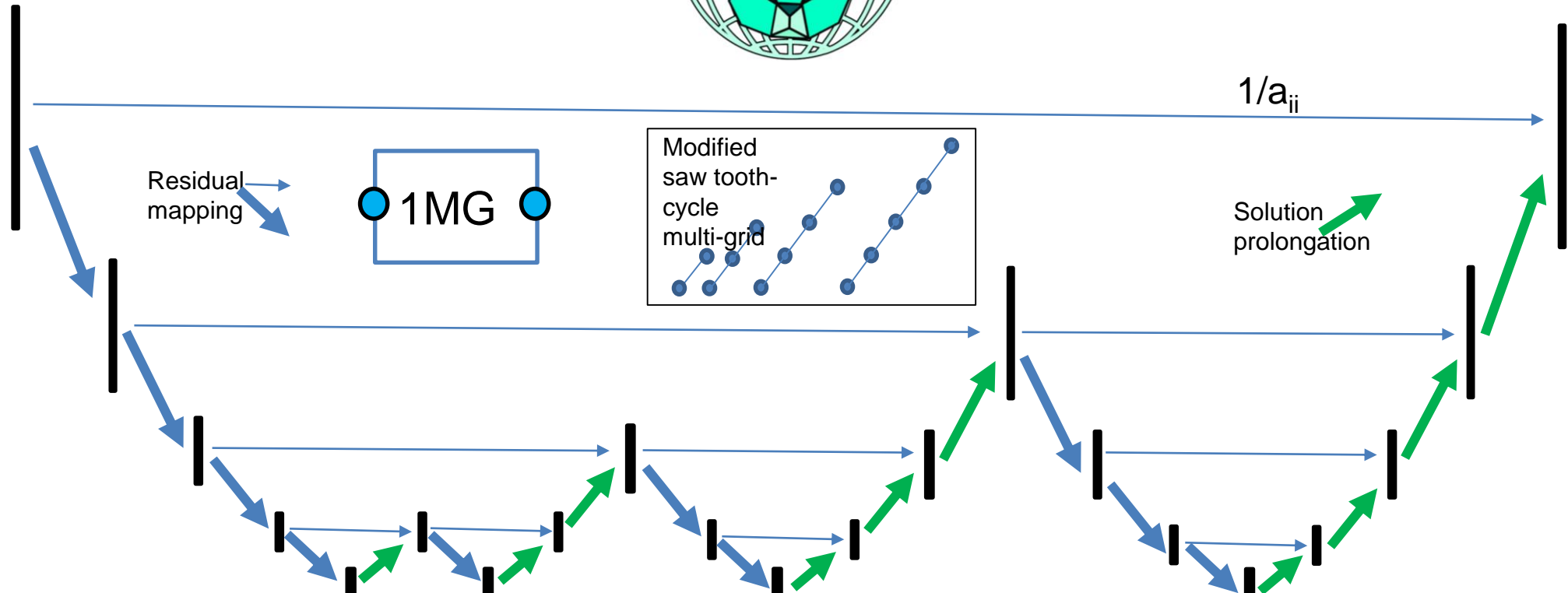


Left: Multi-Grid (MG –saw tooth cycle) CNN skip layers rather than use biases (1MG cycle – U-Net architecture);
Right: Multi-Grid (3 iterations – cycles) solving $Ax = s$, starting from 0:

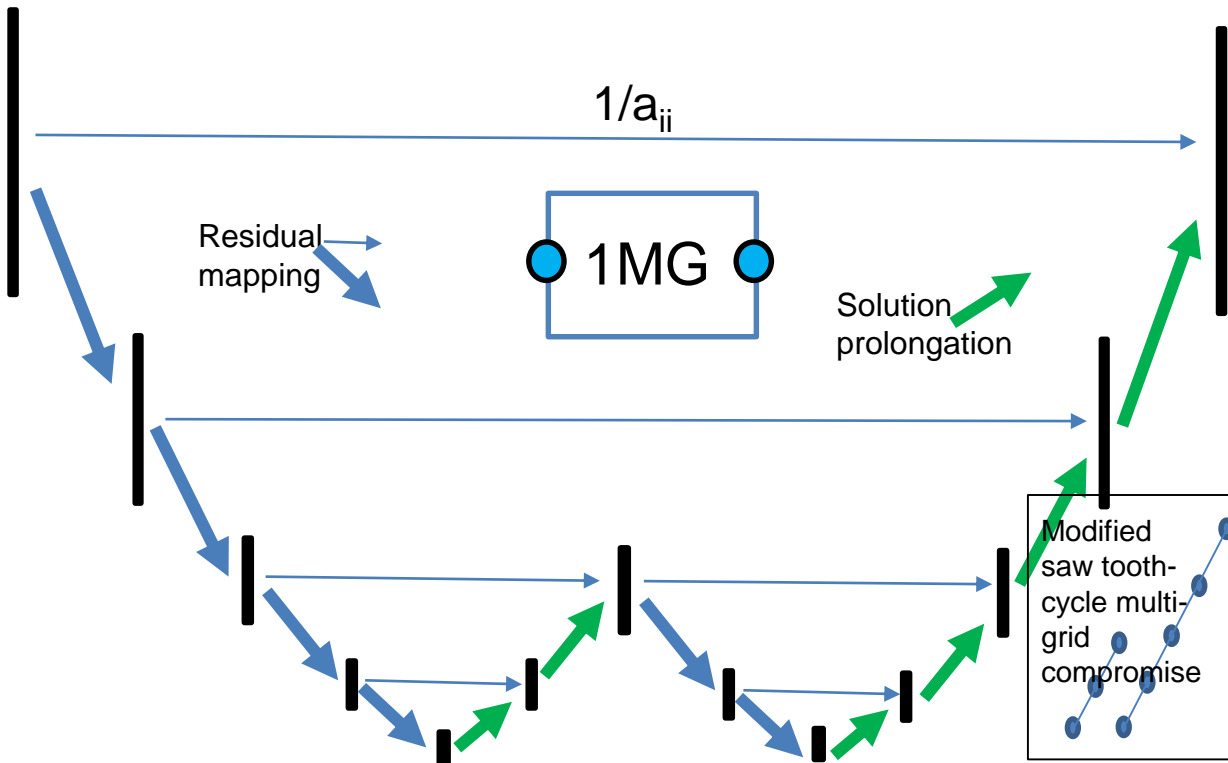


B-Net an extension of U-Net architecture for Multi-Grid (MG) CNN skip layers (1MG cycle):

B-net for UNstructured meshES
(BUNES-Net) or BunnyNet

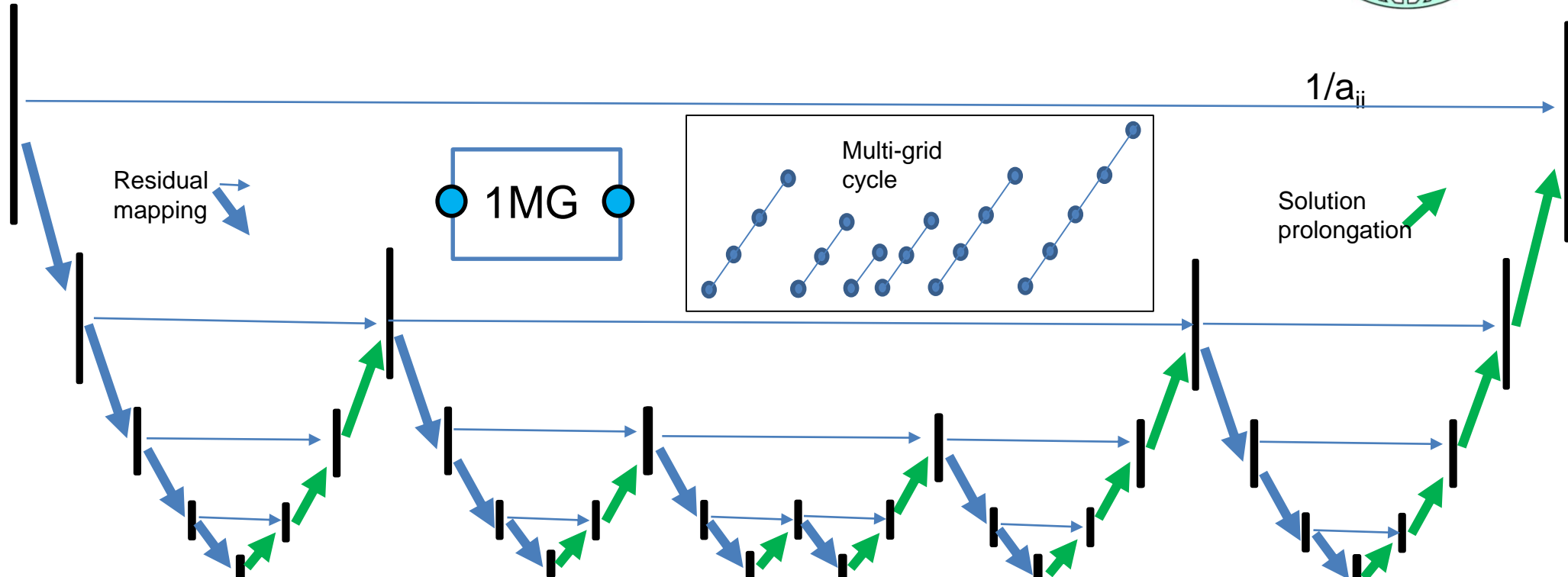


B-Net an extension of U-Net architecture for Multi-Grid (MG) CNN skip layers (1MG cycle). Lots of options can be used that for example use more or less relaxations on the coarsest grid e.g. repeating the upward sweeps through the grids gives you more. A method that gives you less is a compromise between U-Net and B-Net that spends less time on the coarsest grids:



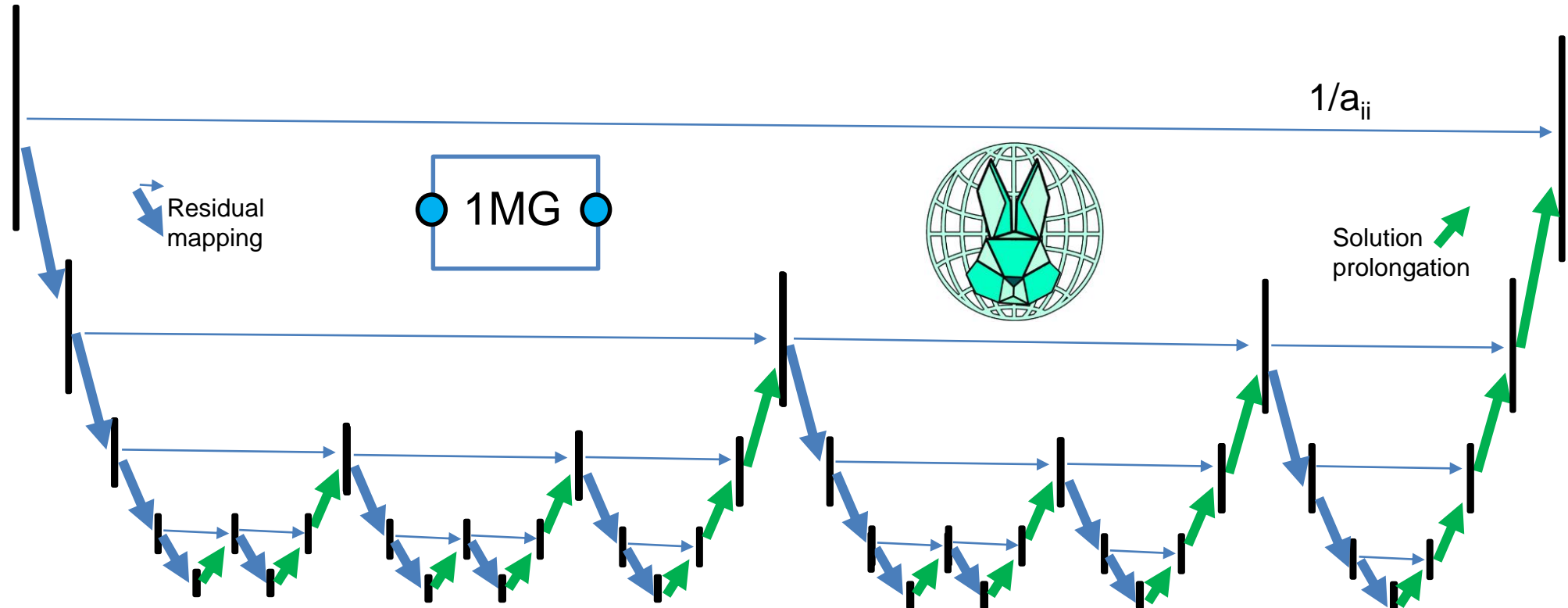
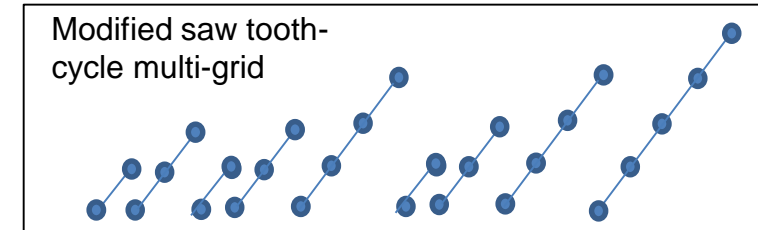
BunnyNet another example: B-Net extension of U-Net architecture for Multi-Grid (MG) CNN skip layers (1MG cycle):

B-net for UNstructured
meshES (BUNES-Net)
or BunnyNet



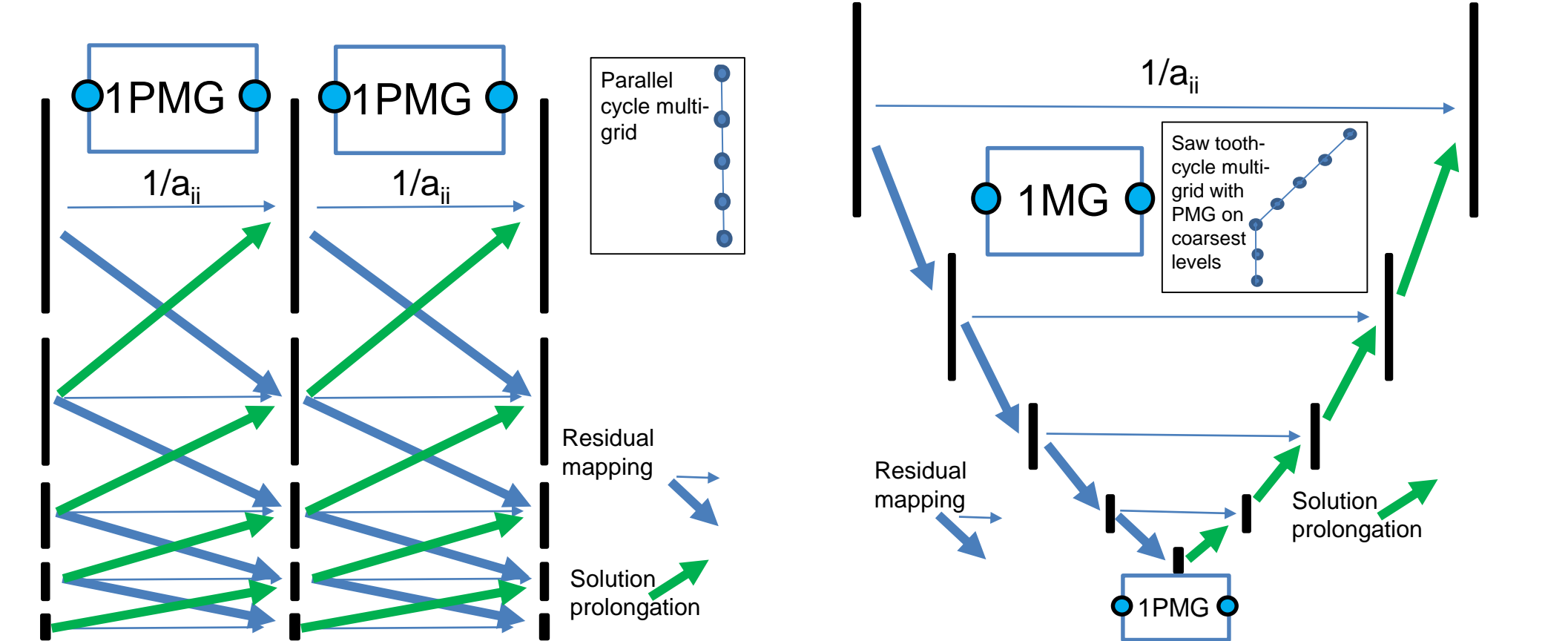
B-Net an extension of U-Net architecture for Multi-Grid (MG) CNN skip layers (1MG cycle) – doing more work on the coarser grids:

B-net for UNstructured meshES (BUNES-Net) or BunnyNet.

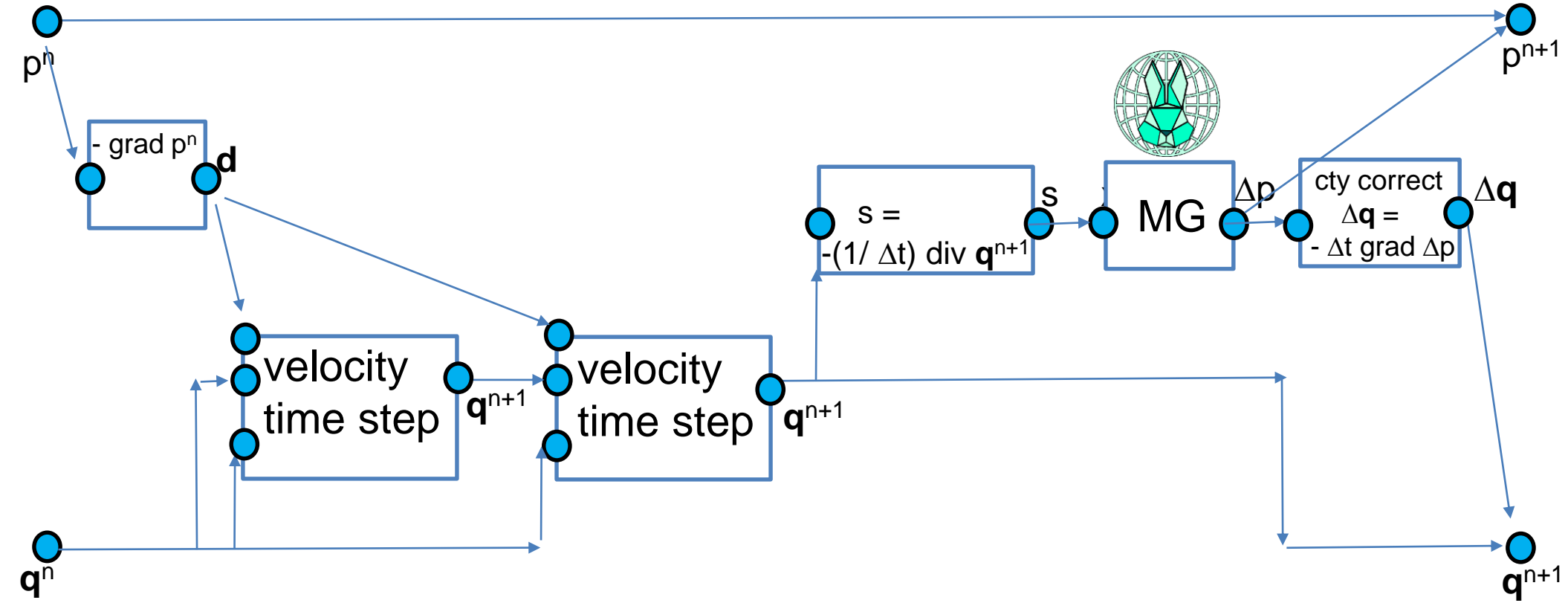


P-Net (Parallel Net) an extension of U-Net architecture for Multi-Grid (MG) CNN skip layers (1PMG cycle)

One can update all grid levels simultaneously and distribute the results to the neighbouring grid levels. This is important as it eliminates the bottle neck associated with the smaller grid levels which can be as expensive as the finer grid levels because one needs to finish this level before proceeding to the next levels. One can also assume the average update on a certain grid level is zero and rely on the coarser grid level to get the mean. Bottom right a combination of U-Net and P-Net to get the best.



CFD time step:



Governing equation for projection base CFD:

Governing eqns ($\mathbf{q} = (u \ v \ w)^T$)

$$\frac{D\mathbf{q}}{Dt} + \sigma \mathbf{q} - \mu \nabla \cdot \nabla \mathbf{q} = - \nabla p,$$
$$\operatorname{div} \mathbf{q} = 0.$$

Derived eqns – solution steps:

$$1) \frac{D\mathbf{q}}{Dt} + \sigma \mathbf{q} - \mu \nabla \cdot \nabla \mathbf{q} = - \nabla p,$$

$$2) \nabla \left(\frac{1}{1 + \Delta t \sigma} \right) \nabla \Delta p = - \left(\frac{1}{\Delta t} \right) \operatorname{div} \mathbf{q},$$

$$\text{or for simplicity } \nabla \cdot \nabla \Delta p = - \left(\frac{1}{\Delta t} \right) \operatorname{div} \mathbf{q}$$

$$3) \Delta \mathbf{q} = - \left(\frac{\Delta t}{1 + \Delta t \sigma} \right) \nabla \Delta p,$$

$$\text{or for simplicity } \Delta \mathbf{q} = - \Delta t \nabla \Delta p$$

$$4) p \rightarrow p + \Delta p$$

$$5) \mathbf{q} \rightarrow \mathbf{q} + \Delta \mathbf{q}$$

Governing equation for projection based interface tracking multi-phase flow CFD (blue difference from single phase):

Governing eqns ($\mathbf{q} = (u \ v \ w)^T$)

$$\rho (\partial \mathbf{q} / \partial t + \mathbf{q} \cdot \nabla \mathbf{q}) + \sigma \mathbf{q} - \nabla \cdot \mu \nabla \mathbf{q} = - \nabla p + \rho g \quad \&$$

$$\partial C / \partial t + \nabla \cdot \mathbf{q} C + \sigma_c C - \nabla \cdot k_c \nabla C = 0 \text{ with } \rho = C \rho_l + (1-C) \rho_g$$

$$\nabla \cdot \mathbf{q} = 0$$

Derived eqns – solution steps:

0) $\rho = C \rho_l + (1-C) \rho_g$

1a) $\rho (\partial \mathbf{q} / \partial t + \mathbf{q} \cdot \nabla \mathbf{q}) + \sigma \mathbf{q} - \nabla \cdot \mu \nabla \mathbf{q} = - \nabla p + \rho g$

1b) $\partial C / \partial t + \nabla \cdot \mathbf{q} C + \sigma_c C - \nabla \cdot k_c \nabla C = 0$

2) $\nabla \cdot (1/\rho) \nabla \Delta p = - (1/\Delta t) \nabla \cdot \mathbf{q}$ & use a harmonic average of $1/\rho$ in multi-grid

3) $\Delta \mathbf{q} = - (\Delta t / \rho) \nabla \Delta p$

4) $p \rightarrow p + \Delta p$

5) $\mathbf{q} \rightarrow \mathbf{q} + \Delta \mathbf{q}$

Governing equation for projection based interface tracking multi-phase flow CFD with hydrostatic pressure (blue difference from single phase):

Governing eqns ($\mathbf{q} = (u \ v \ w)^T$)

$$-\nabla \cdot \nabla p_h = \nabla \cdot \mathbf{s}_u$$

$$\rho (\partial \mathbf{q} / \partial t + \mathbf{q} \cdot \nabla \mathbf{q}) + \sigma \mathbf{q} - \nabla \cdot \mu \nabla \mathbf{q} = -\nabla p_h - \nabla p_{nh} - \mathbf{s}_u \quad \&$$

$$\partial C / \partial t + \nabla \cdot \mathbf{q} C + \sigma_c C - \nabla \cdot k_c \nabla C = 0 \text{ with } \rho = C \rho_l + (1-C) \rho_g$$

$$\nabla \cdot \mathbf{q} = 0$$

Derive eqns – steps (p_h & p_{nh} are hydrostatic & non-hydrostatic pressures):

1) $\rho = C \rho_l + (1-C) \rho_g \quad \& \quad \mathbf{s}_u = \rho \mathbf{g}$

2) $-\nabla \cdot \nabla p_h = \nabla \cdot \mathbf{s}_u$

3) $\rho (\partial \mathbf{q} / \partial t + \mathbf{q} \cdot \nabla \mathbf{q}) + \sigma \mathbf{q} - \nabla \cdot \mu \nabla \mathbf{q} = -\nabla p_h - \nabla p_{nh} - \mathbf{s}_u$

4) $\partial C / \partial t + \nabla \cdot \mathbf{q} C + \sigma_c C - \nabla \cdot k_c \nabla C = 0$

5) $\nabla \cdot (1/\rho) \nabla \Delta p = - (1/\Delta t) \nabla \cdot \mathbf{q} \quad \& \text{ use a harmonic average of } 1/\rho \text{ in multi-grid}$

6) $\Delta \mathbf{q} = -(\Delta t / \rho) \nabla \Delta p$

7) $p \rightarrow p + \Delta p$

8) $\mathbf{q} \rightarrow \mathbf{q} + \Delta \mathbf{q}$

CFD Turbulence Modelling using Petrov-Galerkin Dissipation

Define $c_{xi} = (1/m_i) (A_x C)|_i$, $c_{yi} = (1/m_i) (A_y C)|_i$, $c_{zi} = (1/m_i) (A_z C)|_i$,
 $r_i = 0.33(|u_i|/\Delta x_i + |v_i|/\Delta y_i + |w_i|/\Delta z_i) \hat{A}_{D2} C|_i$ (& \hat{A}_{D2} is for unit element) or $r_i = (1/m_i)(1/3)(|\Delta x_i u_i| + |\Delta y_i v_i| + |\Delta z_i w_i|)|A_{D2} C|_i$ or more accurately $r_i = (1/m_i)(1/3)(|\Delta x_i u_i (A_{D2x} C)|_i| + |\Delta y_i v_i (A_{D2y} C)|_i| + |\Delta z_i w_i (A_{D2z} C)|_i|)$ and even more accurately $r_i = (\nabla \cdot a_i a_i^\top \nabla C)|_i$ (with $a_{xi} = (|u_i|/\Delta x_i)^{1/2}$) in which A_{D2} is the filter for ∇^2 , A_{D2x} is the filter curvature in the x-direction, and $m_i = \Delta x_i \Delta y_i \Delta z_i$ is the mass associated with FEM node i; A_x , A_y , A_z are the filters for the derivative in the x, y and z directions. $P_i = \min\{1/(\sigma + \epsilon), \hat{P}_i\}$, in which ϵ is a small number and in which

$\hat{P}_i = \alpha_k |(u_i, v_i, w_i) \cdot (c_{xi}, c_{yi}, c_{zi})| (1/3)(|2/\Delta x_i| c_{xi}| + |2/\Delta y_i| c_{yi}| + |2/\Delta z_i| c_{zi}|)$ and $|.|$ represents the absolute value with $\alpha_k = 1/2$ and 1 for linear DG and continuous elements. Thus, the diffusion coefficient is $k_i = r_i^2 P_i / (\epsilon_k + c_{xi}^2 + c_{yi}^2 + c_{zi}^2)$, ϵ_k needs to be sufficiently large so that k_i does not get too big. A simple version is given for linear elements by: $k_i = \alpha_k |r_i| h_i / (\epsilon_k + (c_{xi}^2 + c_{yi}^2 + c_{zi}^2)^{1/2})$ with element size $h_i = (\Delta x_i + \Delta y_i + \Delta z_i)/3$ or for efficiency $k_i = \min\{k_{maxi}, \alpha_k |r_i| h_i / (\epsilon_k + (|c_{xi}| + |c_{yi}| + |c_{zi}|)/3)\}$ with a stability criteria $k_{maxi} = 0.25 \min\{\Delta x_i, \Delta y_i, \Delta z_i\}^2 / \Delta t$ and for steady problems $k_{maxi} = |\mathbf{u}_i| h_i$. For steady problems can start with $k_i = k_{maxi}$. The final diffusion matrix multiplication is given by $\frac{1}{2}(k_i (A_{D2} C)|_i + (A_{D2} (K C))|_i - c_i (A_{D2} K)|_i)$ – see variable diffusion coefficient slide. Thus, an ANN channel is needed that stores k_i and A_{D2} is a discretisation (e.g. FEM) of the Laplacian.

Residual calculation along the velocity direction for Petrov-Galerkin Dissipation

Define $c_{xi} = (1/m_i) (A_x C)|_i$, $c_{yi} = (1/m_i) (A_y C)|_i$, $c_{zi} = (1/m_i) (A_z C)|_i$.

The more accurately $r_i = (\nabla \alpha_{oi} \mathbf{o}_i \mathbf{o}_i^T \nabla C)|_i$ (with $a_{xi} = u_i/\Delta x_i$, $a_{yi} = v_i/\Delta y_i$, $a_{zi} = w_i/\Delta z_i$ and $\mathbf{a}_i = (a_{xi}, a_{yi}, a_{zi})^T$ with $\mathbf{o}_i = \mathbf{a}_i / \|\mathbf{a}_i\|_2$ and $\alpha_{oi} = \|\mathbf{a}_i\|_2 = (a_{xi}^2 + a_{yi}^2 + a_{zi}^2)^{1/2}$ with element size $h_i = (\Delta x_i + \Delta y_i + \Delta z_i)/3$ and for efficiency $k_i = \min\{k_{maxi}, \alpha_k |r_i| h_i / (\epsilon_k + (|c_{xi}| + |c_{yi}| + |c_{zi}|)/3)\}$ with for steady problems $k_{maxi} = (u_i^2 + v_i^2 + w_i^2)^{1/2} h_i$ and $\alpha_k = 1$. For steady problems can start with $k_i = k_{maxi}$.

The final diffusion matrix multiplication is given by $\frac{1}{2}(k_i(A_{D2}C)|_i + (A_{D2}(KC))|_i - c_i(A_{D2}K)|_i)$ – see variable diffusion coefficient slide. Thus, an ANN channel is needed that stores k_i and A_{D2} is a discretisation (e.g. FEM) of the Laplacian.

The diffusion is a constant matrix for each direction and is $\alpha_{oi} \mathbf{o}_i \mathbf{o}_i^T =$
 $o_{xx} o_{xy}$ and then $r_i = o_{xx} \partial^2 C / \partial x^2 + o_{xy} \partial(\partial C / \partial y) / \partial x + o_{yx} \partial(\partial C / \partial x) / \partial y + o_{yy} \partial(\partial C / \partial y) / \partial y$
 $o_{yx} o_{yy}$

A more accurate and mathematically more rigorous approach to calculating the residual is to **use the next higher order filters to form the residual** in a discrete sense then divide this discrete residual by the mass.

Summary and our experience of the optimised non-linear Petrov-Galerkin Dissipation

Define $C_{xi} = (A_x C)|_i$, $C_{yi} = (A_y C)|_i$, $C_{zi} = (A_z C)|_i$.

The diffusion based discrete residual (only used for linear elements) is $R_i = m_i (\nabla \alpha_{oi} \mathbf{o}_i \mathbf{o}_i^T \nabla C)|_i$ (with $a_{xi} = u_i/\Delta x_i$, $a_{yi} = v_i/\Delta y_i$, $a_{zi} = w_i/\Delta z_i$ and $\mathbf{a}_i = (a_{xi}, a_{yi}, a_{zi})^T$ with $\mathbf{o}_i = \mathbf{a}_i / \|\mathbf{a}_i\|_2$ and $\alpha_{oi} = \|\mathbf{a}_i\|_2 = (a_{xi}^2 + a_{yi}^2 + a_{zi}^2)^{1/2}$ with element size $h_i = (\Delta x_i + \Delta y_i + \Delta z_i)/3$ and for efficiency

$$k_{1i} = \alpha_{k1} |R_i| h_i / (\epsilon_k + (|C_{xi}| + |C_{yi}| + |C_{zi}|)/3),$$

$$k_{2i} = \alpha_{k2} R_i^2 h_i / (\epsilon_k + ((|u^*_i| + |v^*_i| + |w^*_i|)/3)(C_{xi}^2 + C_{yi}^2 + C_{zi}^2)) , \text{ in which a 2 replaces the 3 in 2D in these 3D eqns}$$

and in which $(u^*_i, v^*_i, w^*_i)^T = ((u_i C_{xi} + v_i C_{yi} + w_i C_{zi}) / (\epsilon_k + C_{xi}^2 + C_{yi}^2 + C_{zi}^2)) (C_{xi}, C_{yi}, C_{zi})^T$.

The final Petrov-Galerkin diffusion coefficient is

$$k_i = \min\{k_{maxi}, k_{1i}, k_{2i}\} \text{ with } k_{maxi} = (u_i^2 + v_i^2 + w_i^2)^{1/2} h_i \text{ and for steady problems and } k_{maxi} = 0.25 \min\{\Delta x_i, \Delta y_i, \Delta z_i\}^2 / \Delta t \text{ for transient problems.}$$

Also $\alpha_{k1} = 0.125 \gamma$, $\alpha_{k2} = 2 \gamma$ with $\gamma = 0.0086$ for linear elements in which case R_i is defined using the diffusion operator (top of page) and otherwise $\gamma = 0.25(2^p)$ in which p is the polynomial order of the FEM expansion ($p=1$ for linear 3x3x3 filters, $p=2$ for quadratic 5x5x5 filters and $p=3$ for cubic filters). When we are using mass lumping or non-centred schemes then we set $\alpha_{k1} = 0.25 \gamma$. The scalar γ gets bigger with increasing p because the residual R_i gets smaller. For $p > 1$ then we calculate R_i with:

$R_i = (u_i C_{xi} + v_i C_{yi} + w_i C_{zi}) - (u_i C_{xi}^{low} + v_i C_{yi}^{low} + w_i C_{zi}^{low})$ in which C_{xi}^{low} , C_{yi}^{low} , C_{zi}^{low} are lower order (by one) filters than those used in the rest of the simulation e.g. if the filter size in 3D is 5x5x5 then the lower order size might be 3x3x3. This R_i effectively forms the residual of the discrete system of equations and results in a particularly impressive performing method. To obtain high rates of convergence use:

$R_i = (u_i C_{xi}^{high} + v_i C_{yi}^{high} + w_i C_{zi}^{high}) - (u_i C_{xi} + v_i C_{yi} + w_i C_{zi})$ in which C_{xi}^{high} , C_{yi}^{high} , C_{zi}^{high} are higher order filters.

Anisotropic residual based diffusion for non-linear Petrov-Galerkin Dissipation

Define $C_{xi} = (A_x C)|_i$, $C_{yi} = (A_y C)|_i$, $C_{zi} = (A_z C)|_i$.

Suppose as in the previous section the residual can be defined by for example:

$R_i = (u_i C_{xi} + v_i C_{yi} + w_i C_{zi}) - (u_i C_{xi}^{\text{low}} + v_i C_{yi}^{\text{low}} + w_i C_{zi}^{\text{low}})$ or using the mixed mass approximation to the residual

$R_i = \alpha_r (M_L^{-1} M - I)(u_i C_{xi} + v_i C_{yi} + w_i C_{zi})$ in which $\alpha_r=2$ has been effective. Now the residual in each direction in turn can also be estimated from: $R_{xi} = \alpha_r (M_L^{-1} M - I) u_i C_{xi}$, $R_{yi} = \alpha_r (M_L^{-1} M - I) v_i C_{yi}$, $R_{zi} = \alpha_r (M_L^{-1} M - I) w_i C_{zi}$.

This provides an opportunity to apply anisotropically the Petrov-Galerkin diffusion – that is to apply different diffusion in different directions. In its simplest form this can be achieved through for example (extending the previous approach): $k_{x1i} = \alpha_{k1} |R_{xi}| \Delta x_i / (\epsilon_k + |C_{xi}|)$, $k_{y1i} = \alpha_{k1} |R_{yi}| \Delta y_i / (\epsilon_k + |C_{yi}|)$, $k_{z1i} = \alpha_{k1} |R_{zi}| \Delta z_i / (\epsilon_k + |C_{zi}|)$.

However, this can be generalised further by not assuming that the diffusion is aligned with the coordinate system. For simplicity initially we will assume the system is 2D. This then enables us to define another residual from: $R_{xyi} = \alpha_r (M_L^{-1} M - I)(u_i C_{xi} + v_i C_{yi})$ with associated diffusion coefficient of $k_{xy1i} = \alpha_{k1} |R_{xyi}| / (\epsilon_k + \frac{1}{2}|C_{xi}|/\Delta x_i + \frac{1}{2}|C_{yi}|/\Delta y_i)$. Now we have 3 diffusion coefficients so one might find the largest of the 3 diffusion coefficients and rotate the coordinate system so that it is aligned with this diffusion direction, either $(u_i, 0)^T$, $(0, v_i)^T$ or $(u_i, v_i)^T$ then project the other two directions so they are orthogonal to this direction and choose the largest of the remaining diffusion coefficients (after the projection). This becomes the orthogonal diffusion then rotate the system back to the original system to form the final diffusion tensor. A similar approach can be applied in 3D but then 6 residuals are formed e.g. $R_{xyz_i} = \alpha_r (M_L^{-1} M - I)(u_i C_{xi} + v_i C_{yi} + w_i C_{zi})$ as well as R_{xyi} as defined above.

Calculating diffusion/gradient ANN filters for $-\nabla \cdot k \nabla c$, ∇c on non-uniform but not distorted grids with variable diffusion

From 1D we can see that assuming $\Delta x=1$ then the diffusion 3 point discretization is
$$-\frac{1}{2}(k_i+k_{i+1})(c_{i+1}-c_i)+\frac{1}{2}(k_{i-1}+k_i)(c_i -c_{i-1}) = -\frac{1}{2}(k_i+k_{i-1})c_{i-1} + (\frac{1}{2}k_{i-1}+k_i+\frac{1}{2}k_{i+1})c_i - \frac{1}{2}(k_i+k_{i+1})c_{i+1} \quad \text{---(D1)}$$

In multi-D this becomes in the x-direction diffusion:

$A_{D2x}C|_i = \frac{1}{2} \Delta x_i \Delta y_i \Delta z_i (k_i (\hat{A}_{D2x}C)|_i + (\hat{A}_{D2x}(KC))|_i - c_i (\hat{A}_{D2x}K)|_i)$ in which $KC = K \odot C$ is a vector.

In differential form this is the identity: $2\nabla \cdot (k \nabla c) = k \nabla^2 c + \nabla^2(kc) - c \nabla^2 k$.

In 1D one can see this is equations eqn (D1) when $\hat{A}_{D2x}=(-1, 2, -1)$.

Here A_{2Dx} is normalised to obtain \hat{A}_{2Dx} with $\Delta x_i=\Delta y_i=\Delta z_i=1$ and \hat{A}_{D2x} is obtained from FEM or FD discretisations.

For non-uniform grid spacing use $k_i = \tilde{k}_i / \Delta x_i$ in which \tilde{k}_i is the diffusion coefficient of node/cell i. If the diffusion is isotropic then $k_i = \tilde{k}_i / h_i$ with $h_i = (\Delta x_i + \Delta y_i + \Delta z_i) / 3$. This k_i uses the approx. for 3 point FD stencils:

$1/(\frac{1}{2}\Delta x_i + \frac{1}{2}\Delta x_{i+1}) \approx 1/(2\Delta x_i) + 1/(2\Delta x_{i+1})$ with an error of 5% when ratio of cell sizes is 1.5.

In y-direction: $A_{D2y}C|_i = \frac{1}{2} \Delta x_i \Delta y_i \Delta z_i (k_i (\hat{A}_{D2y}C)|_i + (\hat{A}_{D2y}(KC))|_i - c_i (\hat{A}_{D2y}K)|_i)$, similarly for A_{D2z} .
The overall diffusion filter operating on C becomes:

$A_{D2}C = A_{D2x}C + A_{D2y}C + A_{D2z}C$ and is a discretization of $\nabla \cdot k \nabla c$

For advection filter A_x this becomes $A_x = (\Delta x_i \Delta y_i \Delta z_i / \Delta x_i) \hat{A}_x$ and similarly for A_y, A_z .

Isotropic diffusion for a uniform grid, that is $-\nabla \cdot k \nabla c$:

In multi-D this becomes in the isotropic diffusion term:

$-(\nabla \cdot k \nabla c)|_i \sim (A_{D2K}C)|_i = \frac{1}{2} (k_i (A_{D2}C)|_i + (A_{D2}(KC))|_i - c_i (A_{D2}K)|_i)$ in which $KC = K \odot C$ is a vector.

In differential form this is the identity: $2\nabla \cdot (k \nabla c) = k \nabla^2 c + \nabla^2(kc) - c \nabla^2 k$.

DG filters on orthogonal but non-uniform grid/meshes

The DG filters are formed for advection based on:

$$\begin{aligned} \int_E N_i (\partial C / \partial x) dV &= - \int_E (\partial N_i / \partial x) C dV + \int_{\Gamma_{in}} n_x N_i C_{bc} d\Gamma + \int_{\Gamma_{out}} n_x N_i C d\Gamma \\ &= - (\Delta x \Delta y \Delta z / \Delta x) \int_{E\eta} (\partial N_i / \partial \eta) C dV + \Delta y \Delta z \int_{\Gamma_{in\eta x}} n_x N_i C_{bc} d\Gamma + \Delta y \Delta z \int_{\Gamma_{out\eta x}} n_x N_i C d\Gamma \\ &= - \Delta y \Delta z \int_{E\eta} (\partial N_i / \partial \eta) C dV + \Delta y \Delta z \int_{\Gamma_{in\eta x}} n_x N_i C_{bc} d\Gamma + \Delta y \Delta z \int_{\Gamma_{out\eta x}} n_x N_i C d\Gamma \end{aligned}$$

in which $E\eta$ represent the unit dimension element and $\Gamma_{in\eta}$ the faces of that element.

Since this represents $A_{x,DG}$ then $A_{x,DG} = \Delta y \Delta z \hat{A}_{x,DG}$, $A_{y,DG} = \Delta x \Delta z \hat{A}_{y,DG}$, $A_{z,DG} = \Delta x \Delta y \hat{A}_{z,DG}$ in which Δx , Δy , Δz represents the dimensions of the local element.

For the 2nd order operator:

- $\int_E (\partial N_i / \partial x)(\partial C / \partial x) dV + \int_{\Gamma} n_x N_i (\partial C / \partial x)|_{bc} d\Gamma$. This requires integrals of the form:
- $\int_E (\partial N_i / \partial x)(\partial C / \partial x) dV + \int_{\Gamma} n_x N_i (C / \Delta x) d\Gamma$
- = $- (\Delta x \Delta y \Delta z / (\Delta x \Delta x)) \int_E (\partial N_i / \partial \eta)(\partial C / \partial \eta) dV + \Delta y \Delta z \int_{\Gamma_{\eta}} n_x N_i (C / \Delta x) d\Gamma$
- = $- (\Delta y \Delta z / \Delta x) \int_E (\partial N_i / \partial \eta)(\partial C / \partial \eta) dV + (\Delta y \Delta z / \Delta x) \int_{\Gamma_{\eta}} n_x N_i C d\Gamma$

Thus, $A_{xx,DG} = (\Delta y \Delta z / \Delta x) \hat{A}_{xx,DG}$, $A_{yy,DG} = (\Delta x \Delta z / \Delta y) \hat{A}_{yy,DG}$, $A_{zz,DG} = (\Delta x \Delta y / \Delta z) \hat{A}_{zz,DG}$.

Thus, the Laplacian operator is $A_{D2DG} = A_{xx,DG} + A_{yy,DG} + A_{zz,DG}$.

This means that having a un-uniform but orthogonal mesh requires simply modifications to the DG filters. The non-uniform diffusion operator can be treated as described previously.

Interface tracking with compressive advection applied to DG

Using the approach of ‘Pavlidis 2016 Compressive...’ eqn 33 we define a –ve diffusion coefficient to maintain a sharp interface and in each direction k_{xi}^- , k_{yi}^- , k_{zi}^- .

Using $(u_i^*, v_i^*, w_i^*) = ((u_i c_{xi} + v_i c_{yi} + w_i c_{zi}) / (\epsilon_x + c_{xi}^2 + c_{yi}^2 + c_{zi}^2))$ (c_{xi} , c_{yi} , c_{zi}) with $\epsilon_x = 1^{-10}$ and $\mu_i^- = -\beta (u_i^2 + v_i^2 + w_i^2) / (\epsilon_x + u_i^{*2} + v_i^{*2} + w_i^{*2})^{1/2}$ with $\beta = 1/4$ and

$k_{xi}^- = \mu_i^- / \Delta x_i$, $k_{yi}^- = \mu_i^- / \Delta y_i$, $k_{zi}^- = \mu_i^- / \Delta z_i$, and the overall diffusion coefficients are:

$k_{xi} = w_{xi} k_{xi}^- + (1 - w_{xi}) k_i^+$, $k_{yi} = w_{yi} k_{yi}^- + (1 - w_{yi}) k_i^+$, $k_{zi} = w_{zi} k_{zi}^- + (1 - w_{zi}) k_i^+$

in which the k_i^+ is positive isotropic diffusion from the previous Petrov-Galerkin method.

Suppose the cells are arranged 

in which the cells are arranged in the direction of the flow from cell c_c .

Define the face value of c as $\check{c}_f = \varphi_f (c_d - c_u) + c_u$ and

$\varphi_f = f_{\text{limit}}(\psi_f, \psi_c)$ if $\psi_c \in [0, 1]$ else $\varphi_f = \psi_c$ with $f_{\text{limit}}(\psi_f, \psi_c) = \min\{\max\{1/(3C_{xi}), 2\} \psi_c, \max\{0, \psi_f\}\}$

and the Courant number is $C_{xi} = \Delta t (\epsilon_x + |u_i|) / \Delta x_i$.

Also define $\psi_f = (c_f - c_u) / H(c_d - c_u)$, $\psi_c = (c_c - c_u) / H(c_d - c_u)$ where $H(c) = (\epsilon_x + |c|) \text{ sign}(c)$; $\text{sign}(c) = c/|c|$.

in which the face value using the trapezium rule $c_f = 1/2 (c_d + c_c)$.

Also $w_{xi} = (\varphi_f - \psi_f) / H(\psi_c - \psi_f)$ and similarly for w_{yi} , w_{zi} .

Interface tracking with compressive advection applied to cty elements

Using the approach of 'Pavlidis 2016 Compressive...' eqn 33 we define a -ve diffusion coefficient to maintain a sharp interface and in each direction k_{xi}^- , k_{yi}^- , k_{zi}^- .

Using $(u_i^*, v_i^*, w_i^*) = ((u_i c_{xi} + v_i c_{yi} + w_i c_{zi}) / (\epsilon_x + c_{xi}^2 + c_{yi}^2 + c_{zi}^2)) (c_{xi}, c_{yi}, c_{zi})$ with $\epsilon_x = 1^{-10}$ and $\mu_i^- = -\beta (u_i^2 + v_i^2 + w_i^2) / (\epsilon_x + u_i^{*2} + v_i^{*2} + w_i^{*2})^{1/2}$ with $\beta = 1/4$ and

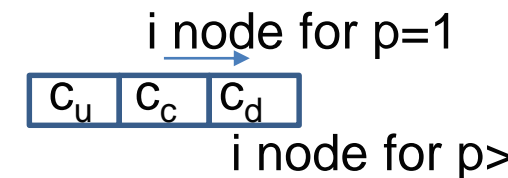
$k_{xi}^- = \mu_i^- / \Delta x_i$, $k_{yi}^- = \mu_i^- / \Delta y_i$, $k_{zi}^- = \mu_i^- / \Delta z_i$, and the overall diffusion coefficients are:

$$k_{xi} = w_{xi}^- k_{xi}^- + w_{xi}^+ k_i^+, \quad k_{yi} = w_{yi}^- k_{yi}^- + w_{yi}^+ k_i^+, \quad k_{zi} = w_{zi}^- k_{zi}^- + w_{zi}^+ k_i^+,$$

in which the k_i^+ is positive isotropic diffusion (k_i^{Petrov}) based on the previous Petrov-Galerkin method but multiplied by 300. The nodes are arranged as shown below – right.

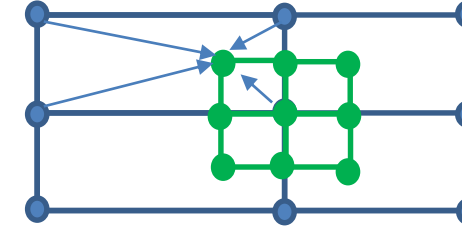
For node i we define an oscillation detecting variable:

$S_{xi} = (c_c - c_u)(c_d - c_c)$ and thus if $S_{xi} > 0$ there is no change of sign in gradient and thus no oscillation. However, if either $c_i > 1$ or $c_i < 0$ or this is true of any of the 3x3x3-1 surrounding nodes, to node i, then we assume there is an oscillation and define $S_{xi} = -1$. We define $w_{xi}^+ = -\max\{-1, \min\{0, S_{xi}\}\}$, $w_{xi}^- = \max\{-1, \min\{0, S_{xi}\}\}$, and similarly for w_y^+ , w_z^- , w_y^+ , w_z^+ . Also $k_{xi}^+ = k_{yi}^+ = k_{zi}^+ = 300 k_i^{\text{Petrov}}$. For stability we limit k_{xi} with $k_{xi} = \min\{k_{\text{max1}i}, k_{\text{max2}i}, k_{xi}\}$ with $k_{\text{max1}i} = (u_i^2 + v_i^2 + w_i^2)^{1/2} h_i$ and $k_{\text{max2}i} = 0.25 \min\{\Delta x_i, \Delta y_i, \Delta z_i\}^2 / \Delta t$.

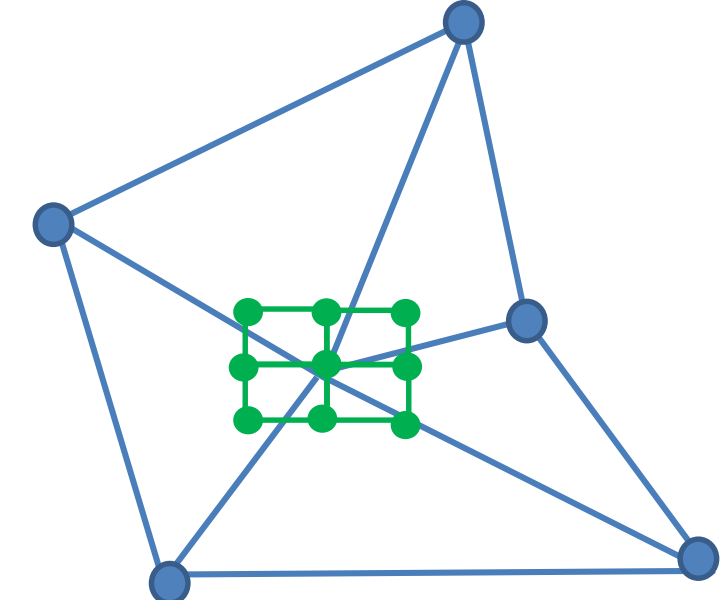


Structured-unstructured mesh discretisation for rapid/simple discretisation and on the fly filter formation with graph ANNs

One could have used interpolation to extend/diffusion filters to grids with non-uniform spacing. Imagine interpolating from the larger variables Δx , Δy spacing grid to the smaller uniform grid. On the right interpolate from blue nodes to green nodes. The FEM solution variables are the blue nodes.



On unstructured grid shrink to small element. The unknowns are on the unstructured grid. If high order elements are used then one might have to interpolate by mapping to certain polynomials. One can also mix discretisation types. e.g. map to rectangular DG structured grid discretisation from a continuous grid of triangles. Care must be taken to avoid singularities in the resulting matrix because values of the unstructured nodes are not defined.



Using the FEM basis functions to perform the interpolation from and too orthogonal but non-uniform meshes as well as for unstructured meshes

A simple way to interpolate is assuming an element with sides of length 2 then for bi-linear elements then $\zeta = \Delta x / 2$, $\eta = \Delta y / 2$ and then these local coordinates can be used to perform the interpolation or extrapolation to the element of length 2.

Then $C_i = \sum_j N_j(\zeta_i, \eta_i) C_j$ in which ζ_i, η_i is the position of node i.

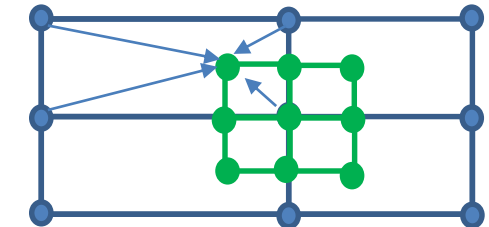
Many of the nodes to interpolate too or from are positioned along an edge in which simple 1D interpolation can be used which greatly simplifies these equations.

This interpolation effectively forms a matrix R and an inverse matrix P to interpolate too and from the standard element with sides of length 2.

Thus the filter becomes for example:

$$A_x = P \hat{A}_x R$$

This approach can readily be applied to distorted grids and may also be applied to fully unstructured grids but care must be taken to ensure the resulting matrices are non-singular.



Quadratic and higher order continuous FEM approach to producing stencils on structured grids – Convolutional FEM (CFEM)

The basic idea is to add discretisation stencils and take an average.

This is necessary because the stencils look different from node to node (see bottom pic). The basis functions for one of the

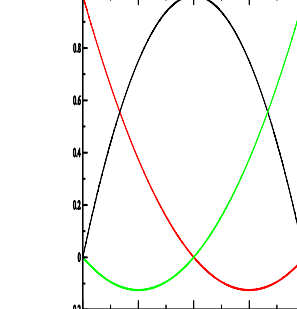
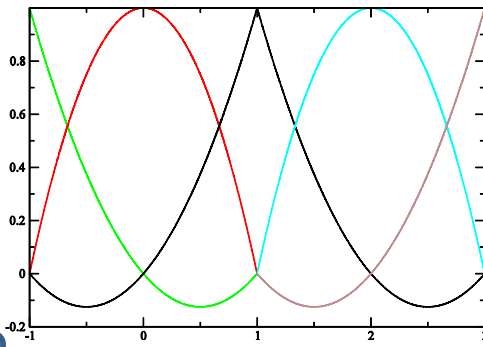
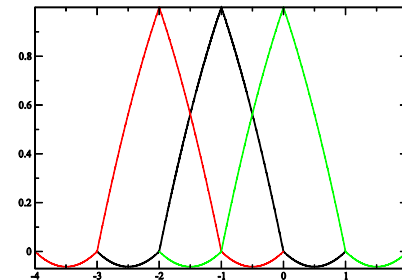
discretisations is shown right (middle) with the solid lines and for

another discretisation is shown below in the graph that. These

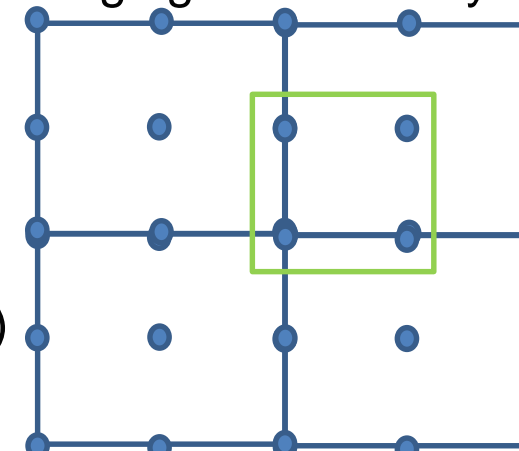
discretisations are simply added together. If there is a lumped basis function then it looks like an average of the 2 basis functions – see

graph top right. At the bottom we have highlighted (green box) the 4 nodes around which the stencils need to be averaged for 2D and for

3D there are similarly 8 nodes around which averaging is necessary.



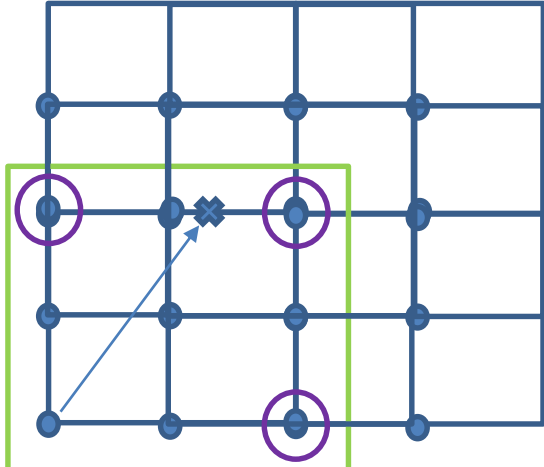
For mass the discretisation becomes:

$$\int_E \frac{1}{2} (N_i \sum_j N_j C_j + S_i \sum_j S_j C_j) dV$$
 in which N_i and S_i are the basis functions of the 2 discretisation in 1D (N_i & S_i middle & bottom right pics) and for diffusion we have: $\int_E \frac{1}{2} (((\partial N_i / \partial x) \sum_j (\partial N_j / \partial x) C_j) + ((\partial S_i / \partial x) \sum_j (\partial S_j / \partial x) C_j)) dV$.

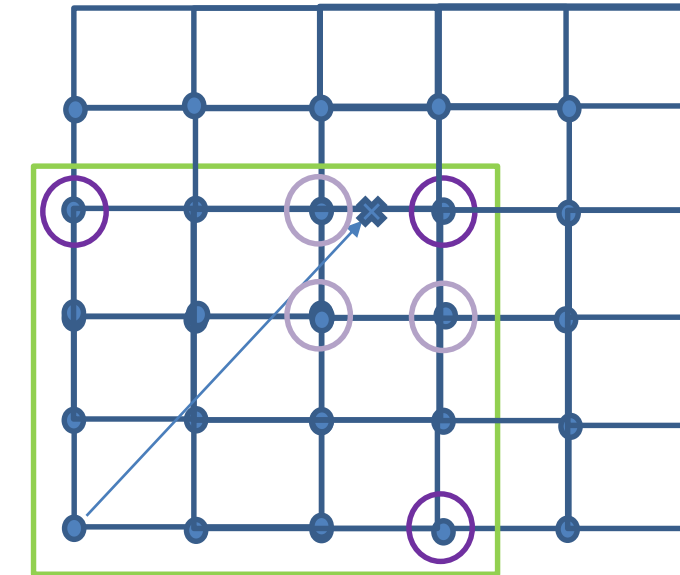
None-centred schemes from the quadratic and higher order continuous FEM approach to producing stencils on structured grids

The basic idea is to add discretisation stencils and take an average. This is necessary because the stencils look different from node to node and for the cubic element (bottom left) and quintic element (bottom right) we highlight how to form the average and what the candidate nodes are for upwind averaging of the discrete equations. The arrow shows the possible direction of advection and the cross the interpolation point which would be some linear combination of the node equations circles in purple.

Cubic element

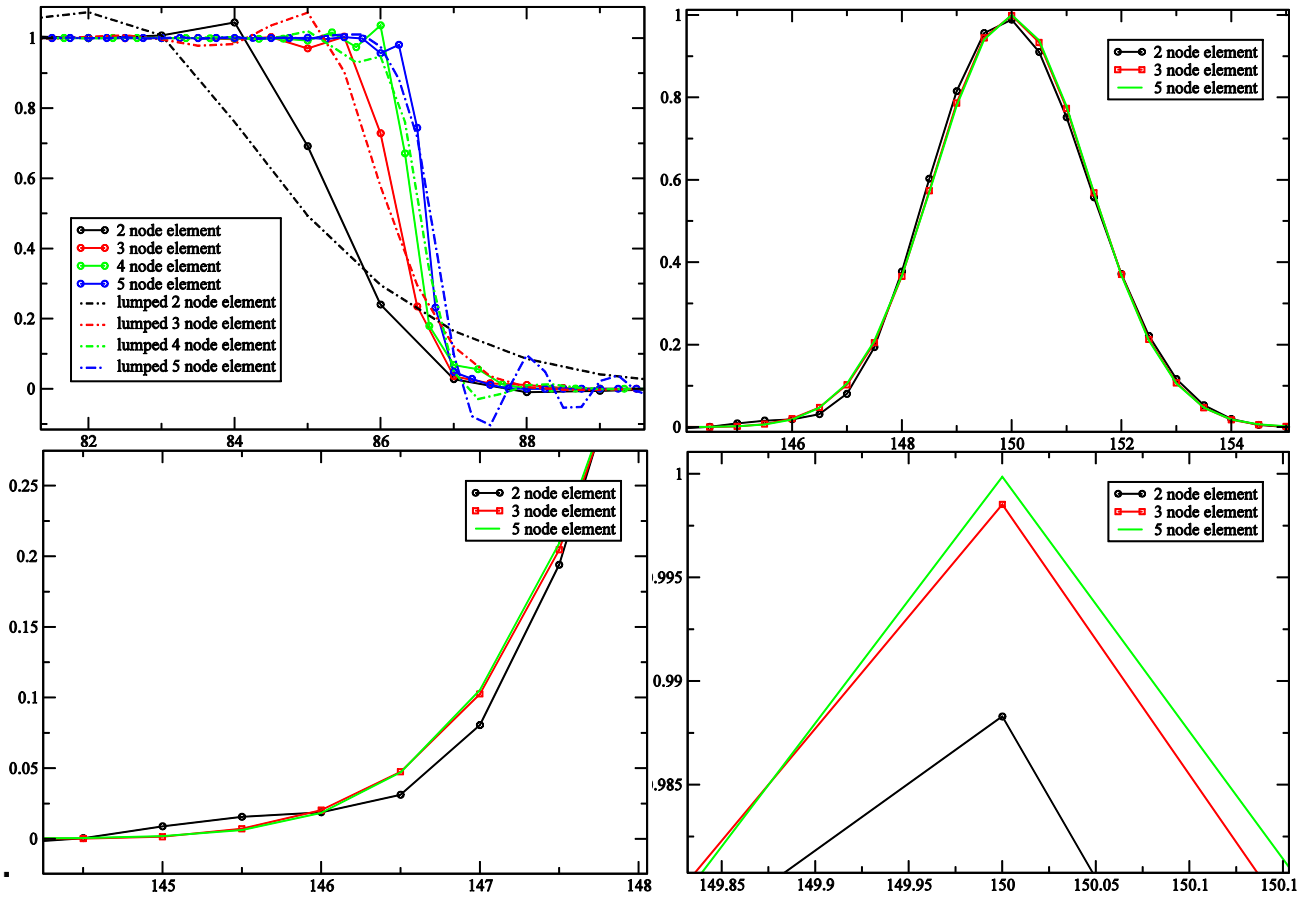


Quintic element



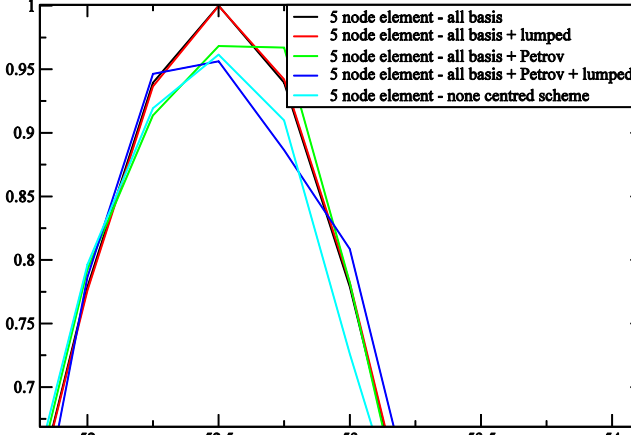
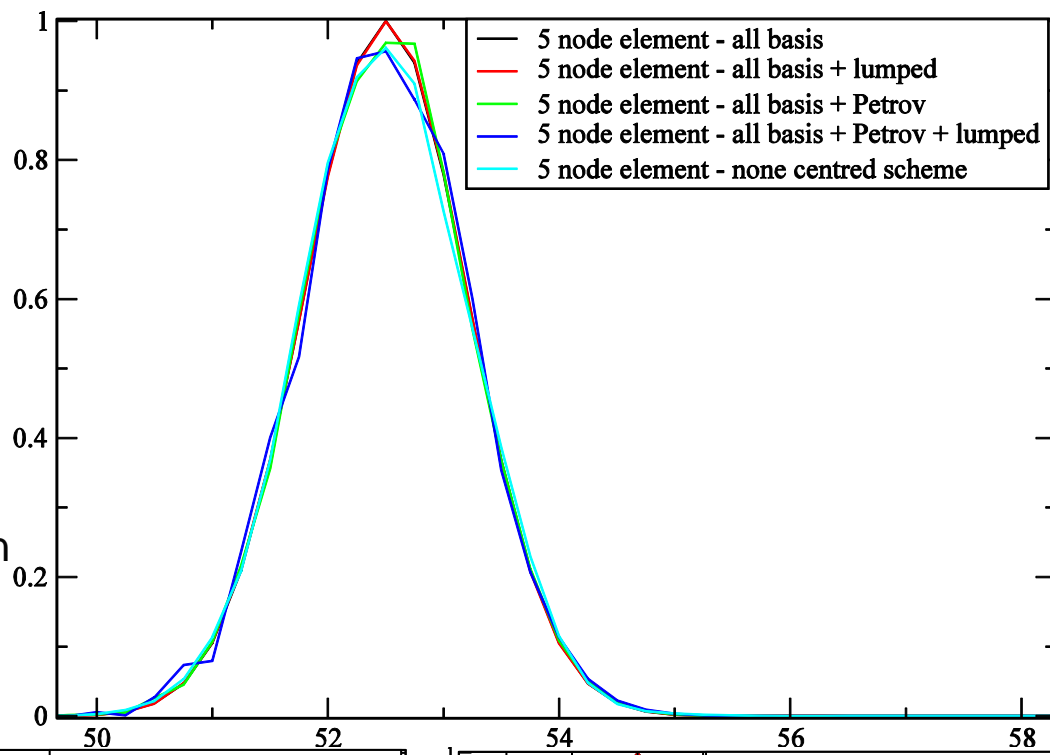
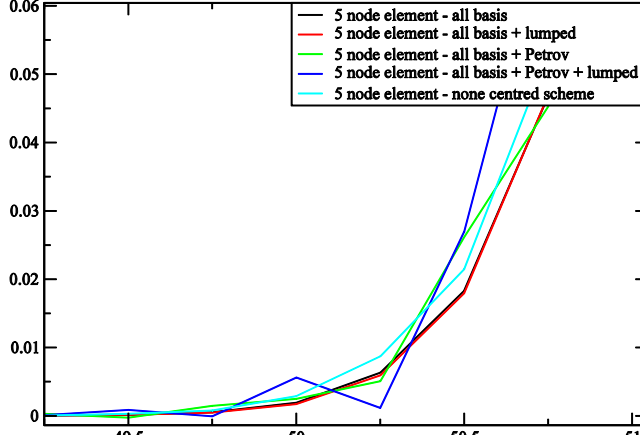
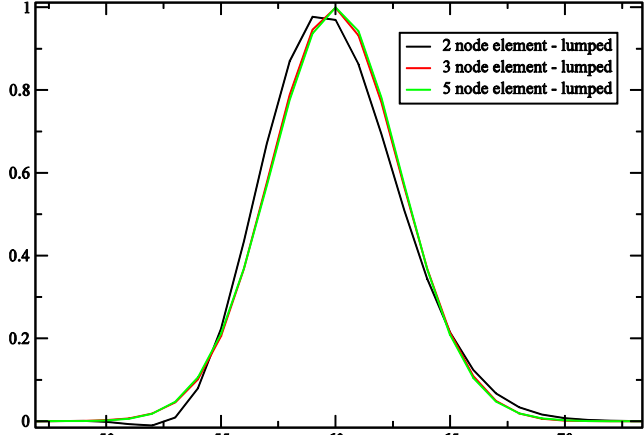
Results of Lagrange continuous elements but with the same stencil every where – designed for simple convolutional methods (CFEM)

The results are shown for the square wave problem (left-top pic) in which no benefit is observed for using high order methods when adjusted for number of variables other than for the lowest order method – the non-linear Petrov-Galerkin method is used here. For the Galerkin method we advect a Gaussian using elements of different orders of polynomials p1,p2,p4 with 2,3,5 nodes per element and the results are shown for the other graphs right including for focussed areas. One may assume that the 5 node quintic method is the most accurate followed by the cubic then the linear method (max Gaussian should be 1).



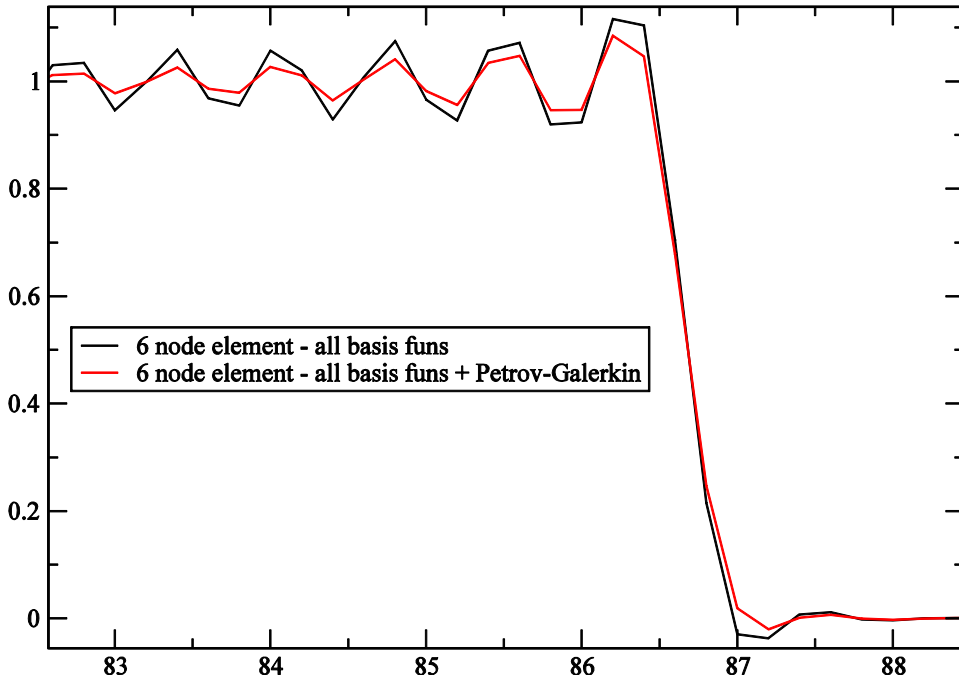
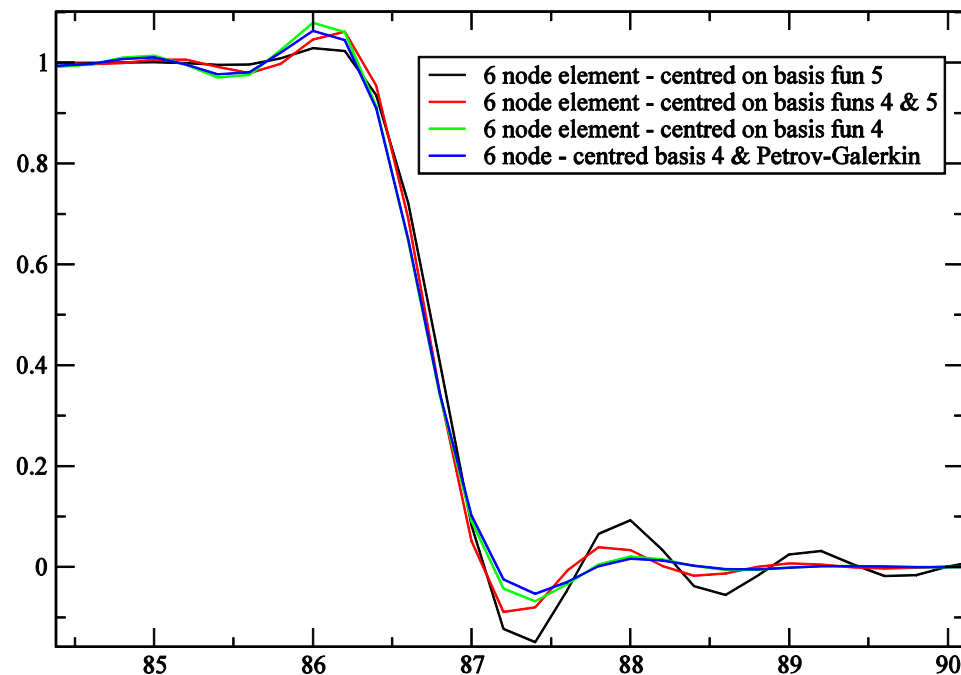
Results of Lagrange continuous elements (CFEM) with the same stencil every where – designed for simple convolutional methods – results for 5 node element and lumped approx.

The results are shown for the advection of a Gaussian. One can observe that the all basis function with and without mass lumping is the most accurate possibly followed by the none-centred scheme. The Petrov-Galerkin scheme's reduce the accuracy (max Gaussian should be 1). Bottom left – lumped in which the high order lumped schemes are accurate.



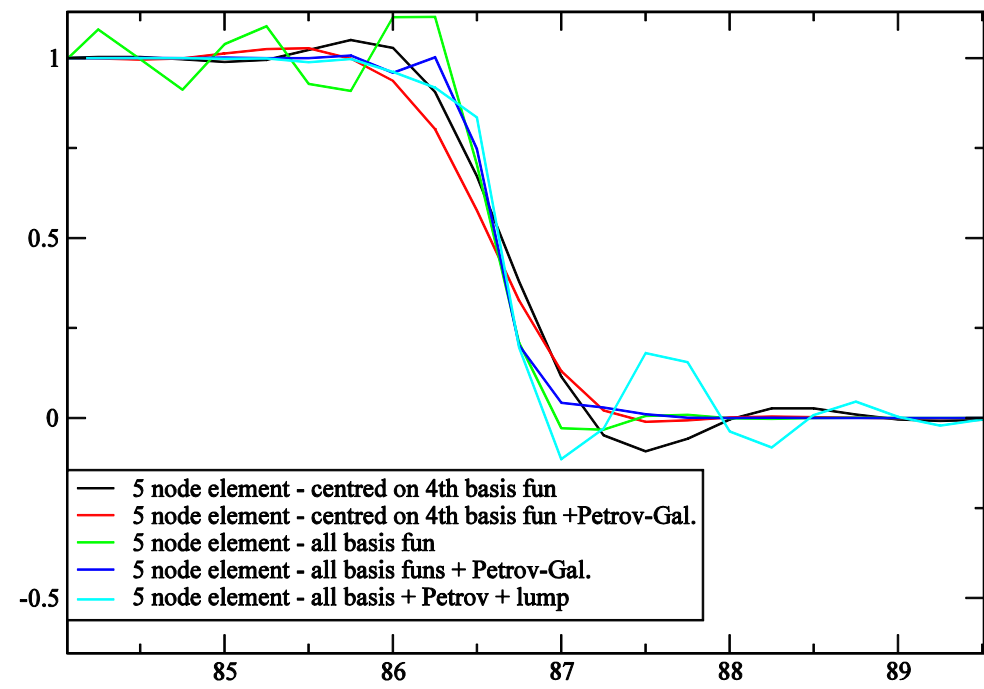
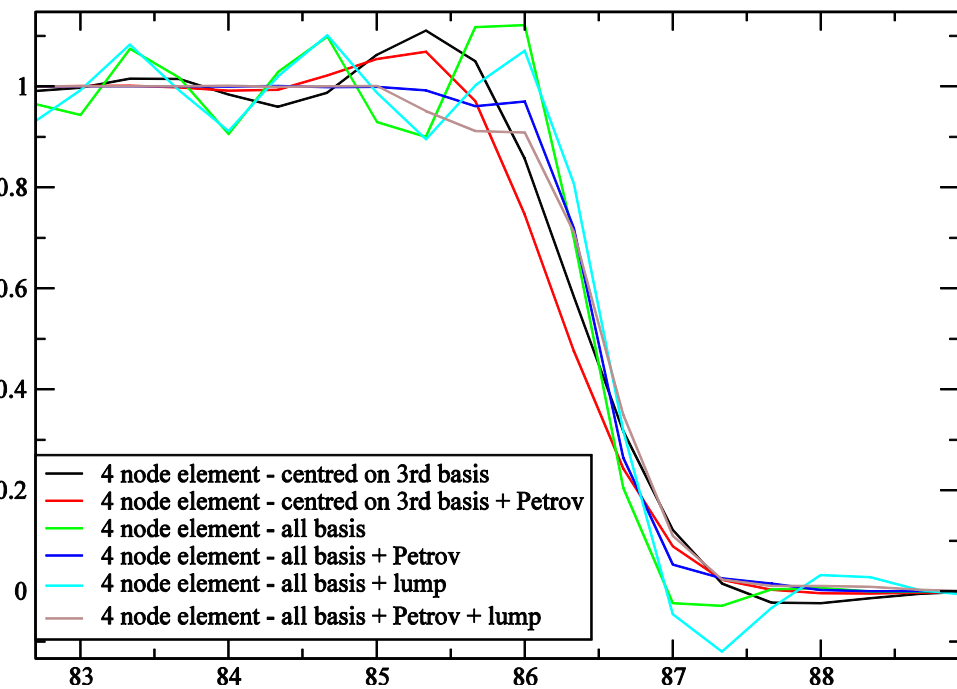
Results of Lagrange continuous elements but with the same stencil every where – 1D 6 node element results

We upwind the solution by using only basis function 4 & 5 to weight the governing eqns. We also show the all basis function method with and without the non-linear Petrov-Galerkin method.



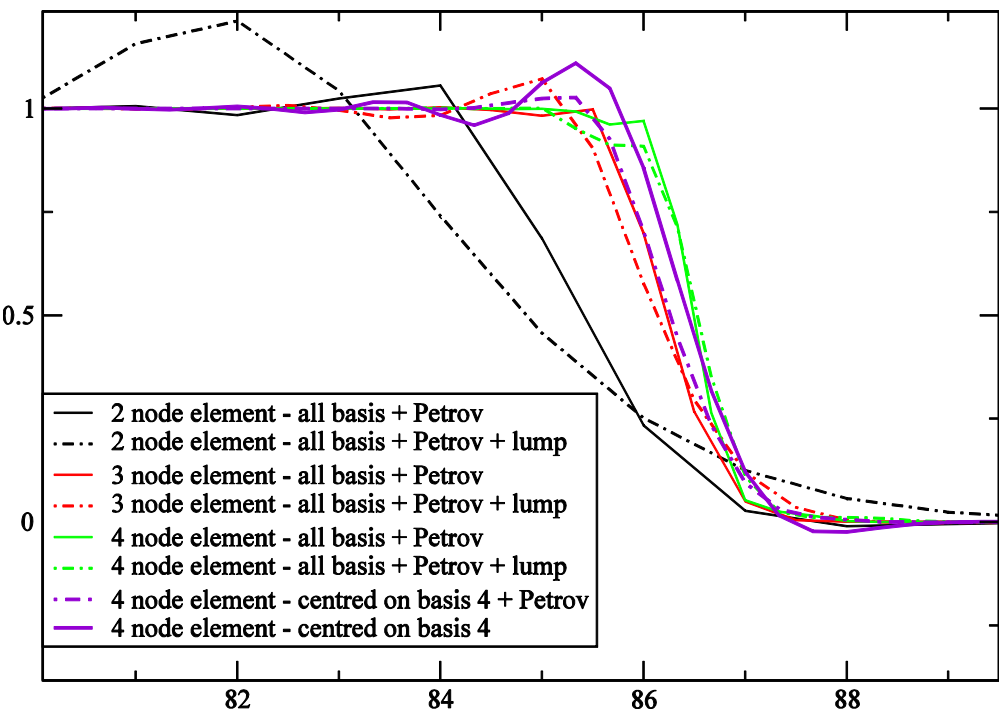
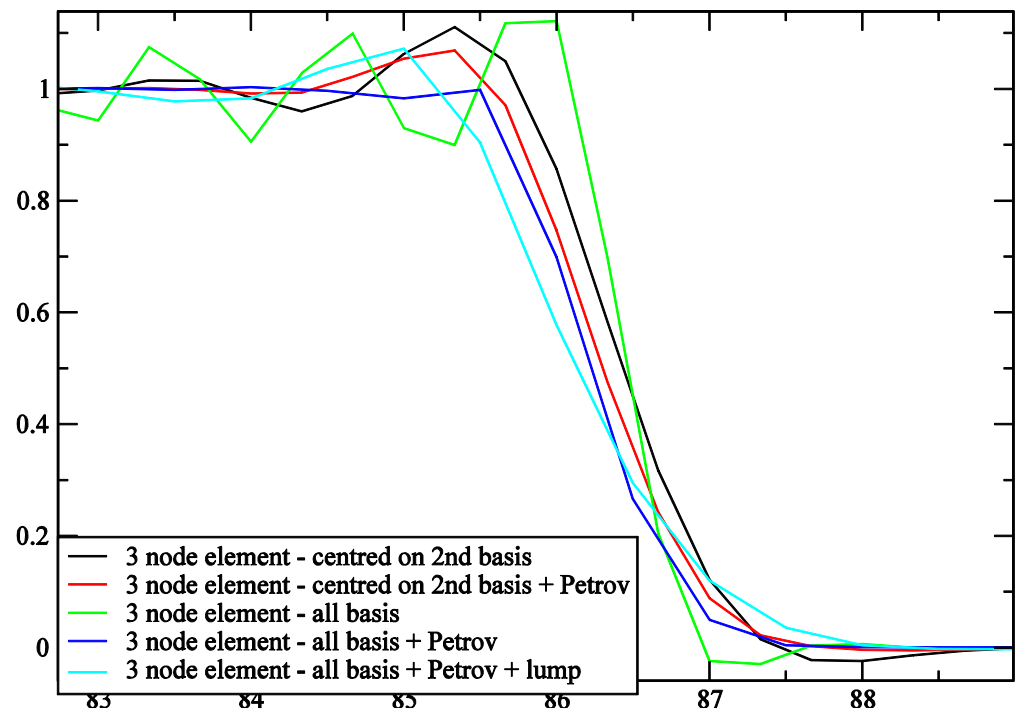
Results of Lagrange continuous elements but with the same stencil every where – 1D 4 & 5 node element results

We upwind the solution by using only basis function 3 (for 4 node element) and 4 (for 5 node element) to weight the governing eqns. We also show the all basis function method with and without the non-linear Petrov-Galerkin method.



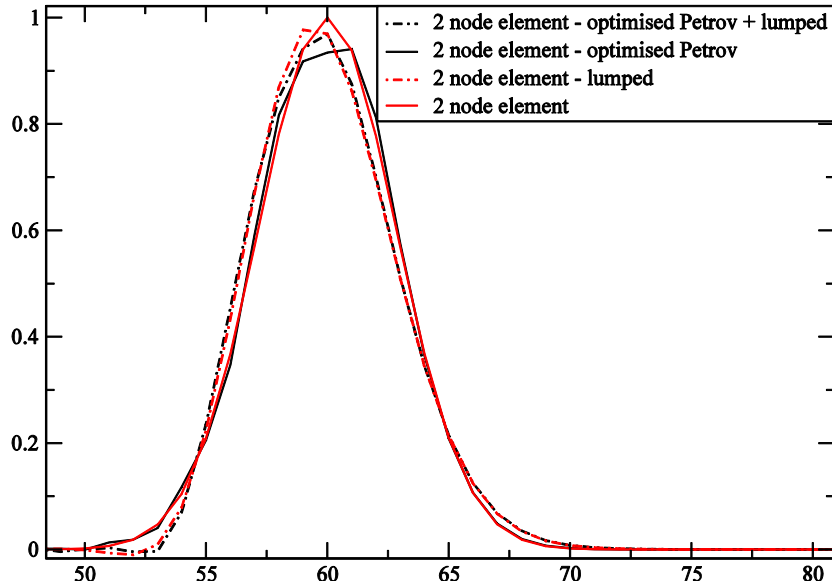
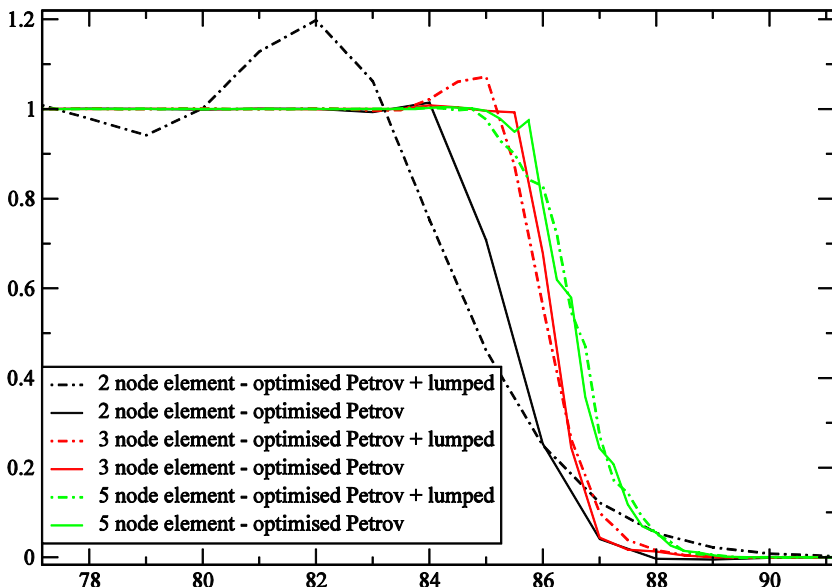
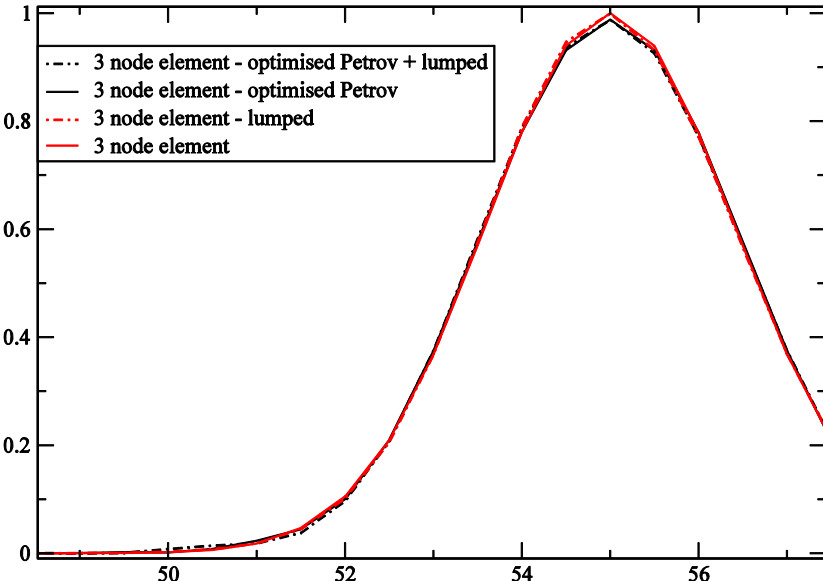
Results of Lagrange continuous elements but with the same stencil every where – 1D 3 node element results (left) and comparison of lumped, consistent mass results and none centred schemes (right)

We upwind the solution by using only basis function 2 to weight the governing eqns (left graph). We also show the all basis function method with and without the non-linear Petrov-Galerkin method. Mass lumping seems to matter more for 2 node element than other elements. Using mass lumping with none-centred schemes does not work well.



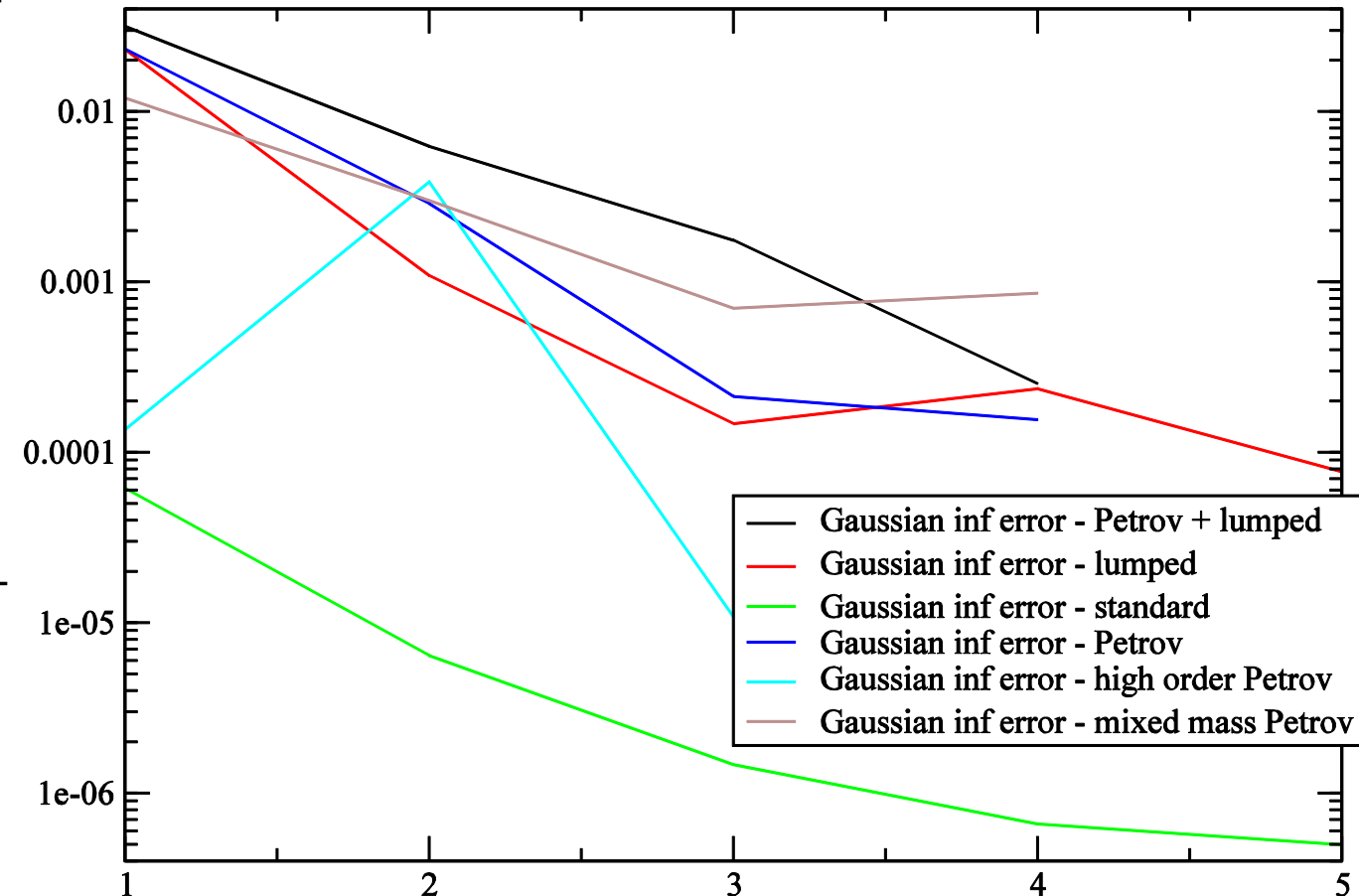
Results of Lagrange continuous elements with the optimised non-linear Petrov-Galerkin method formed (when possible) using a residual calculation that mixes low and high order filters

Notice that the Petrov-Galerkin method produces nearly identical exact Gaussian results for the 3 node per element element and higher order elements are even more accurate. The shock capturing (top right) is particularly good.

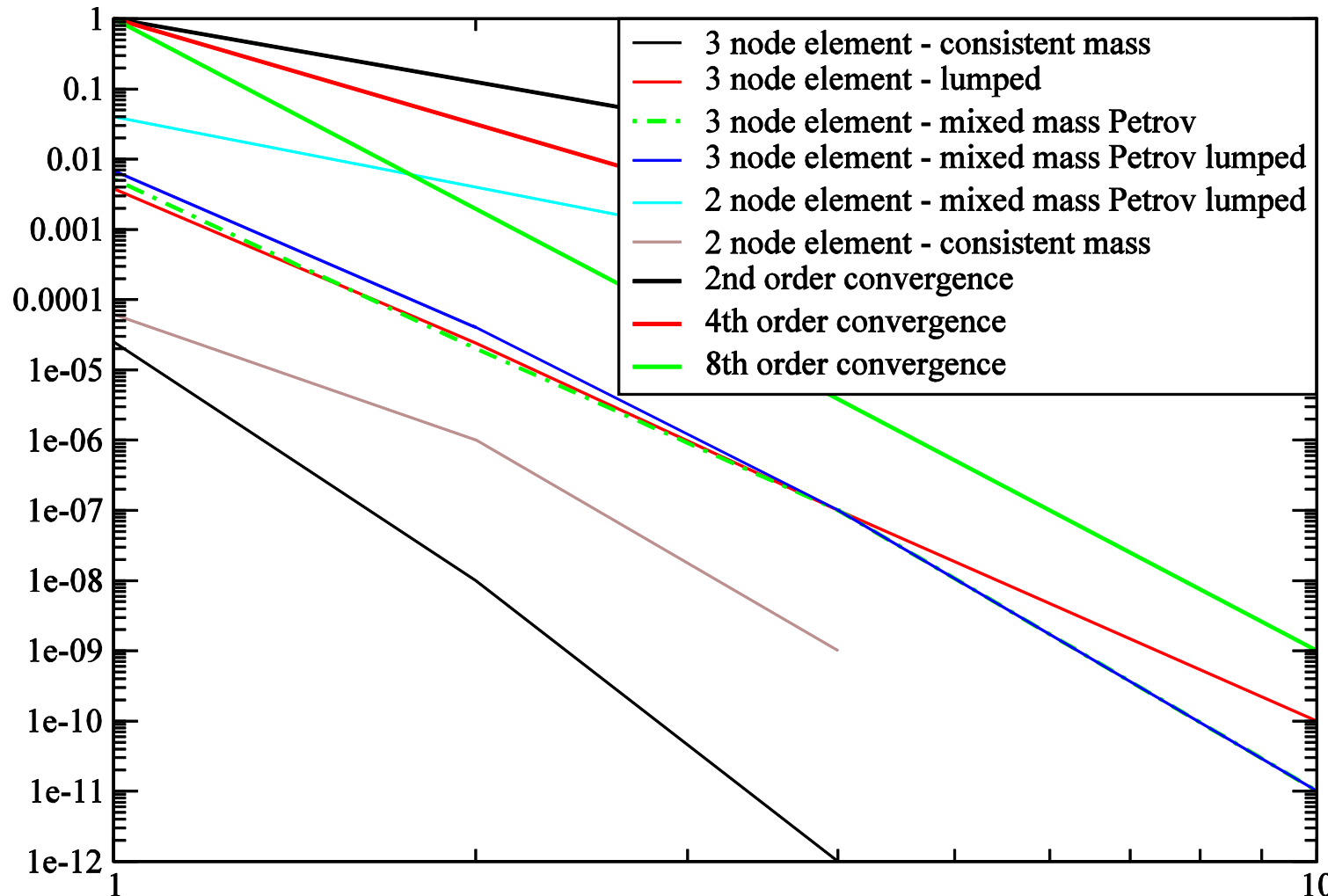


Convergence with increased polynomial order p of Convolutional Lagrange continuous FEM (CFEM) with the optimised non-linear Petrov-Galerkin method formed using a residual calculation that mixes low and high order filters

Infinity norm of error v
polynomial order for advection of
a smooth Gaussian. The mixed
mass Perov-Galerkin residual is
defined by $R_i = \beta_R (M_L^{-1}M -$
 $I)(u_i C_{xi} + v_i C_{yi} + w_i C_{zi})$ in which M is
consistent mass matrix (filter)
and M_L is the lumped filter.
Notice that the high order
residual calculation method can
be a little unpredictable and in
which β_R is an order one scalar –
here $\beta_R = 2$ other than for linear
element in which case $\beta_R = 160$
or one can treat linear elements
with the same coefficient as $p > 1$
elements.



Convergence with increased spatial resolution (x-axis in graph) for the Convolutional Lagrange FEM CFEM – graph shows good accuracy of method for advection of a Gaussian – results focus on the best performing Petrov Galerkin method: the mixed mass Petrov-Galerkin method



Unstructured mesh discretisation for rapid/simple discretisation and on the fly filter formation with graph and classical ANNs

As an alternative to the structured-unstructured approach one could use the FEM representation of the differential equation or, often equivalently, using mass lumping by having quadrature points at the FEM nodes. This is particularly suitable for high order elements as it makes implementation rapid and simple and allows high order derivatives in the differential equation to be used directly (see right picture). One can use higher order quadrature but this will be roughly twice as expensive and one still needs to mass lump.

The 1st order derivative of a field can be discretised FEM over an element:

$$\int_E N_i (\partial C / \partial x) dV = - \int_E (\partial N_i / \partial x) C dV + \int_{\Gamma_{in}} n_x N_i C_{bc} d\Gamma + \int_{\Gamma_{out}} n_x N_i C d\Gamma$$

Using:

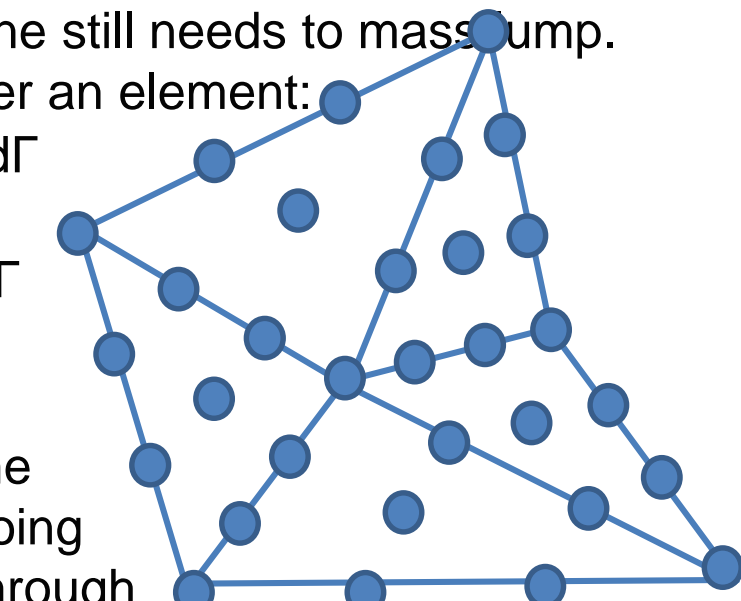
$$\int_E N_i (\partial C / \partial x) dV = - \int_E (\partial N_i / \partial x) C dV + \int_{\Gamma_{in}} n_x N_i C d\Gamma + \int_{\Gamma_{out}} n_x N_i C d\Gamma$$

then

$$= \int_E N_i (\partial C / \partial x) dV + \int_{\Gamma_{in}} n_x N_i (C_{bc} - C) d\Gamma$$

and C_{bc} is from the neighbouring element and Γ_{in} , Γ_{out} are the boundary of the element associated with incoming and outgoing information respectively. Using mass lumping and dividing through

by the lumped mass: $\partial C / \partial x \approx \partial C / \partial x|_i + (M_p n_x / \Delta x)(C_{bc} - C)|_i$ and $M_p = \text{no nodes normal to } \Gamma_{in}$.



Unstructured mesh discretisation for rapid/simple discretisation and on the fly filter formation with ANNs (cont)

For second order terms this becomes:

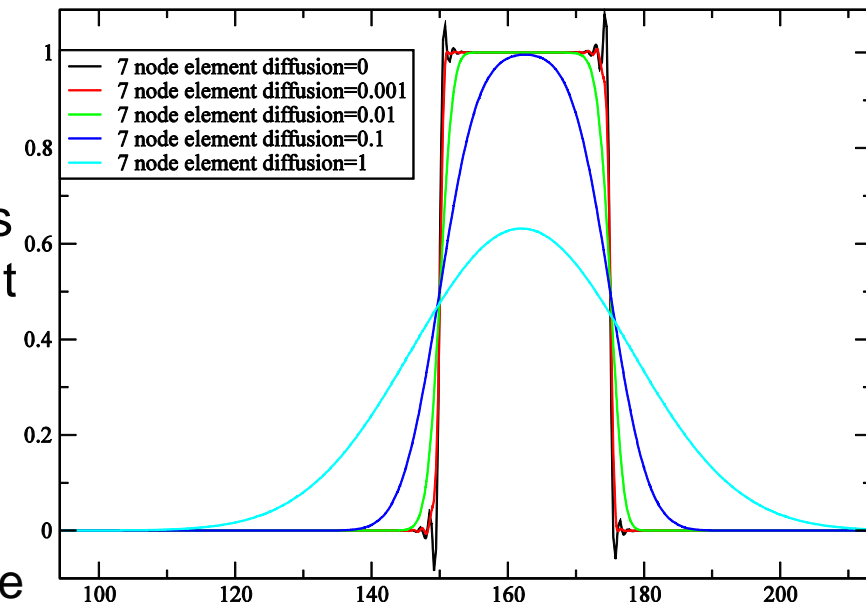
$$\int_E N_i (\partial^2 C / \partial x^2) dV = - \int_E (\partial N_i / \partial x)(\partial C / \partial x) dV + \int_{\Gamma} n_x N_i (\partial C / \partial x)|_{bc} d\Gamma.$$

Using mass lumping and dividing through by the lumped mass:

$$(\partial^2 C / \partial x^2)|_i \approx (\partial^2 C / \partial x^2)|_i + (1/(m_i \Delta x_i))(C_{bci} - C_i) - (n_x s_i / m_i)(\partial C / \partial x)|_i$$

in which s_i and m_i are the volume and surface masses associated with node i on the boundary of the element E .

If node i is not on the boundary $s_i=0$. For continuous FEM the same approach can be applied but one may form for each element a value of the derivatives like $(\partial^2 C / \partial x^2)|_i$ at node i and then the final value of $(\partial^2 C / \partial x^2)|_i$ is calculated by taking an area/volume weighting of these derivatives. The effectiveness of solving with various diffusion coefficients is shown in the right picture for advection of a square wave used later.



Consistent mass Chebyshev DG: Unstructured mesh discretisation for rapid/simple discretisation and on the fly filter formation with graph and classical ANNs

The DG discretization with a Chebyshev polynomial and a consistent mass matrix (solved using a Jacobi iteration) if formed through:

$$\int_E N_i (\partial C / \partial x) dV = - \int_E (\partial N_i / \partial x) C dV + \int_{\Gamma_{in}} n_x N_i C_{bc} d\Gamma + \int_{\Gamma_{out}} n_x N_i C d\Gamma$$

Key to this are 4 things.

- (1) forming C at the quadrature points** before evaluating the above integrals.
- (2) using a consistent mass matrix** which is solved for using a Jacobi style iteration.
- (3) we need to multiply the surface integrals in the above using the simple compact filter** without indirect addressing before
- (4) sending the above surface integral for equation i** to the neighbouring element with the graph neural network.

Unstructured mesh discretisation for rapid/simple discretisation and on the fly filter formation with ANNs – on the fly shape function derivatives:

To form $\partial C / \partial x$ at a node i we use:

$(\partial C / \partial x)|_i = \sum_j (N_{xj})|_i C_j$ in which we form $(N_{xj})|_i$ using (Fortran code):

```
do GI=1,NGI
    AGI=0.
    BGI=0.
    CGI=0.
    DGI=0.
```

```
do L=1,NLOC
    AGI=AGI+NLX(GI,1,L)*x_loc(1,L)
    BGI=BGI+NLX(GI,1,L)*x_loc(2,L)
    CGI=CGI+NLX(GI,2,L)*x_loc(1,L)
    DGI=DGI+NLX(GI,2,L)*x_loc(2,L)
```

end do

DETJ= AGI*DGI-BGI*CGI

! For coefficient in the inverse mat of the Jacobian.

A11= DGI /DETJ

A21=-BGI /DETJ

A12=-CGI /DETJ

A22= AGI /DETJ

do L=1,NLOC

NX(GI,1,L)= A11*NLX(GI,1,L)+A12*NLX(GI,2,L)

NX(GI,2,L)= A21*NLX(GI,1,L)+A22*NLX(GI,2,L)

end do

end do

Thus in 2D one stores, at each FEM node, the 2x2 inverse of the FEM Jacobian matrix which becomes a 3x3 matrix in 3D. Then form on the fly $(N_{xj})|_i$ when forming the discretisation for each element and to form the discretisation of terms like $(\partial C / \partial x)|_i = \sum_j (N_{xj})|_i C_j$. This makes the method fast and memory efficient. In FEM form this is:

$$\begin{Bmatrix} \frac{\partial N_i}{\partial x} \\ \frac{\partial N_i}{\partial y} \\ \frac{\partial N_i}{\partial z} \end{Bmatrix} = \mathbf{J}^{-1} \begin{Bmatrix} \frac{\partial N_i}{\partial \xi} \\ \frac{\partial N_i}{\partial \eta} \\ \frac{\partial N_i}{\partial \zeta} \end{Bmatrix} ; \quad \mathbf{J} = \begin{bmatrix} \sum \frac{\partial N_i}{\partial \xi} x_i, & \sum \frac{\partial N_i}{\partial \xi} y_i, & \sum \frac{\partial N_i}{\partial \xi} z_i \\ \sum \frac{\partial N_i}{\partial \eta} x_i, & \sum \frac{\partial N_i}{\partial \eta} y_i, & \sum \frac{\partial N_i}{\partial \eta} z_i \\ \sum \frac{\partial N_i}{\partial \zeta} x_i, & \sum \frac{\partial N_i}{\partial \zeta} y_i, & \sum \frac{\partial N_i}{\partial \zeta} z_i \end{bmatrix}.$$

Efficient discretisation for each direction in turn :

One can greatly speed up discretisation and derivative formation when one can separate out the components of the basis functions. This is extensively used in spectral element discretisation to make them very fast and is also easily achieved on structured grids – see picture.

For example suppose one wishes to evaluate at quadrature point g:

$$(\partial C / \partial x)|_g = \sum_k (N_{xk})|_g C_k = \sum_i \sum_j (N_i^x N_j^y)|_g C_{ij} = \sum_i \sum_j (N_i^x N_j^y)|_{xg} C_{ij} = \sum_j N_j^y|_g \sum_i (N_i^x)|_{xg} C_{ij}$$

Suppose quadrature points g are also at the collocation point and g is separated using (g_i, g_j) .

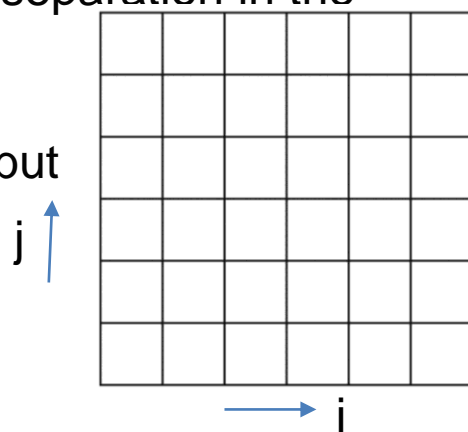
Thus:

$$(\partial C / \partial x)|_{(g_i, g_j)} = \sum_j N_j^y|_{gj} \sum_i (N_i^x)|_{gi} C_{ij} = N_j^y|_{gj} \sum_i (N_i^x)|_{gi} C_{igj}$$

Thus there is only summation over a 1D array greatly speeding up calculations.

This separation is easily extended to unstructured grids as long as there is separation in the local coordinates ζ, η . That is $N_k = N_i^\zeta N_j^\eta$. Then $(N_k)_x = (J^{-1})_{xx} N_i^\zeta + (J^{-1})_{xy} N_j^\eta$ in which $(J^{-1})_{xx}, (J^{-1})_{xy}$ are contributions from the inverse Jacobian matrix.

Thus this approach can also be used for triangle and tetrahedral elements but further research may be needed.

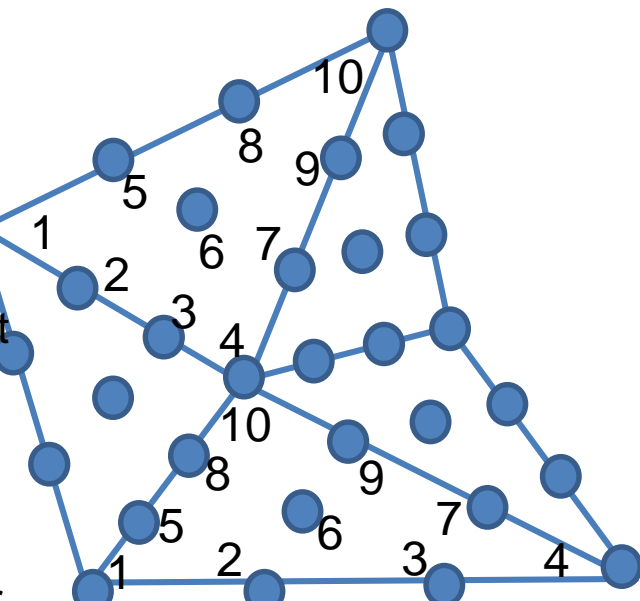


DG Unstructured mesh discretisation data structure:

To form an efficient data structure for the neural network one may split the data structure into two 1D CNNs. Assuming the nodes are ordered consecutively local to each element then **one filter is structured** with lopsided (not centred) filters and a filter specific for each local element. Then each of these filters has a stride of M_{loc} which is the number of local nodes per element (on the right its 10 for 2D cubic elements (see right pic) and 20 for 3D tetrahedral elements).

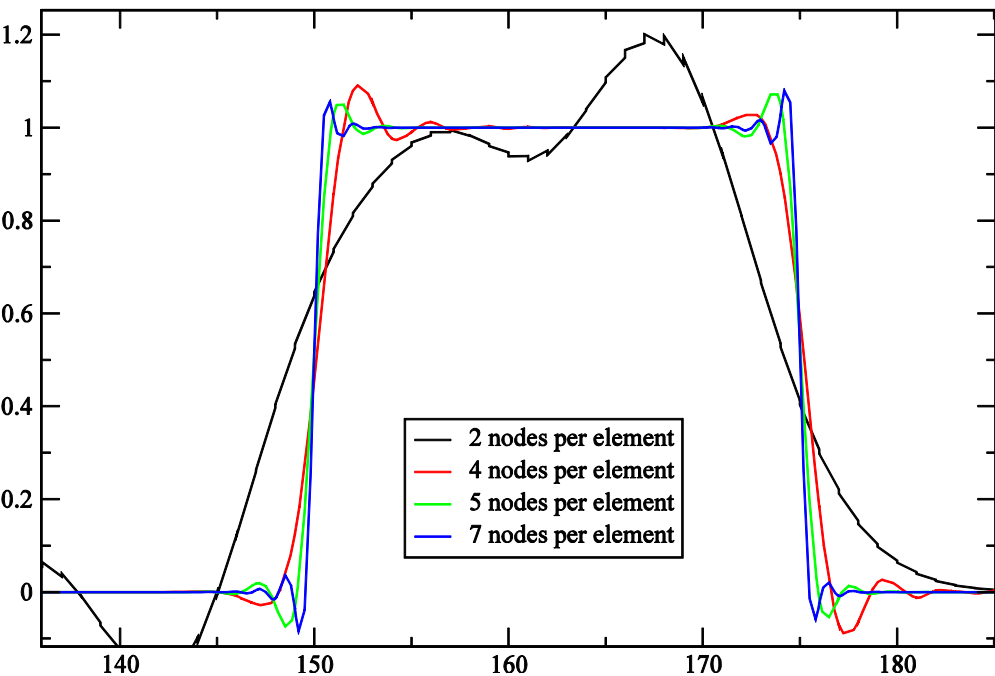
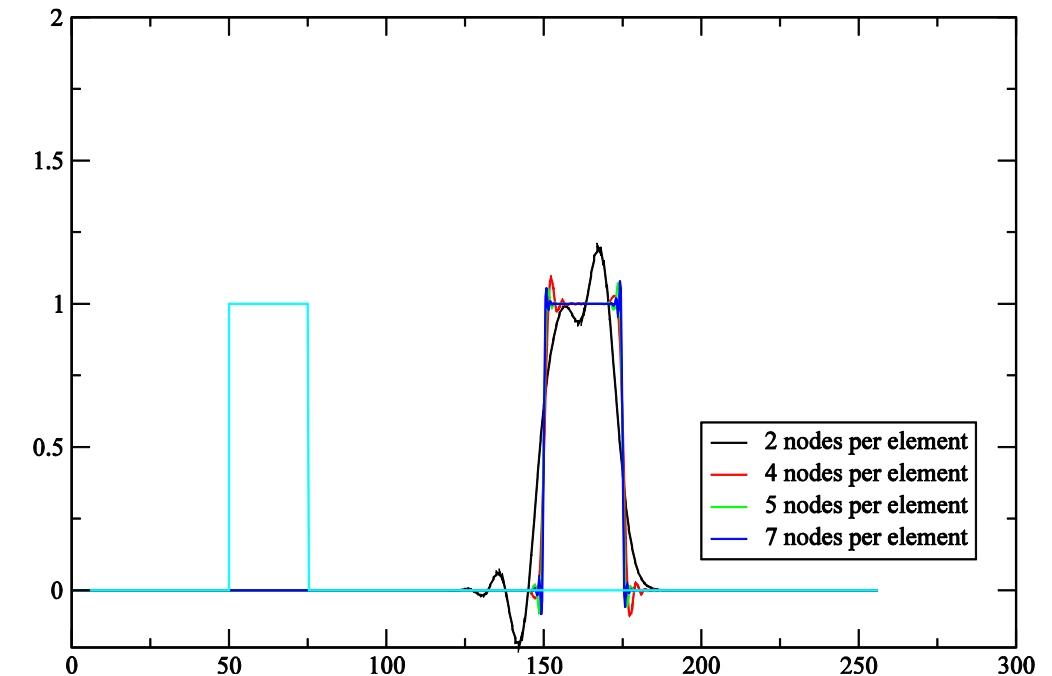
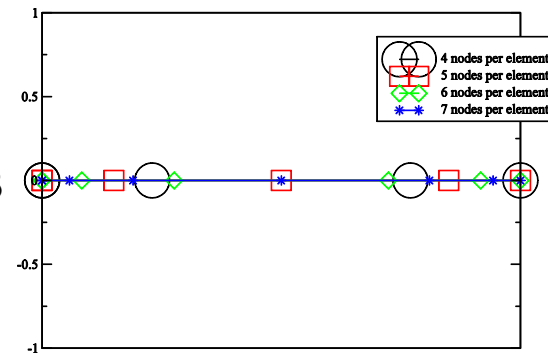
The second set of filters are formed from this 1D vector but with **graph neural networks but with limited connectivity** – just connecting to the single node on the other side of the face (see previous section on lumping). However, there may be a number of faces a node is opposite ~5 at corner nodes, 2 at edge nodes, 1 at face nodes, 0 in interior nodes in 3D (mean 2.4 graph connections per cubic DG node) and max of 2 in 2D. Even more efficient data structures are possible which only take into account the connectivity of the elements in the graph neural networks but these are more complex.

To solve the equations efficiently it is suggested that one would perform lots of Jacobi style iterations on the finest grid (possibly only updating the nodes within an element for efficiency) then use the Space Filling Curve (SFC) multi-grid applied to the collapsed to one variable per element. The SFC must go through all the element of the mesh.



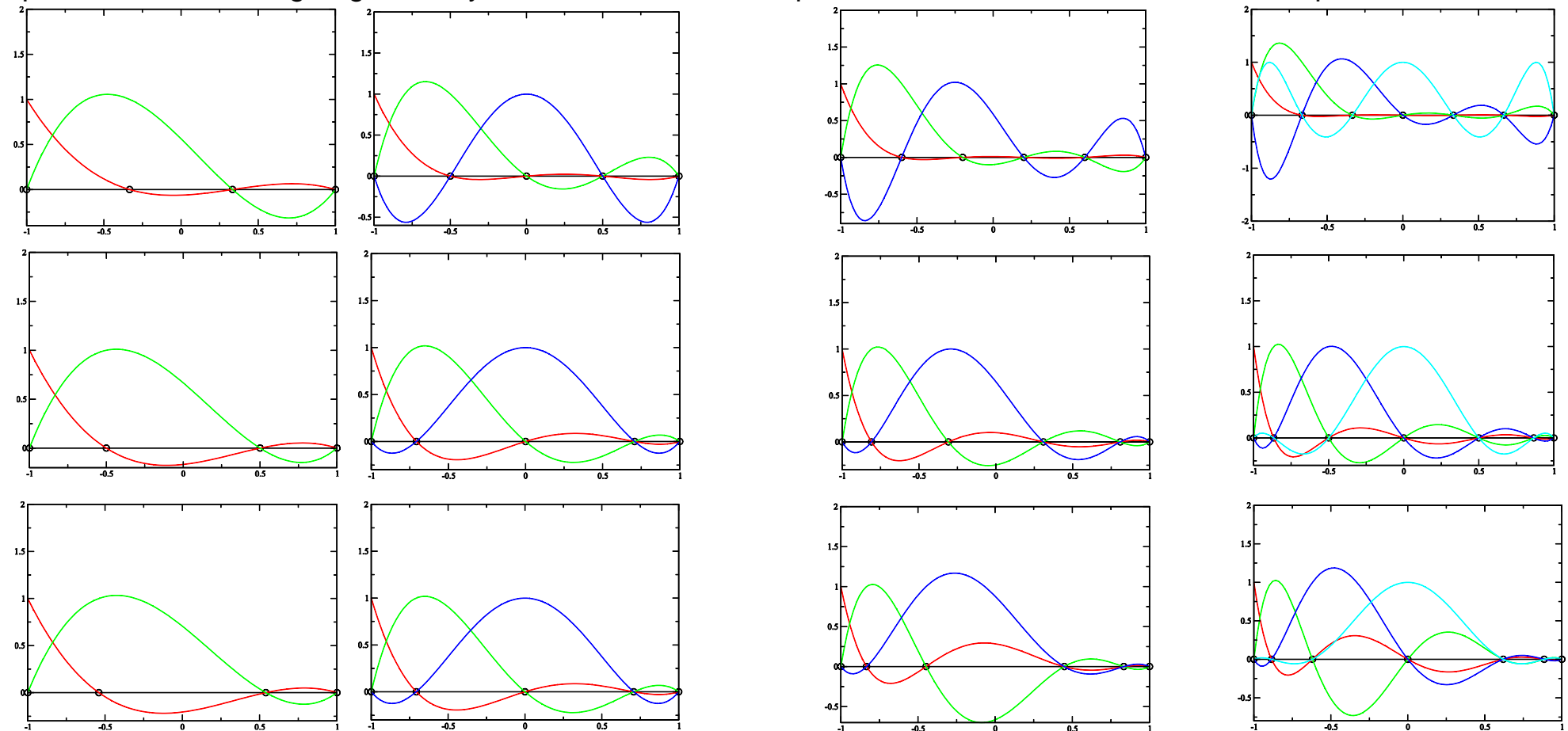
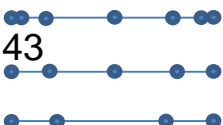
DG high order methods comparison for different numbers of nodes per element using non-uniform node spacing in an element: 2 nodes per element is linear, 3 nodes is quadratic etc. Advection of a square wave in 1D

We use the on the fly approach with quadrature at the nodes. The method uses a non-uniform grid in 1D (right pic) in which the nodes are clustered towards the boundaries of the elements. The ratio between the node spacing distances is 0.43 (works well in $[0.43, 0.54]$ or $[(1/5)^{1/2}, (2/7)^{1/2}] - 0.43$ similar to low order Chebyshev spectral elements (4 or 5 nodes per 1D element). Initial condition is shown in the 1st graph on the left in cyan colour – blow up of wave on the 2nd graph.



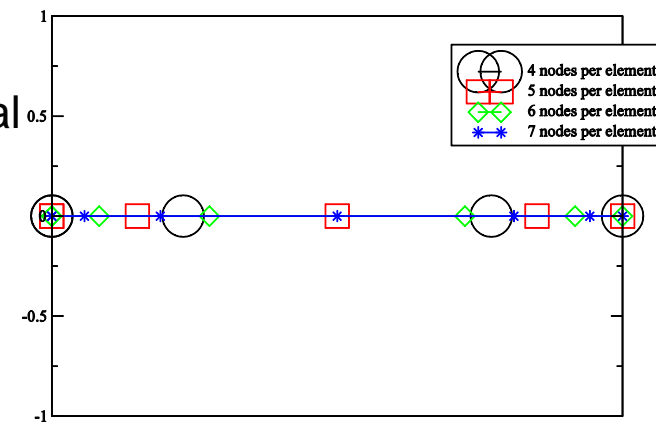
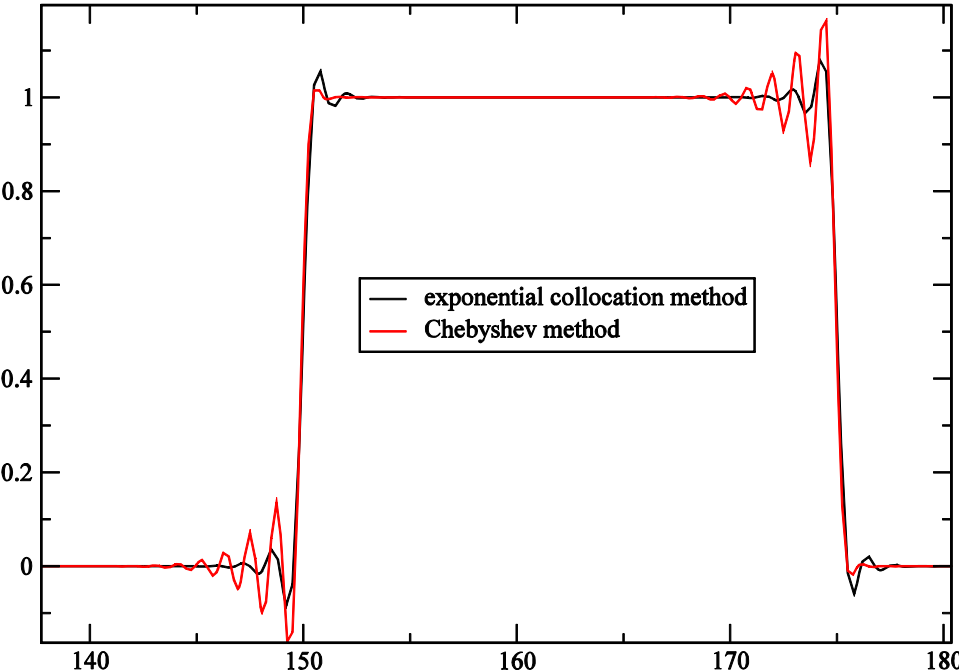
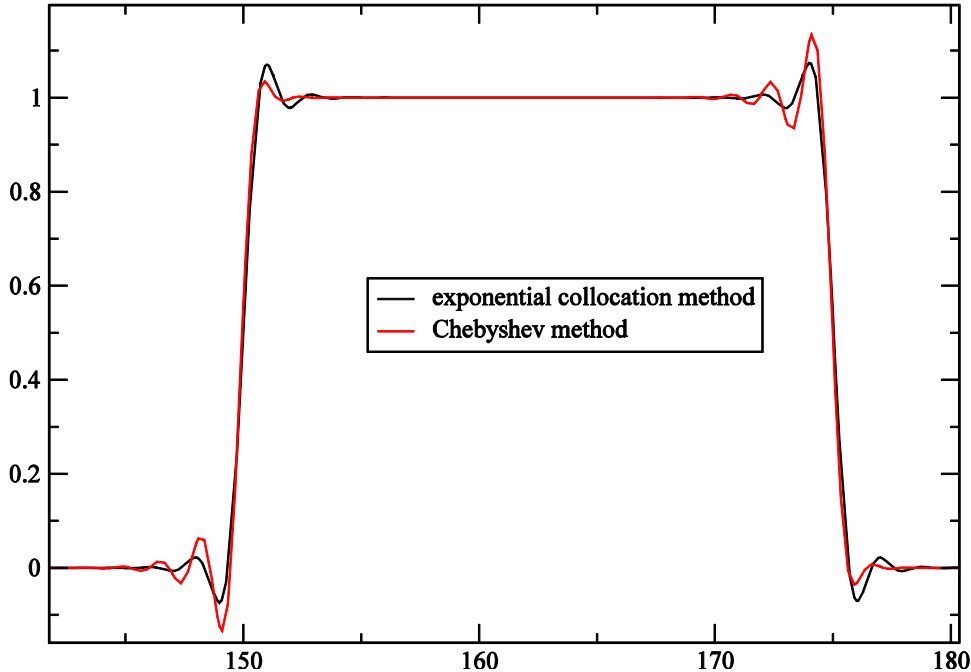
DG high order methods basis functions in 1D comparison of Lagrange, Chebyshev and exponential collocation basis functions

We use the on the fly approach with quadrature at the nodes. The ratio between the node spacing distances is 0.43 for exponential collocation method – similar to low order Chebyshev spectral elements.
Top to bottom rows, Lagrange, Chebychev-Gauss-Lobatto, exponential collocation and 4,5,6,7 nodes per element.



DG high order methods comparison of Chebyshev and exponential collocation of nodes methods for advection of a square wave in 1D

Results for 4 and 5 nodes per element are visually identical. Exponential collocation shown on the right for 4,5,7 nodes per element. 6 nodes on the left graph and 7 nodes per element on the right graph. Unstable results seen for Lagrange elements.

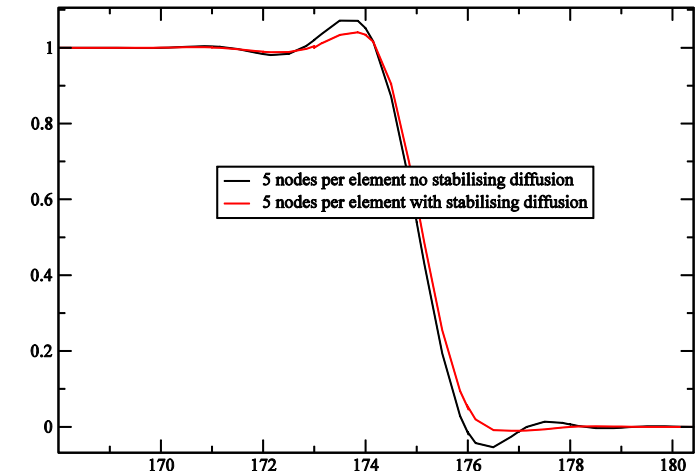


DG high order methods adding stabilising Petrov-Galerkin hyper-diffusion to square wave advection for lumped approach

Here we add the term:

$$\int_E N_i \frac{\partial^2(k(\partial^2 C/\partial x^2))/\partial x^2}{\partial x^2} dV = - \int_E (\partial^2 N_i/\partial x^2) k(\partial^2 C/\partial x^2) dV \\ + \int_{\Gamma_E} n_x N_i k(\partial^2 C/\partial x^2)|_{bc} d\Gamma.$$

We remove the last term in this equation as it's the natural boundary condition to the element. The hyper diffusion coefficient is k is formed as described for the Petrov-Galerkin methods by multiplying by Δx which is the element size. The advantage of using this form of hyper-diffusion is that it is much more scale selective than classical second order diffusion. That is it will try to act on the smaller scale oscillations rather than the larger scale structures. Higher order hyper-diffusion can also be applied in a similar approach to the above.



Within the Petrov-Galerkin method the residual of the equation is estimated from :

$$r = \alpha \Delta x^4 u \partial^5 C / \partial x^5$$

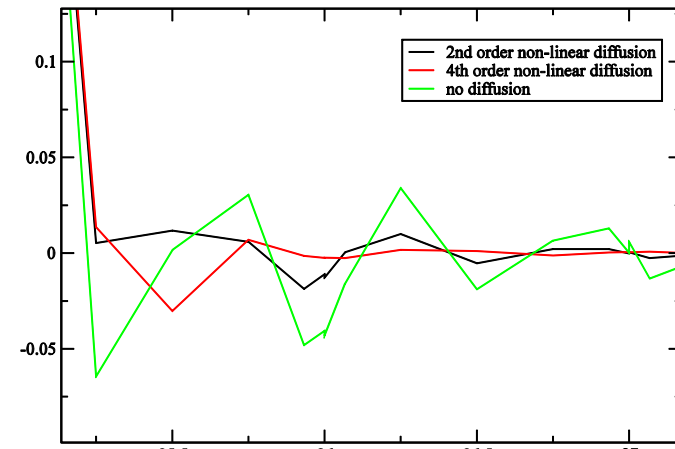
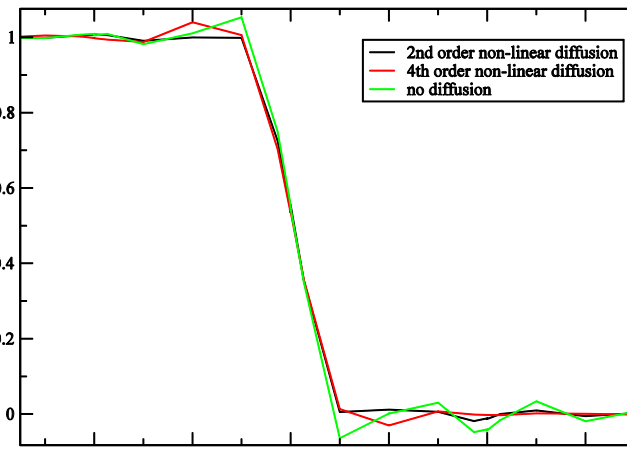
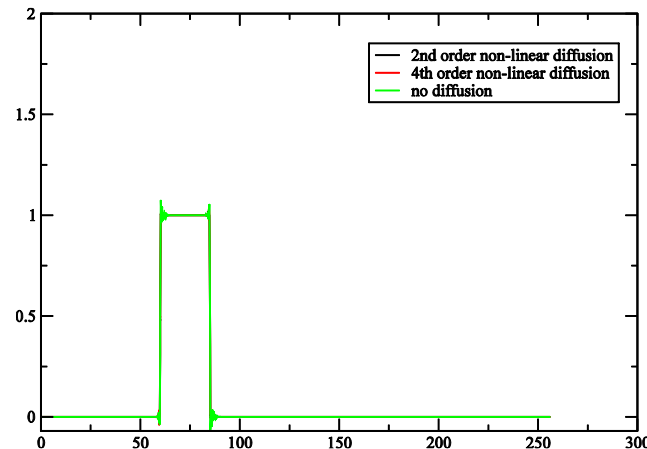
because a 5th order polynomial is used within the element (see right picture) in which α is an O(1) coefficient.

DG 6th order using stabilising 2nd and 4th order non-linear Petrov-Galerkin – comparison of advection of a square wave

We are advecting a square wave and a Gaussian from left to right and with 256 7-node DG elements and using the non-linear Petrov-Galerkin or Galerkin Chebyshev approaches. The residual of the equation is estimated from: $r = \alpha_r (u/\Delta x) \partial^2 C / \partial \zeta^2$ in which ζ is the local coordinate with $\alpha_r=1$. The diffusion coefficient is defined previously as $k_i = \alpha_k |r_i| h_i / (\epsilon_k + (c_{xi}^2 + c_{yi}^2 + c_{zi}^2)^{1/2})$ and the form of the dissipation is for 4th order non-linear Petrov-Galerkin diffusion:

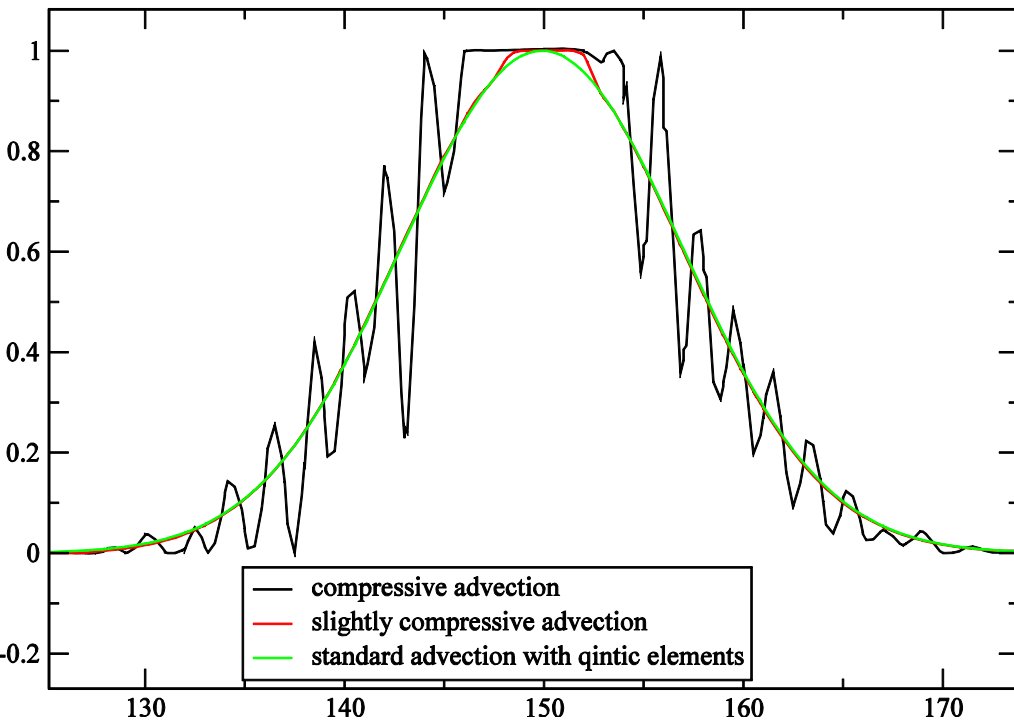
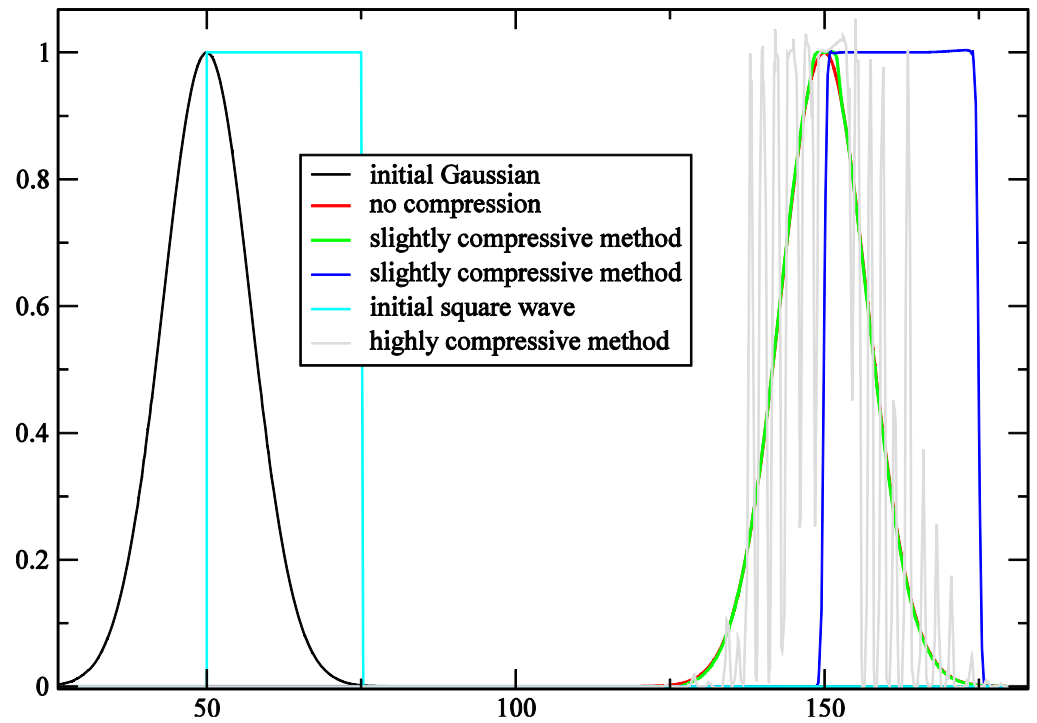
$$\int_E (\partial^2 N_i / \partial \zeta^2) k (\partial^2 C / \partial \zeta^2) dV \text{ with } \alpha_k = 0.0000125 \text{ and for 2}^{\text{nd}} \text{ order diffusion: } \int_E (\partial N_i / \partial \zeta) k (\partial C / \partial \zeta) dV \text{ with } \alpha_k = 0.00125.$$

Notice that both dissipation methods perform well. The 4th order dissipation seems to reduce the persistent oscillations (bottom right) more than the 2nd order dissipation possibly because it works more effectively on the smaller scale oscillations without effecting the larger scale structures.

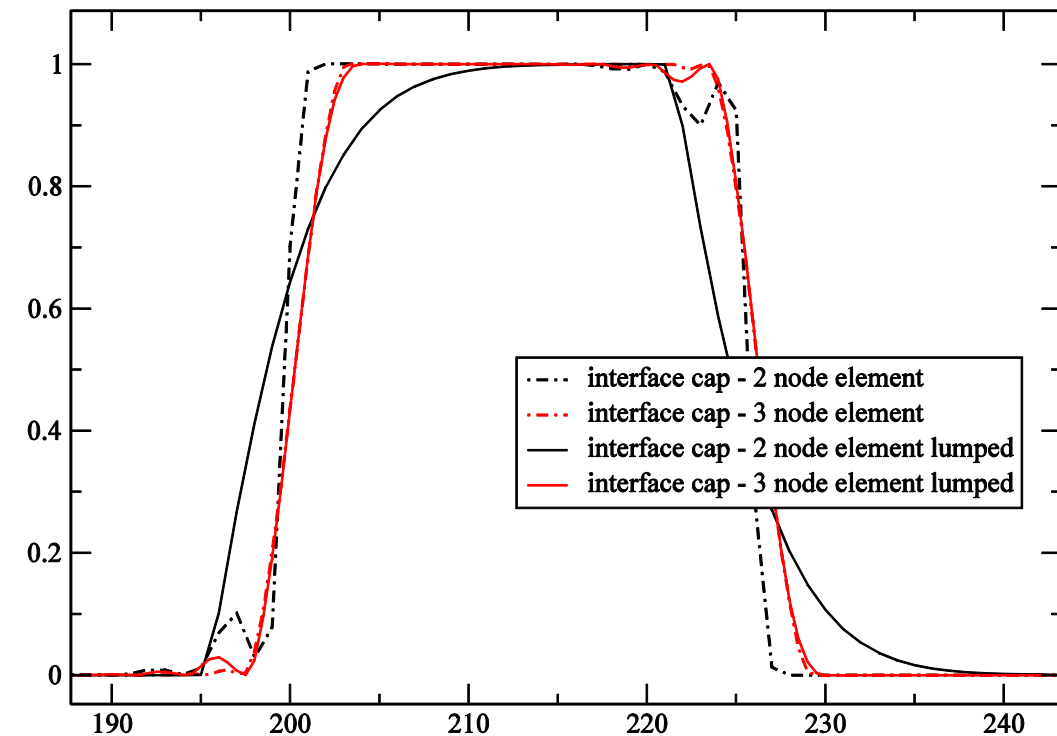
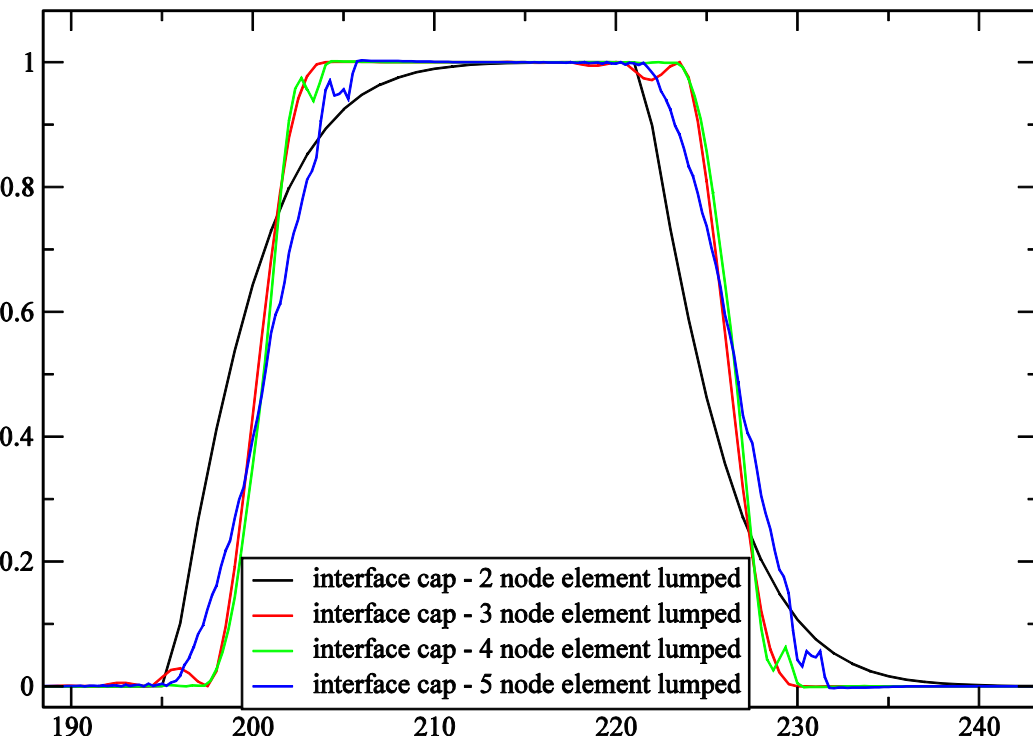


DG 5th order with interface capturing using stabilising second order Petrov-Galerkin and –ve diffusion interface capturing as described previously – comparison of advection of a square wave and a Gaussian

We are advecting a square wave and a Gaussian from left to right and with 256 5-node DG elements (quantic polynomials). Notice that the Gaussian becomes fragmented when the highly compressive interface capturing method is applied. The Petrov-Galerkin stabilisation is applied to to avoid oscillations and the interface capturing Petrov-Galerkin is applied to sharpen the interfaces, see pics.

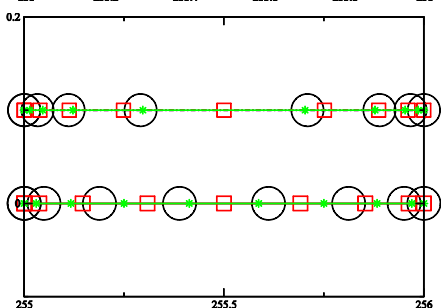
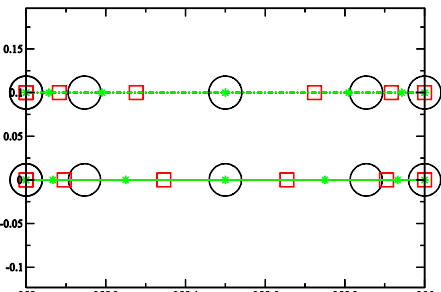
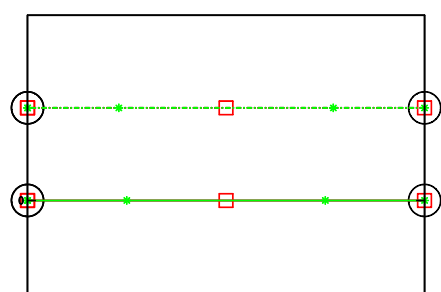
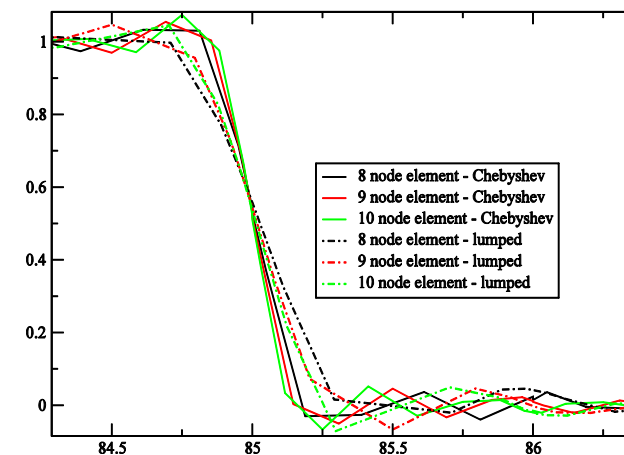
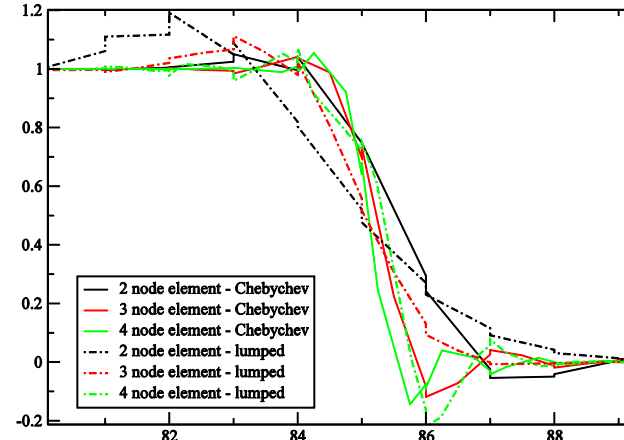
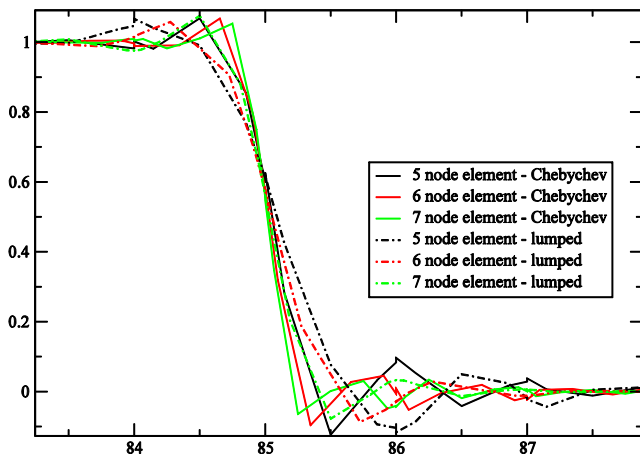
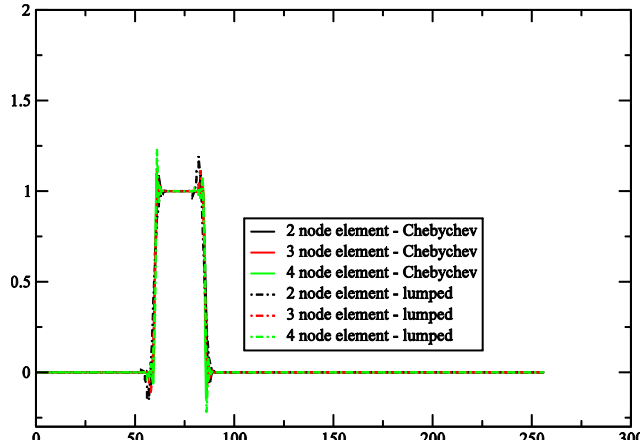


Continuous convolution FEM with interface capturing using Petrov-Galerkin and –ve diffusion interface capturing – comparison of different polynomial orders with lumped mass (left) and lumped and consistent mass approaches (right)



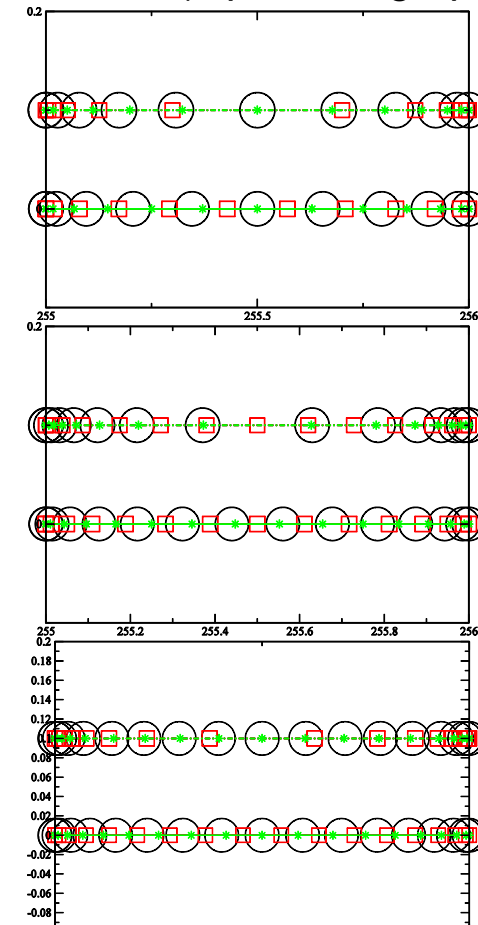
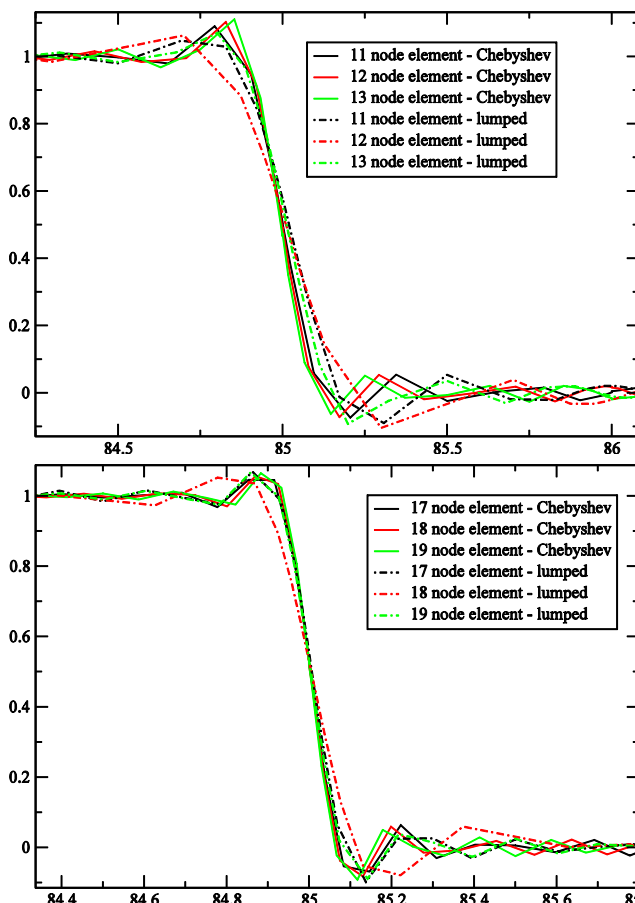
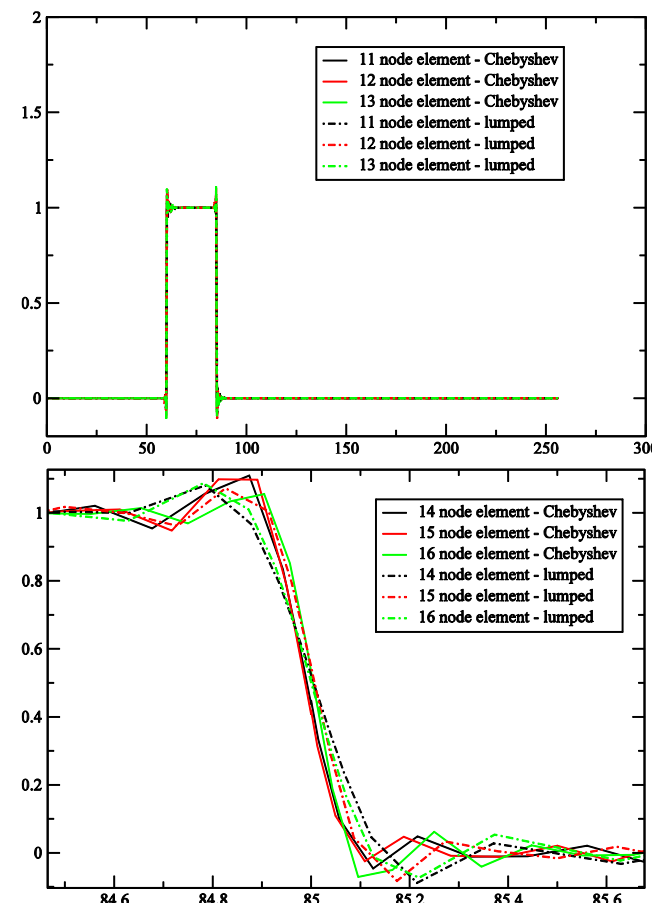
Comparison of Chebyshev-Gauss-Lobatto spectral element and exponential collocation (lumped) DG methods for different numbers of nodes per element

Left 4 graphs: Whole domain for square wave advection, focussed results for 2,3,4 nodes per element and 5,6,7 node per element and 8,9,10 nodes per element. Right 3 graphs: Corresponding collocation points or nodes for Chebyshev (bottom line of graph) and exponential collocation method (top line of each graph).



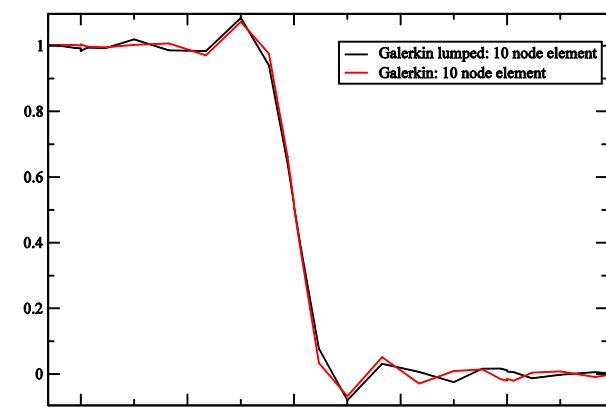
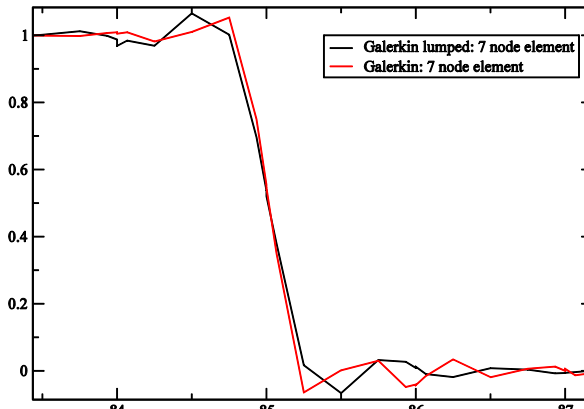
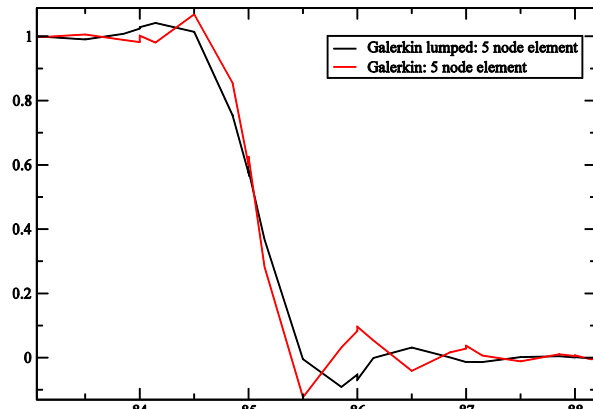
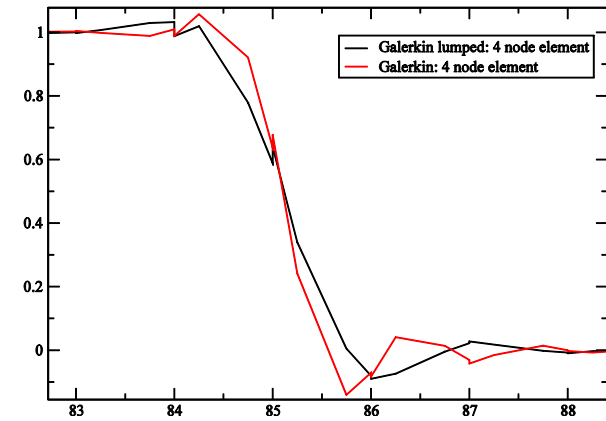
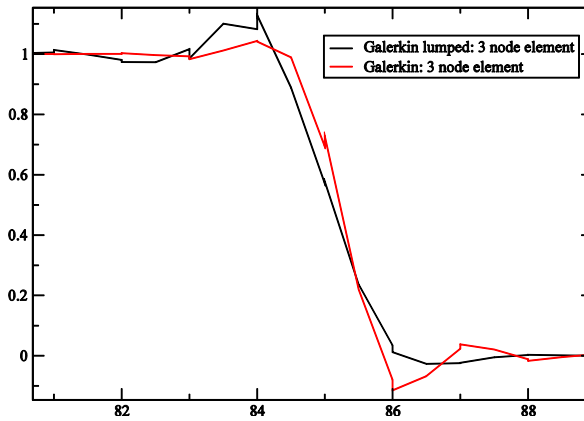
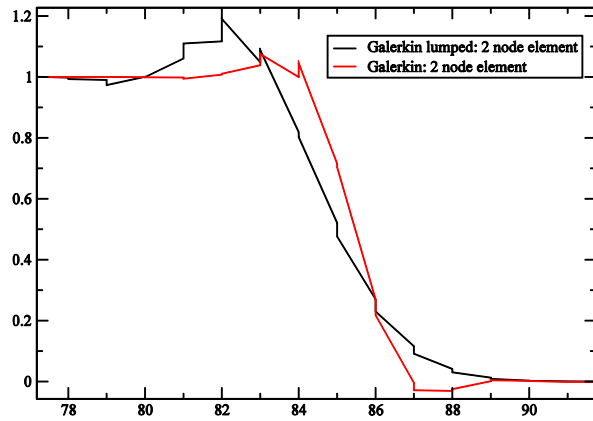
Comparison of Chebyshev-Gauss-Lobatto spectral element and exponential collocation (lumped) DG methods for different numbers of nodes per element (cont)

Left 4 graphs: Whole domain for square wave advection, focussed results for 11,12,13 nodes per element and 14,15,16 node per element and 17,18,19 nodes per element. Right 3 graphs: Corresponding collocation points or nodes for Chebyshev (bottom line of graph) and exponential collocation method (top line of graphs).



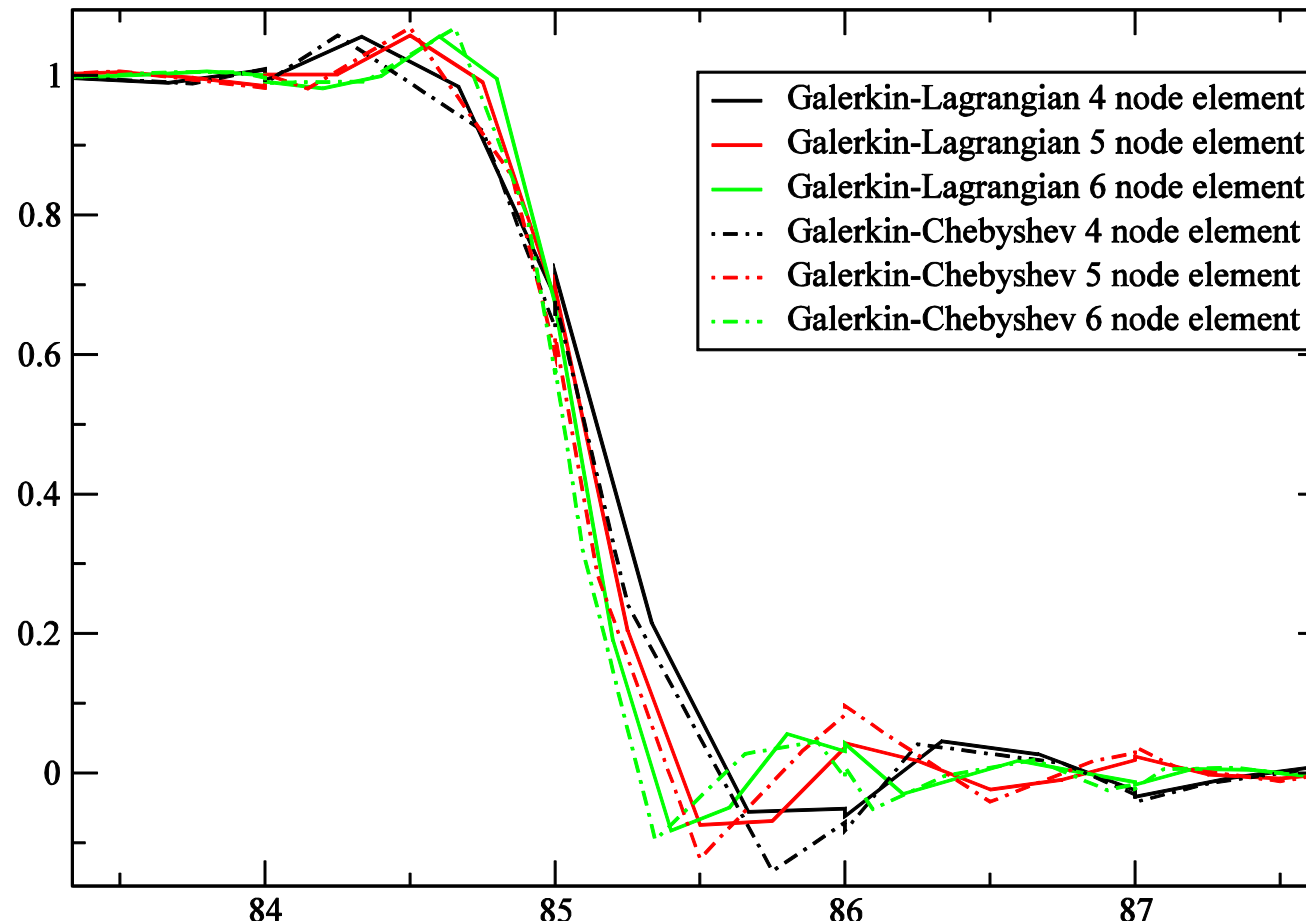
Comparison of Chebyshev-Gauss-Lobatto spectral element with and without row sum lumping

The graphs show that the results get closer to one another as the order of the polynomial (or number of nodes per element) increase.



Comparison of Chebyshev-Gauss-Lobatto spectral DG element with standard Lagrange DG element

The graphs show that the results for 4,5 & 6 node per element. For 2 and 3 nodes per element the results are identical and after 6 nodes per element the Lagrange element becomes highly oscillatory.

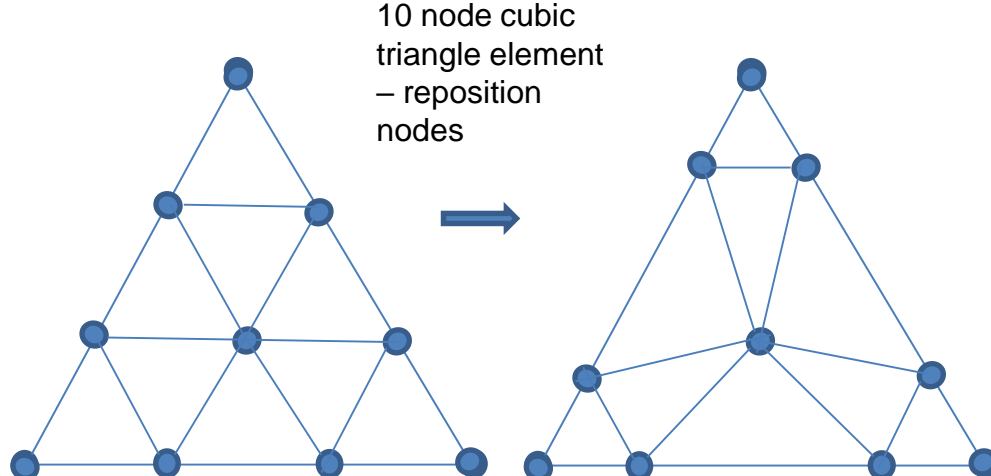


DG triangle and tetrahedral elements with non-uniform node spacing

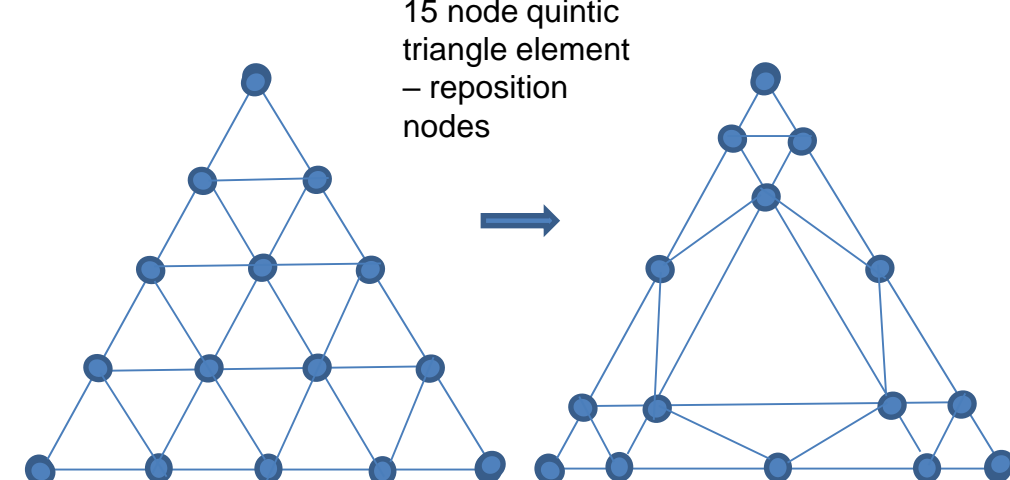
Using the non-uniform spacing of the nodes approach in 1D that is used to suppress oscillations and achieve good accuracy one can extend the approach to triangle and tetrahedral elements as shown below with each edge of the element having the same non-uniform spacing as the corresponding 1D element.

In 2D for triangle elements we have: 10 nodes per element for cubic; 15 for quintic; 21 for 5th order polynomials; 28 for 6th order polynomials.

In 3D tetrahedral elements this becomes: 20 nodes per element for cubic elements; 35 for quintic; 56 for 5th order polynomials; 84 for 6th order polynomial expansions.

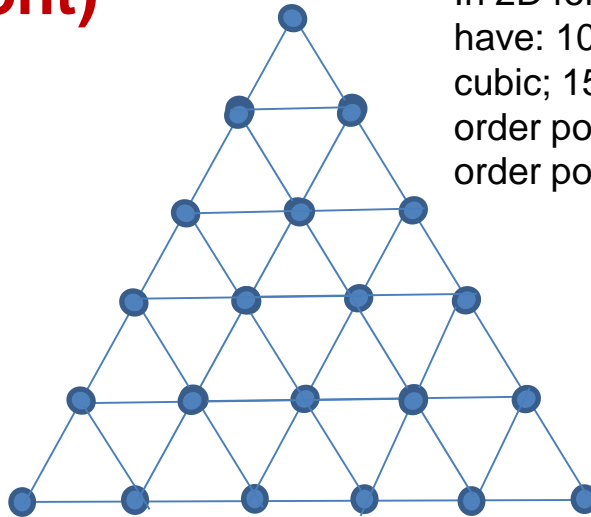


10 node cubic
triangle element
– reposition
nodes

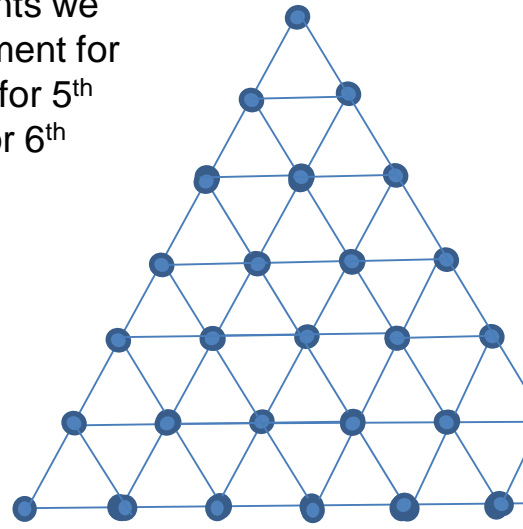


15 node quintic
triangle element
– reposition
nodes

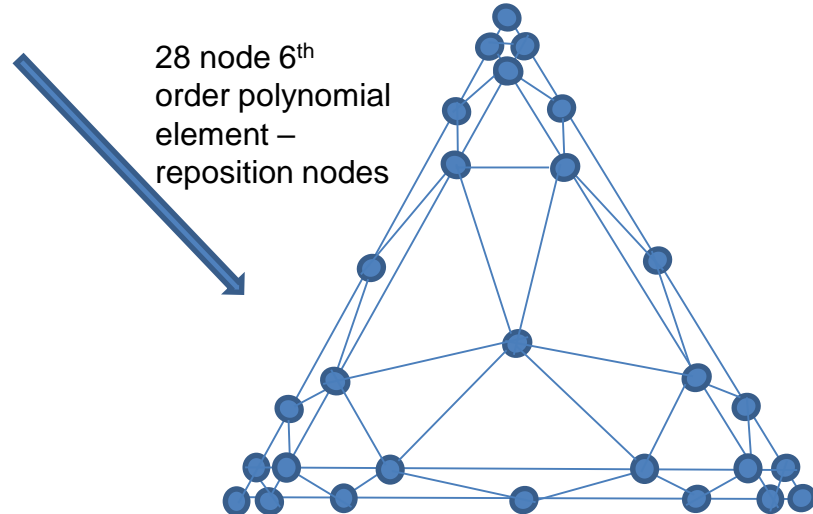
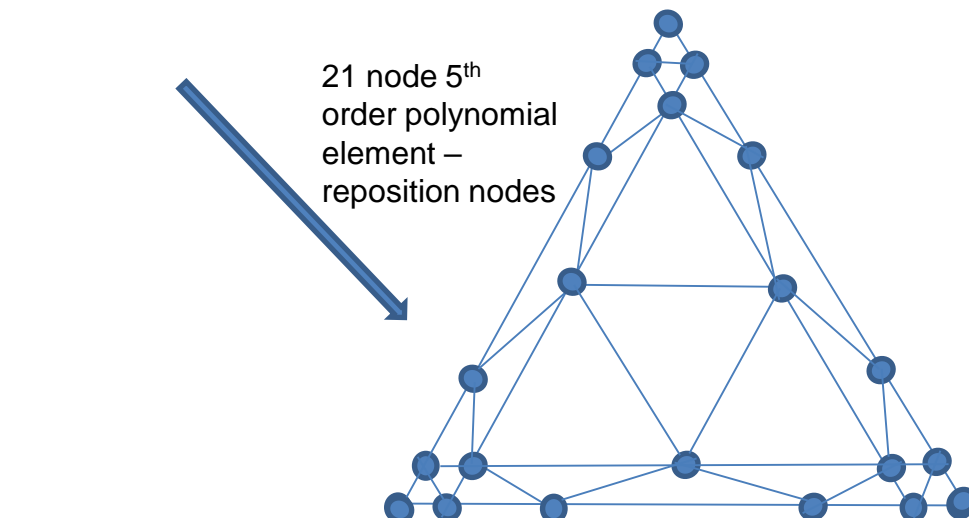
DG triangle and tetrahedral elements with non-uniform node spacing (cont)



In 2D for triangle elements we have: 10 nodes per element for cubic; 15 for quintic; 21 for 5th order polynomials; 28 for 6th order polynomials.



For 2D specifying the position of the nodes along the edges of the elements use the local coordinates that are consistent with the corresponding 1D positioning of the nodes. One can use the lower order elements to position the nodes in super-triangles inside the element e.g. for the 6th order polynomial element it has a 3rd order polynomial element in its centre.



Stokes Flow Solution Method in AI-CFD

Governing eqns ($\mathbf{q} = (u \ v)^T$)

Derived eqns – solution steps:

$$1) \sigma \mathbf{q} - \mu \nabla \cdot \nabla \mathbf{q} + \nabla p = 0,$$

$$2) \nabla \cdot \mathbf{q} + (\mu / \Delta x^2) p - (\Delta x / L) \mu \nabla \cdot \nabla p = (\mu / \Delta x^2) p,$$

in which the term just before $=$ avoids pressure modes and the terms $(\mu / \Delta x^2) p$ are to make it easier to apply block Jacobi smoothing.

Use Harmonic average of σ in multi-grid.

Also in multi-grid method form a block Jacobi relaxation which couples u, v, w, p and thus the ANN channel weights for this are the inverse of the associated block.

Multi-phase Darcy Flow Solution Method in AI-CFD

Governing eqns ($\mathbf{q}_1^n = (u_1^n \ v_1^n \ w_1^n)^T$) for phase 1 and ($\mathbf{q}_2^n = (u_2^n \ v_2^n \ w_2^n)^T$) for phase 2 where n is the time level and l is the iteration level e.g. ($\mathbf{q}_1^{n+1})^l$). The derived eqns solution steps are:

- 1) $\sigma_1^l(\mathbf{q}_1^{n+1})^{l+1} + d_{1q}^l(\mathbf{q}_1^{n+1})^{l+1} - \nabla \cdot \mathbf{k}_{1ql} \nabla (\mathbf{q}_1^{n+1})^l + \nabla (p^{n+1})^l = d_{1q}^l(\mathbf{q}_1^{n+1})^l ,$
- 2) $\sigma_2^l(\mathbf{q}_2^{n+1})^{l+1} + d_{2q}^l(\mathbf{q}_2^{n+1})^{l+1} - \nabla \cdot \mathbf{k}_{2ql} \nabla (\mathbf{q}_2^{n+1})^l + \nabla (p^{n+1})^l = d_{2q}^l(\mathbf{q}_2^{n+1})^l ,$
- 3) $\nabla \cdot \varphi (c^{n+1} \mathbf{q}_1^{n+1} + (1-c^{n+1}) \mathbf{q}_2^{n+1})^l + d_p^l (p^{n+1})^{l+1} - \nabla \cdot \mathbf{k}_p^l \nabla (p^{n+1})^l = d_p^l (p^{n+1})^l ,$
- 4) $((c^{n+1})^{l+1} - c^n)/\Delta t + d_c^l (c^{n+1})^{l+1} - \nabla \cdot \mathbf{k}_c^l \nabla (c^{n+1})^l = - \nabla \cdot ((\mathbf{q}^{n+1})^l (c^{n+1})^l) + dcl(c^{n+1})^l ,$

with $d_{1q}^l = k_{1q}^l / (\Delta x)^2$, $d_{2q}^l = k_{2q}^l / (\Delta x)^2$, $d_p^l = (\sigma_1^l + \sigma_2^l) / (\sigma_1^l \sigma_2^l (\Delta x)^2) + k_p^l / (\Delta x)^2$,

$d_c^l = (\|(\mathbf{q}_1^{n+1})^l\|_2 / \Delta x) + kcl / (\Delta x)^2$ in which the term involving kpl avoids pressure modes and the terms involving d_{1ql} , d_{2ql} , dpl , d_c^l are to make it easier to apply block Jacobi smoothing and φ is the porosity. Use Harmonic average of σ in multi-grid. Also in multi-grid method one could form a block Jacobi relaxation which couples u,v,w,p and thus the ANN channel weights for this are the inverse of the associated block. However, this is often not necessary and also since the gradient operators, using central discretisations) often have zero's on the diagonal this may not help with the solution method.

For eqns 1,2 & 3 above we use the diffusion from: $k_{1i} = \alpha_{k1} |R_i| h_i / (\epsilon_k + (|C_{xi}| + |C_{yi}| + |C_{zi}|) / 3)$, and $k_i = \min\{k_{maxi}, k_{1i}\}$ for equation 4 we apply the optimal Petrov-Galerkin method involving mixing 2 schemes.

CFD DG CNN filters – Pressure/Diffusion operator with interior penalty function method

For the diffusion operator $\nabla^2 p$ which we might solve for pressure, say, have a 3x3 but with a stride of 2. Need for of these in 2D rectangular elements and 8 in 3D.

For multi-grid collapse to element the 4 variables in each element in 2D. Thus getting the same stencil used for the continuous FEM.

Apply each filter by missing out every other node in each direction (stride =2).

The green square, in the figure, shows the stencil associated with local node 1 – this has a 3x3 stencil. Diffusion discretisation:

$$\int_{V_e} N_i \nabla^2 p \, dV = - \int_{V_e} (\nabla N_i) \cdot (\nabla p) \, dV + \int_{\Gamma_e} N_i n \cdot (\nabla p) \, d\Gamma$$

In which n is the normal to the element. The filter then becomes for local node 1 using the interior penalty function method:

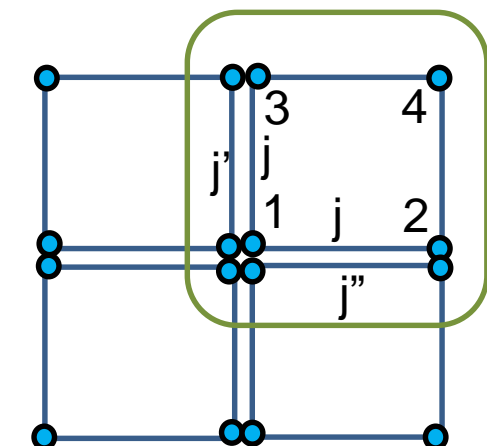
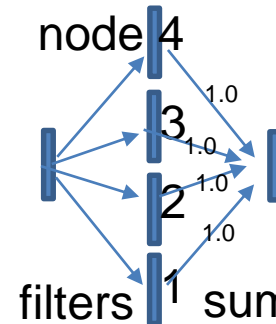
$$A_{\text{filtD1}_j} = - \int_{V_e} (\nabla N_1) \cdot (\nabla N_j) \, dV - \int_{\Gamma_e} N_1 \lambda N_j \, d\Gamma ;$$

$$A_{\text{filtD1}_{j'}} = \int_{\Gamma_e} N_1 \lambda N_{j'} \, d\Gamma ; A_{\text{filtD1}_{j''}} = \int_{\Gamma_e} N_1 \lambda N_{j''} \, d\Gamma$$

in which $\lambda = 2/\Delta x$.

This is repeated for the 4 local nodes as shown in diagram at bottom to get all filters

$$A_{\text{filtD1}}, A_{\text{filtD2}}, A_{\text{filtD3}}, A_{\text{filtD4}} .$$



CFD DG CNN filters – For advection discretization $\mathbf{u} \cdot \nabla C$ or for non-linear momentum

Use two versions of each component of the derivative ∇ – one for positive and one for negative direction (e.g. u_1) of advection $\mathbf{u} = (u \ v)^T$. in which subscript 1 indicates its for node 1. The basic idea is to form the filter centred around node 1, say, depending on if u_1 is positive or negative and then pre-multiply the resulting filter by u_1 to form a discretisation of $u_1 \partial C / \partial x$. That is:

$u_1 A_{\text{filt}u1} = u_1 (H(u_1) A_{\text{filt}u1}^{\text{right}} + H(-u_1) A_{\text{filt}u1}^{\text{left}})$ in which $A_{\text{filt}u1}^{\text{right}}$, $A_{\text{filt}u1}^{\text{left}}$ are filter associated with up and down advection (they contain the same volume integrals) and $H(H(a)=1 \text{ if } a \geq 0 \text{ otherwise } 0)$ is the heavy side function.

Similarly for v_1 :

$$v_1 A_{\text{filt}v1} = v_1 (H(v_1) A_{\text{filt}v1}^{\text{up}} + H(-v_1) A_{\text{filt}v1}^{\text{down}})$$

The discretisation for the horizontal derivative is:

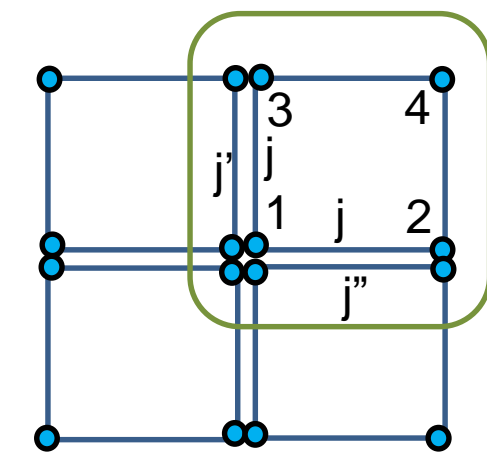
$$\int_{V_e} N_1 \mathbf{u} \cdot (\nabla C) dV \approx u_1 \int_{V_e} N_1 \partial C / \partial x dV + v_1 \int_{V_e} N_1 \partial C / \partial y dV$$

Thus $\int_{V_e} N_1 \partial C / \partial x dV$:

$$A_{\text{filt}u1j}^{\text{right}} = \int_{V_e} \partial N_1 / \partial x N_j dV ; A_{\text{filt}u1j'}^{\text{right}} = \int_{V_e} N_1 n_x N_{j'} dV \text{ with } n_x = -1;$$

$$A_{\text{filt}u1j}^{\text{left}} = \int_{V_e} \partial N_1 / \partial x N_j dV + \int_{V_e} N_1 n_x N_j dV$$

and similarly for the vertical to form $A_{\text{filt}v1}^{\text{up}}$ & $A_{\text{filt}v1}^{\text{down}}$ and for all the other local nodes 2,3,4 to produce $A_{\text{filt}u2}, A_{\text{filt}v2}, A_{\text{filt}u3}, A_{\text{filt}v3}, A_{\text{filt}u4}, A_{\text{filt}v4}$.



DG CNN filters – How to use stride=2 for the discretization of advection and diffusion

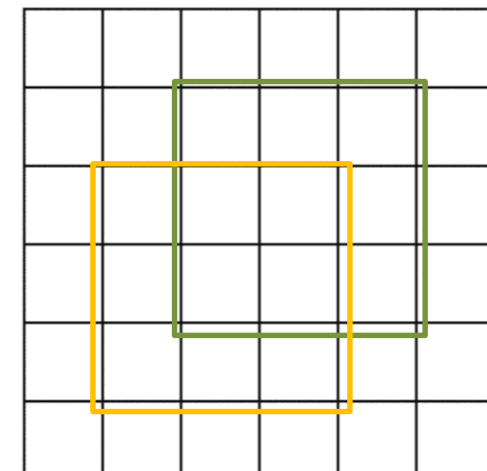
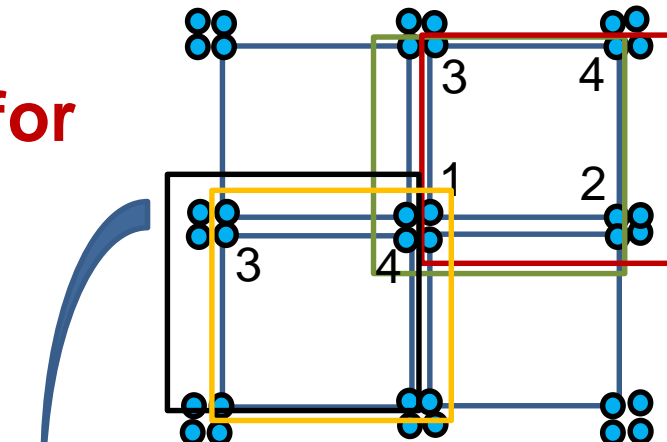
– need 4 channels or filters in 2D one for each local node

Nodes inside green box shows filter for local nodes 1, red for nodes 2, black 3, yellow 4.

Bottom diagram shows how the 4 DG elements are mapped to a regular grid where a 3x3 filter is placed over the domain (an example is shown in green which corresponds to the green filter shown in the top diagram) in order to form a CNN that can do DG discretization on a structured grid.

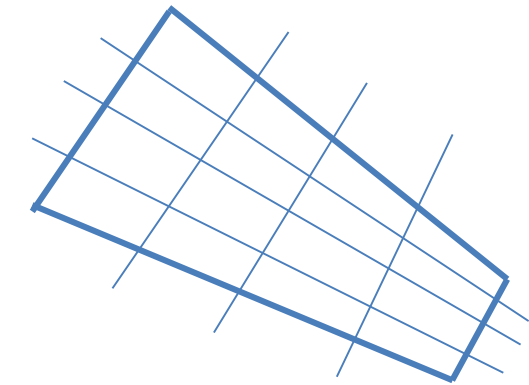
For advection-diffusion the filter for node 1 (green) is:

$A_{filt1} = kA_{filtD1} + u_1 A_{filtu1} + v_1 A_{filtv1}$ in which k is diffusion and similarly to produce all filters $A_{filt1}, A_{filt2}, A_{filt3}, A_{filt4}$.



CFD DG CNN filters – Distorted blocks or unstructured meshes

For local node 1, say, need a 2 filters (for advection to define incoming and outgoing information) and 1 filter for diffusion for each face touched by local node 1. That is 2 faces in 2D and 3 faces in 3D. For advection need 2 filters in 2D (associated with each advection direction) in 3D for the volume of each element and 3 filters in 3D. Repeat for each of the local nodes.



CFD DG CNN filters – Conservative advection $\nabla \cdot uC$ rather than $u \cdot \nabla C$

This is similar to the previous non-conservative approach (using the same filters) to discretising but a rapid way to do this is simply operate on the product uC , directly, rather than C . When one needs to decide if we have to use incoming or outgoing direction information on surfaces associated with node i , say, then use the average velocity $0.5(u_i + u_{i'})$ to determine this in which i' is the node on the other side of the face and use the normal n to the normal to the face to help determine if we have incoming or outgoing information and also could advect with this velocity $0.5(u_i + u_{i'})$ across faces.

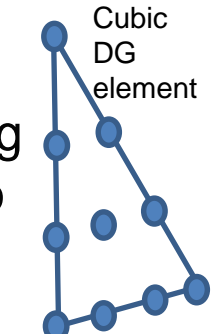
High order DG CNN filters with or without distorted blocks or unstructured meshes using 1D CNNs or 1D structured weights

One can order the nodes along a line element wise so that the element nodes are all grouped together. This means that a N filters with a structured compact representation can be applied to all the elements simultaneously in which N is the number of local nodes. This means that it will be just as fast as the 1D CNN approach. The coupling between the elements is then where the indirect addressing occurs and a graph neural network is needed for this coupling. However, mass lumping of the surface integrals can be used so that the sparsity of this coupling could be very limited.

In addition, further reductions in the indirect addressing may be possible taking into account the structure of the surface integrals across neighbouring elements.

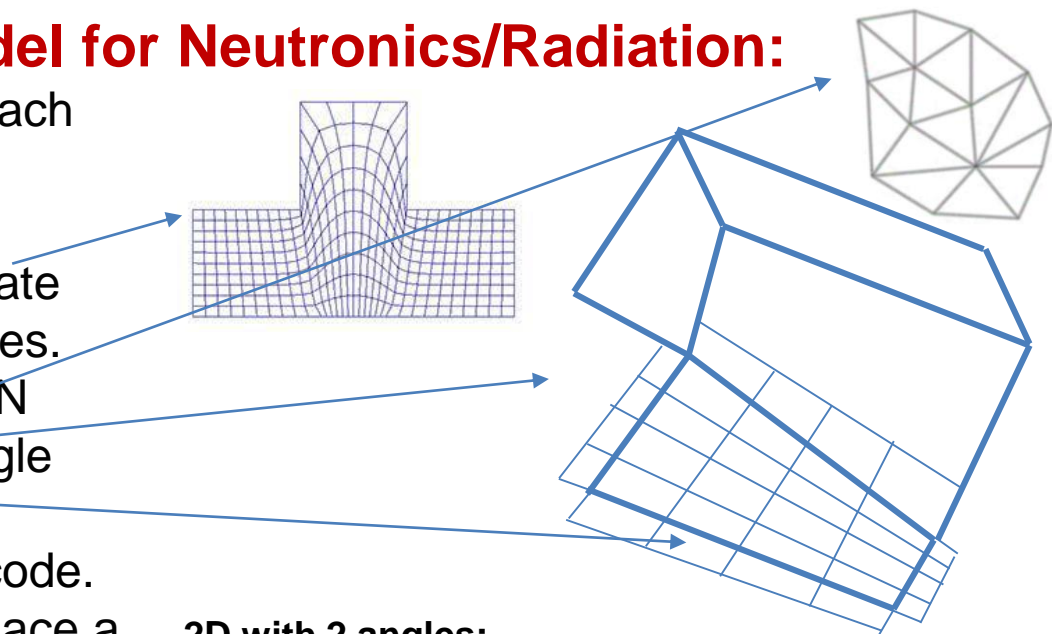


For the DG multi-grid method one can use a Space Filling Curve (SFC) within each element and collapse the nodes, for algebraic multi-grid method, in pairs along the SFC. When one finally has one variables within each element then one needs to resort to a fully unstructured representation (for an unstructured mesh) but an SFC multi-grid method can then be applied at this level to achieve good solver scaling.

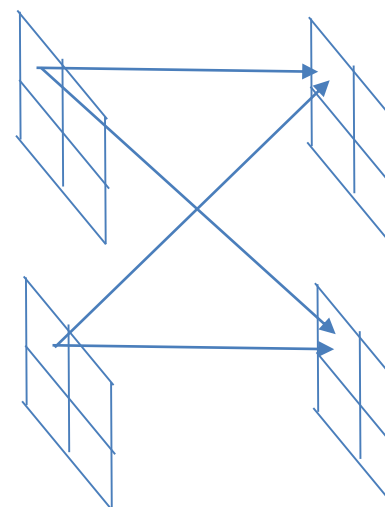


Matrix Free Boltzmann Transport Model for Neutronics/Radiation:

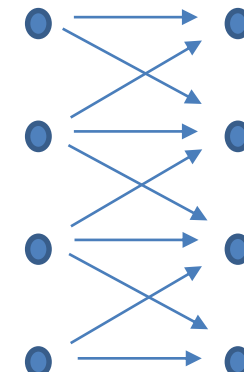
- 1) Have a single filter for advection layer for each SN direction to make method matrix free.
- 2) Each SN direction has a channel.
- 3) For distorted blocks have filters that interpolate between different orientations & element shapes.
- 4) Use Multi-Grid in DG Cartesian Space and SN angle. Collapse each structured block to single cell/node. Halo cells/DG nodes still structured.
- 5) Use block unstructured e.g. structured DG code.
- 6) For linear DG in 1D have 2 channels and replace a_{ii} with the inverse of the element block diagonal matrix. Similarly 3D have 8 channels.
- 7) Start simple with 1 block and 1 direction.
- 8) For scattering removal. Could have a filter for each material in layer or have different weights of the connections – see pics bottom right.
- 9) If massive number of angles can efficiently have a single element in a structured block.



2D with 2 angles:



CNN Layers in 1D:
Advection/absorption



Boltzmann Details: Formation of SN DG Filters:

- 1) For structured block that is not distorted then a single filter is enough to represent $\Omega \cdot \nabla \Phi$ for each SN direction as each sub-element is the same.
- 2) For distorted blocks have form filters from spatial tables for each element and face of elements.
- 3) The filters for 3D DG 8 node bi-linear elements have 3 inner element contributions for each component of ∇ . These are multiplied by Ω to achieve a discretization of $\Omega \cdot \nabla \Phi$ internal to an element. Each of these 3 filters has 8x8 values operating on the nodes of the element.
- 4) For the 3D DG 8 node element there for each face there is an incoming and an outgoing contribution filter set. Each of these has 3 components (filters) and the filters are each of size 4x4. There are thus 8 of these two surface filters (one for each element face) and thus there are 8 times 2 times 3 surface (=48) filters to represent the surface integrals.
- 5) For SN in angle multi-grid formation and using CNN then choose SN directions so as to map to a square grid.

Boltzmann Details: Solution Free Boltzmann transport – the solution vector too large to fit on computer e.g. for some GPU or AI computers say

The coarse grid in angle equation is:

$$A \Phi + B \Psi = s_\Phi$$

The fine grid equation is:

$$C \Phi + D \Psi = s_\Psi$$

In which Φ is the coarse grid in angle solution vector (e.g. scalar flux or low SN order angular flux) and Ψ is the fine SN angular vector. D is the discretized transport operator. The coarse grid in angle equation could be from diffusion theory (DSA) or low order SN.

Combining these the coarse grid equation becomes:

$$(A - B D^{-1} C) \Phi = s_\Phi - B D^{-1} s_\Psi$$

The basic idea is only to use the coarse (in angle solution) vector Φ and never actually form the whole solution vector Ψ or in the above $D^{-1} C \Phi$. Instead each direction is solved for with D^{-1} and is discarded after operating on B .

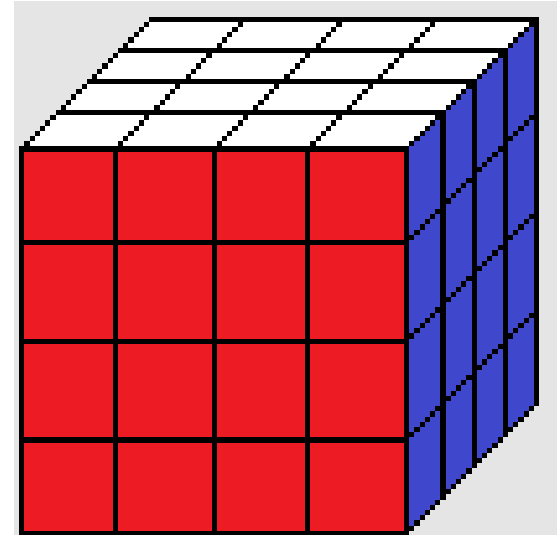
A multi-grid in angle and space can be applied to the SN in angle discretized system.

For time dependent one can only resolve the low order SN solution in time. For SN only include transport and total cross section terms in matrix D put other terms into the sources.

Boltzmann Details: Discretization in SN Angle and Cartesian Space on Structured Grids

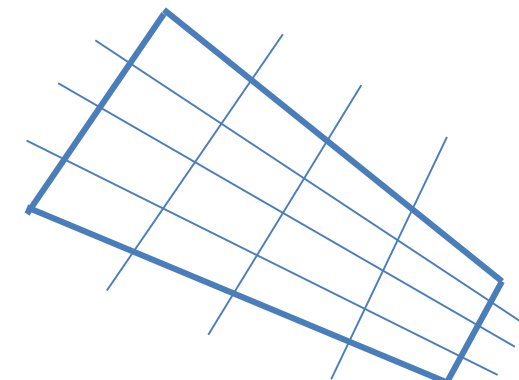
Discretization in SN Angle:

- 1) Use hexahedra on unit sphere and then put a rectangular grid across each square. See figure.
- 2) Have a power of 2 of the number of cells across on this rectangle e.g. 4 in the figure.
- 3) Each cell then represents an SN direction.



Discretization in Cartesian space:

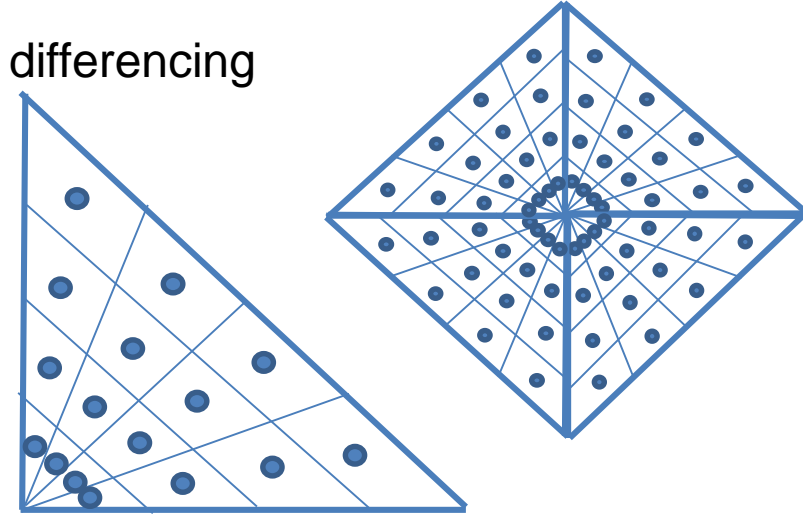
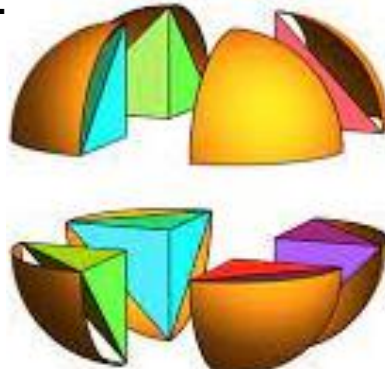
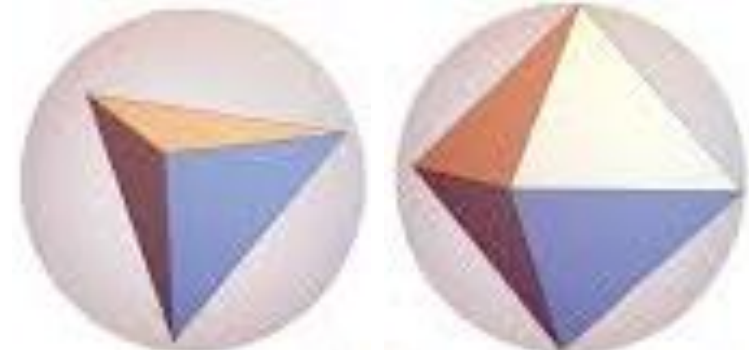
- 1) Use DG in space with $N \times N$ elements and N is a power of 2 – needed for multi-grid method. See figure bottom right in which $N=4$.
- 2) For 4-node DG linear 2D element have 4 convolutional channels. One for each node.



Boltzmann Details: Discretization in SN Angle using collapsed nodes to help form 5D (space and angle) multi-grid

Discretization in SN Angle:

- 1) Use octahedron on unit sphere (bottom left pictures) and then put a rectangular grid across each triangle face with a collapsed edge/node (figure bottom right on a 4x4 grid as well as 4 grids put together to form grid of the top of the sphere). Then place each octant together to form the final grid across the unit sphere (top right).
- 2) Have a power of 2 of the number of cells across on this rectangle e.g. 4 in the figure.
- 3) Each cell then represents an SN direction.
- 4) Each of the 8 faces has separate filters for upwind or DG differencing because the directions are similar.



Boltzmann Details: Convolutional Filters in SN Angle and Cartesian Space on Structured Grids

- 1) Assuming 1D in space and in angle (similar in multi-dimensions) have a different filter for each SN direction but same across space. See figure.
- 2) Add discretization filters together to form coarser filters.
- 3) In angle just add them together to form coarser SN discrete equations.
- 4) In Cartesian space use the prolongation and restriction matrices to form coarse discrete equations.

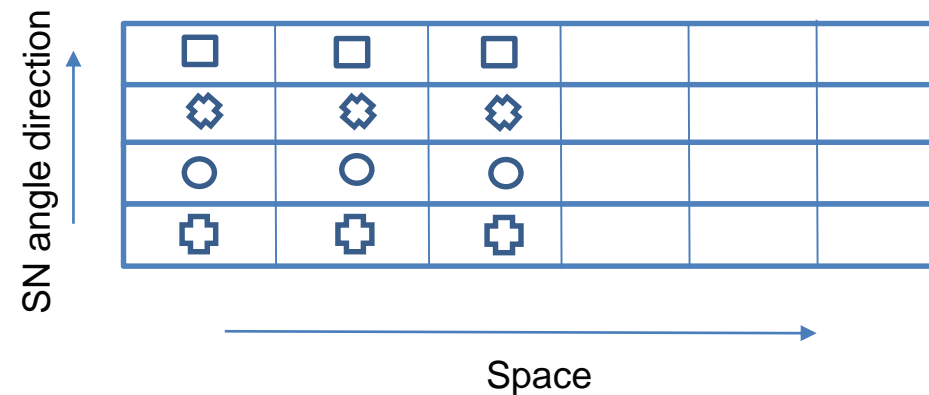


Figure: Space - SN angle CNN filters

Boltzmann Details: DG Prolongation and Restriction Matrices

Fine to coarse grid equation is:

$$\int N_i^c (\Psi_c - \Psi_f) dV; \quad \Psi_c = \sum N_j^c \Psi_{cj}; \quad \Psi_f = \sum N_j^f \Psi_{fj};$$

$$M^c \Psi_c = N^{cf} \Psi_f;$$

$$\text{Thus: } \Psi_c = (M^c)^{-1} N^{cf} \Psi_f = P^{cf} \Psi_f.$$

Course to fine grid:

$$\int N_i^f (\Psi_f - \Psi_c) dV;$$

$$M^f \Psi_f = N^{fc} \Psi_c;$$

$$\Psi_f = (M^f)^{-1} N^{fc} \Psi_c = P^{fc} \Psi_c.$$

Therefore the fine grid matrix equation is: $A^f \Psi_f = s_f$.

The coarse matrix: $P^{cf} A^f P^{fc} \Psi_c = P^{cf} s_f = s_c$.

Or: $A^c \Psi_c = s_c$.

The filters are similarly operated on by these prolongation and restriction matrices: P^{fc} , P^{cf} .

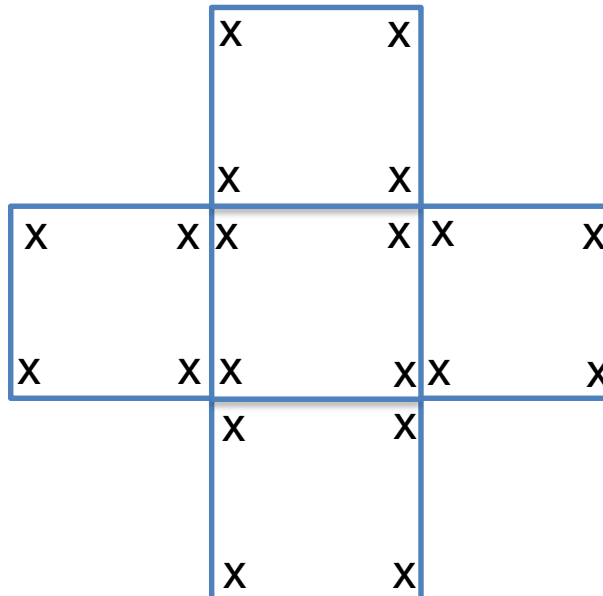
Boltzmann Details: Structured mesh linear DG CNN filters in 2D

Suppose ψ^p is the SN direction angular flux with angle Ω^p and $\psi^p = \sum N_j \psi_j^p$.

The filter is the entire discretization centred on the inner element in the figure in which DG nodes are represented by x.

The filter is defined through the discretization for element e at the centre of figure:

$$\begin{aligned} & -\int_{V_e} (\nabla N_i) \cdot \Omega^p \psi^p dV + \int_{\Gamma_e(\Omega \cdot n < 0)} N_i \Omega^p \cdot n \psi_{bc}^p d\Gamma + \int_{\Gamma_e(\Omega \cdot n > 0)} N_i \Omega^p \cdot n \psi^p d\Gamma \\ & + \int_{V_e} N_i \sigma^p \psi^p dV = s^p \end{aligned}$$



Test cases to demonstrate approach – simple to complex:

- 1) Time dependent 2D advection diffusion equation on structured grid with central difference discretization. (done)
- 2) 2D Burgers equation discretization and solution with non-linearity built into network. (done)
- 3) Multi-grid on 2D advection diffusion equation. (done)
- 4) Discretize fluids equation with central difference and projection method Poisson equation for pressure so can use an A grid. (done)
- 5) 2D Burgers equation to demonstrate adjoint.
- 6) Differentiate fluids equation to find adjoint by defining activation functions.
- 7) Discretize Boltzmann Transport equation with 4D multi-grid on a structured grid – start with diamond differencing then DG in 2D and with SN.
- 8) Solve OPS/2 test cases: convection test case.
- 9) Parallel for structured grid advection-diffusion, fluids and AI model. (done)
- 10) Unstructured and semi-structured mesh multi-grid based on space-filling curves or Earth mover distance optimization (see unstructured mesh slides).

Demonstrations:

- 1) **South Ken air flow** 34 Billion structured mesh nodes $(1024^8)^2 \cdot 512 = 34$ Billion nodes (4km x 5km x 256m) with 0.5m resolution. Have a smaller 4.3 Billion cell problem with a 1m resolution. Add green/blue/grey physics.
- 2) **Multi-phase:** i) collapsing water coln $1024^3 = 1.B$ nodes. ii) 1km long 7cm diameter pipe with $64 \times 64 \times (2^{18} = 262144) = 1.074$ Billion nodes or $128 \times 128 \times (2^{19}) = 8.7B$ nodes. iii) Fluidised beds.
- 3) **Train model & ventilation.** Train carriage dimensions 3m x 3m x 22.5m with 1cm resolution $= 300 \times 300 \times 2250 = 202.5M$ nodes or for multi-grid convenience $256 \times 256 \times 2048 = 134M$ nodes. And 0.25cm (2.5mm) resolution gives $1024 \times 1024 \times (2048^4) = 8.6$ Billion nodes.
- 4) **Flow past loads of cylinders** (porous media): i) Stokes flows (a coupled u-p solver) ii) Turbulent flow. ~1.2Billion nodes.
- 5) **Turbines.**

Nuclear:

- 5) Transport DG RT reactor model.
- 6) Coupled transport and single phase model.
- 7) Coupled Solution criticality 50cm x 50cm x 2m domain with 1mm resolution. $500 \times 500 \times 2000 = 0.5$ Billion nodes. With 0.33mm resolution =15 Billion nodes. Need 1D Rayleigh Taylor and nucleation model.
- 8) Boiling model with phase change with 1mm resolution in nuclear reactors.

Demonstrations (cont) and developments:

Unstructured meshes:

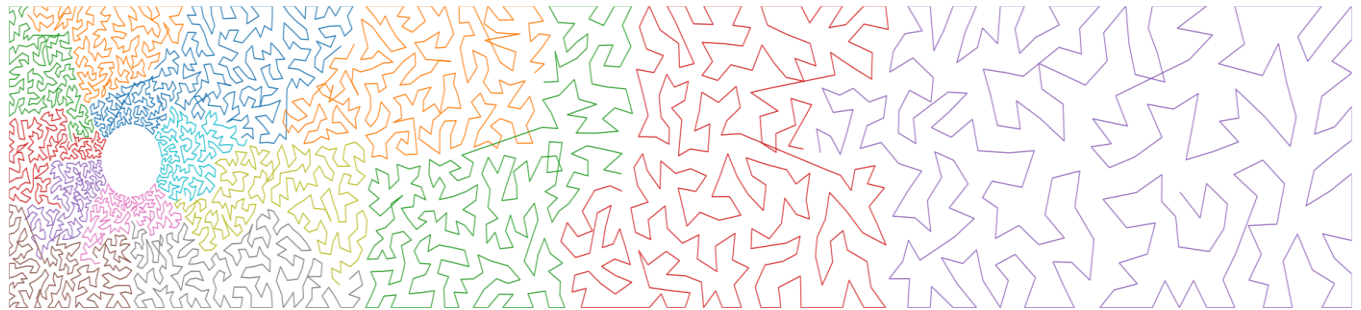
- 9) **Reservoir model** with explicit wells and 20 Billion DG nodes (10^{12} nodes aim).
- 10) **Turbines** with focussed resolution.
- 11) **Shock flows** past aircraft.
- 12) **Solid mechanics model and coupling with fluids.**
- 13) **Cloud formation above city** with coupled RT and Fluids.
- 14) **Environmental: Weather, Ocean and flooding models.**

Main developments:

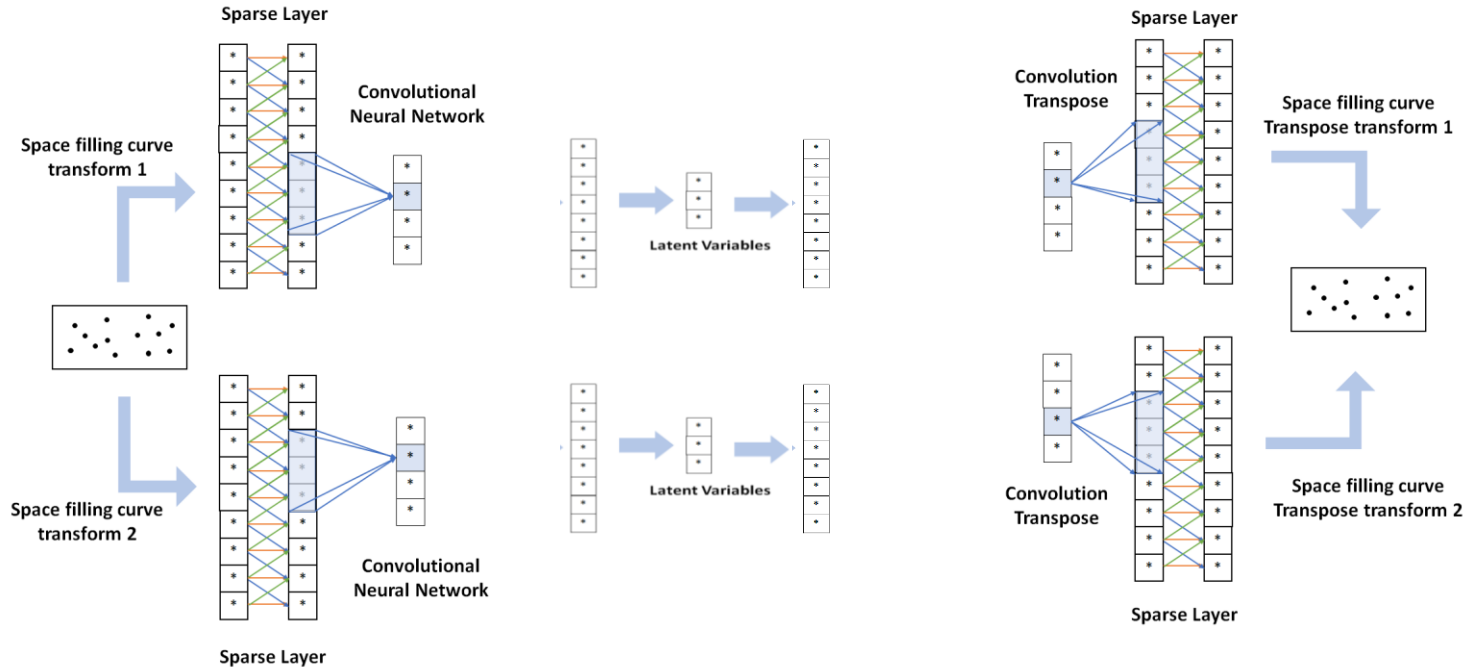
- 1) Structured/orthogonal mesh (done) still needs DG.
- 2) Semi-structured.
- 3) Fully unstructured FEM (done).
- 4) Rapid DG moderate order with tetrahedral meshes unstructured mesh model.
- 5) Mesh adaptivity i) AI mesh generation ii) 4D mesh adaptivity with time slabs allowing Lagrangian accuracy and variable space-time resolution.
- 6) Solid-fluids coupling and solids model.
- 7) Coupling with SGS models within each element with enhanced resolution.
- 8) Static condensation so less needs to be stored.
- 9) On the fly compression.
- 10) Digital twins: DA, UQ, Optimisation.

Unstructured mesh CNN - Multi-dimensional convolutional methods – extension of 1D Space Filling Curve (SFC) method

Space Filling Curve going through all the nodes of an unstructured mesh (right)



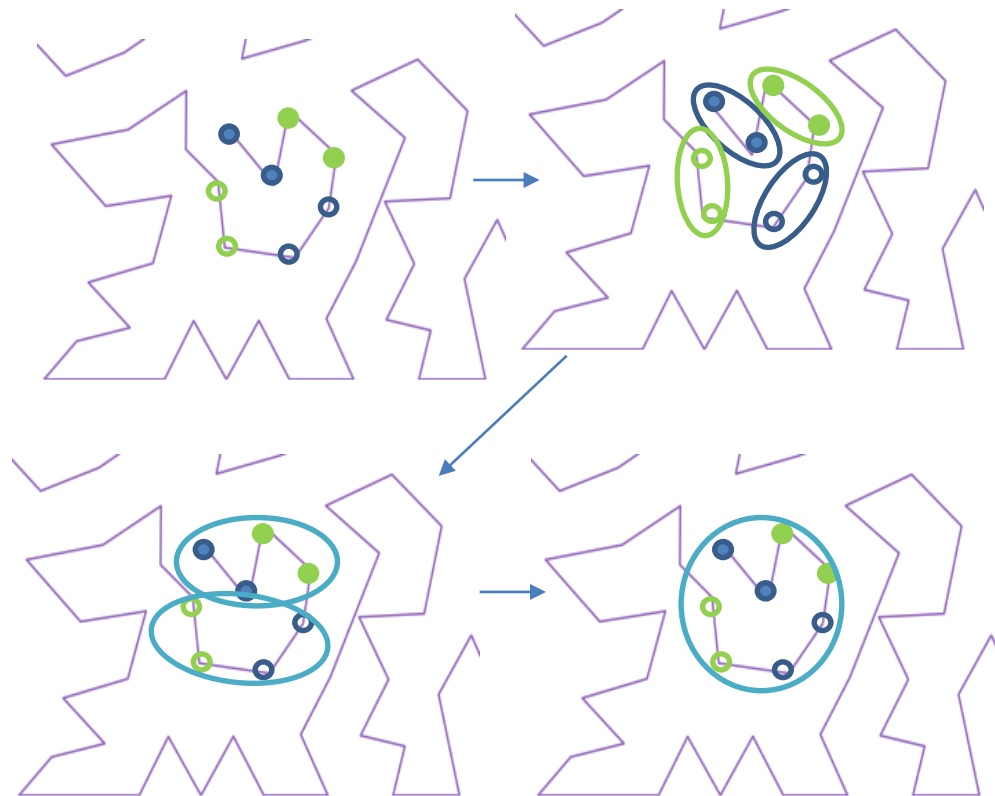
2 Space Filling Curve multi-grid methods (right)



Unstructured mesh CNN - Multi-dimensional convolutional methods – extension of 1D Space Filling Curve (SFC) method

In the multi-grid method one first collapses the nodes with the same color to reduce the number of nodes by a factor of 2 on the coarse grid (see picture on the right). Then repeat to reduce by a factor of two and so on until we get to one node.

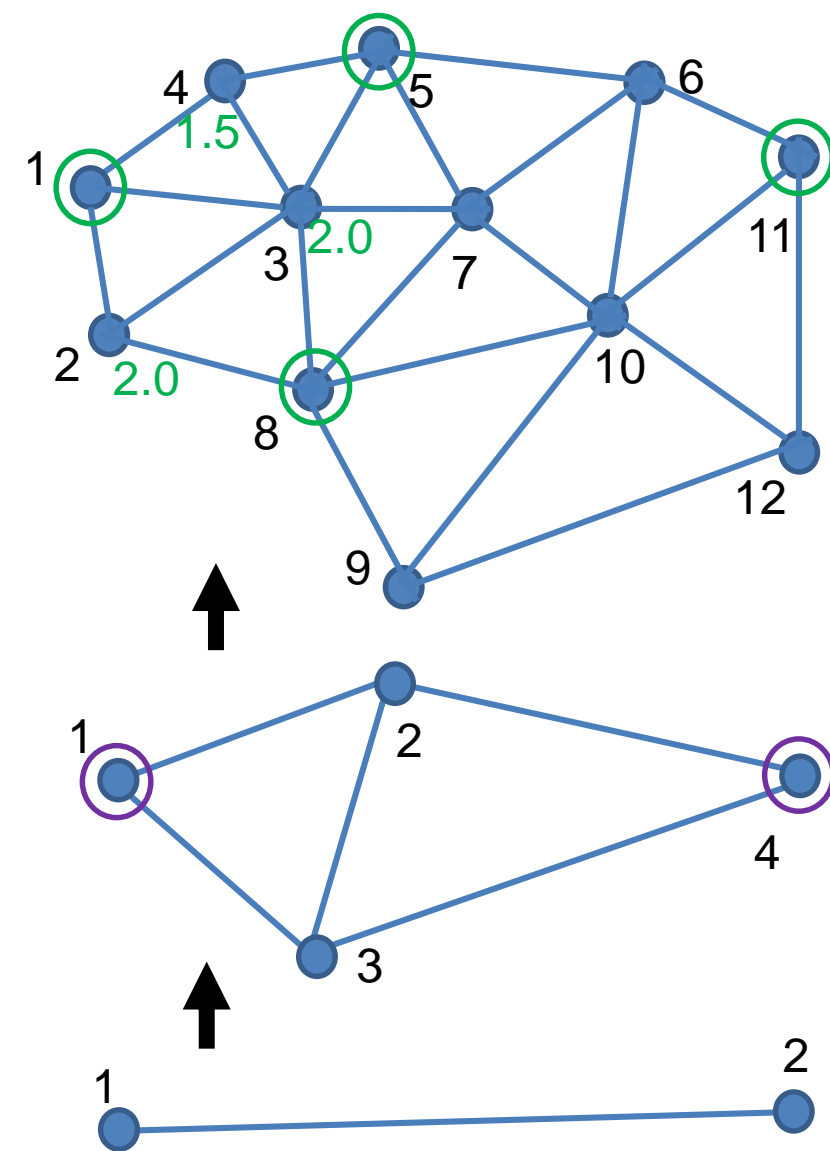
The matrices are formed on each grid level simply by summing the edge values from the finest grid.



Algebraic node coarsening along the SFC – the circles/ellipses represent coarsened nodes

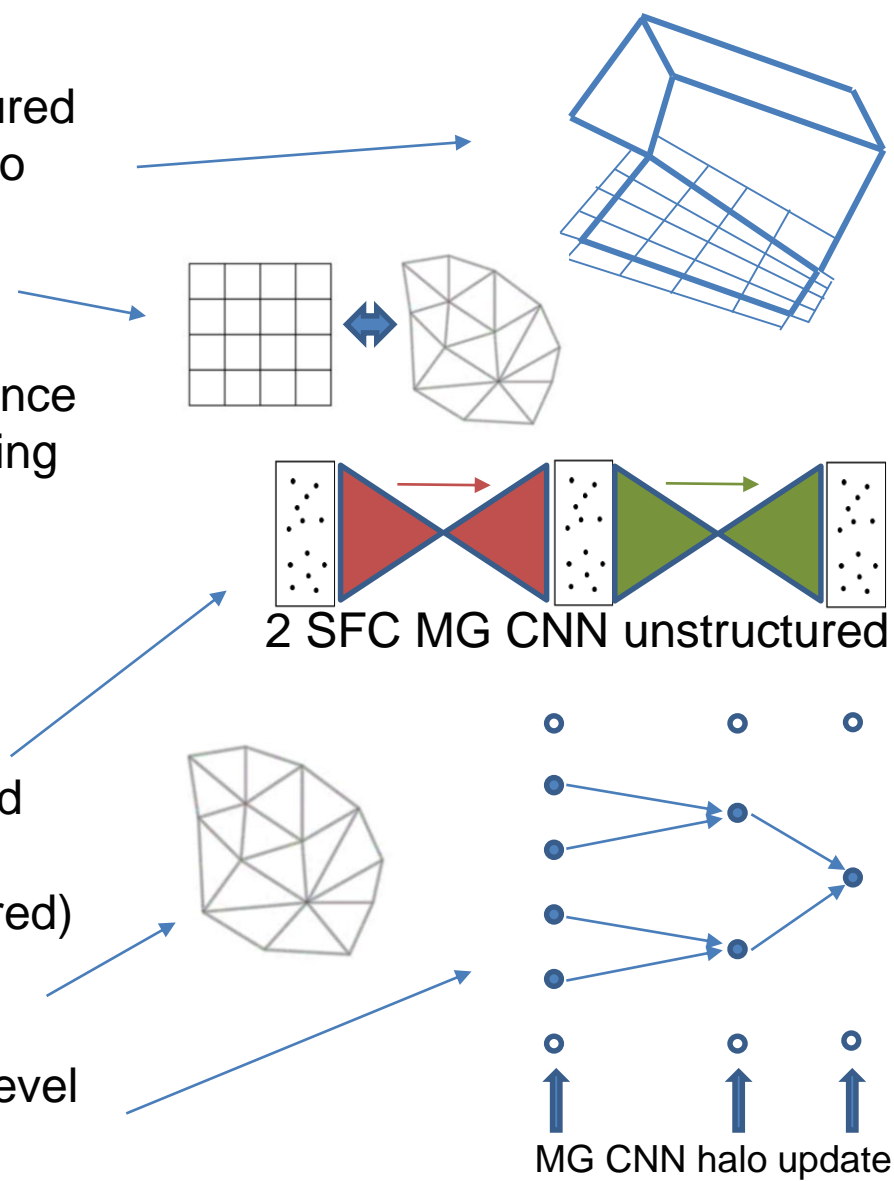
Rapidly forming the Space Filling Curves (SFCs) for unstructured meshes using automatic mesh coarsening

Form a series of graph coarsenings using graph colouring, say. Form an SFC ordering on the coarsest level and pass this ordering to the next finest mesh. Give a number to each node of the finer mesh (green real numbers) depending on the SFC ordering on the coarser mesh by finding the mean SFC node order of the surrounding nodes. One visits each of the coarser mesh nodes on the finer grid in the SFC order and numbers the nodes on the finer grid.



Unstructured meshes and parallel

- 1) Use semi-structured or block approach with unstructured grid representing the interaction between the blocks to start with. See figure.
- 2) Use optimal mappings between unstructured and structured meshes (interaction between structured blocks or elements) based on the earth mover's distance (the Wasserstein metric) using a NN for: a) the mapping of the subdomains to the AI computer cores taking its architecture; b) mapping subdomains to a 2D or 3D structured grid on which the multi-grid CNN can be applied.
- 3) For multi-grid solver either use SFC approach on unstructured representation or structured CNN formed from earth movement distance optimization.
- 4) For fully unstructured meshes (not nec. block structured) use a graph structure for the CNN and have different weights on all the edges of this graph.
- 5) For parallel have a halo update on each coarsening level of the multi-grid CNN method.



Incorporating physics volumetrically into AI models: example of a room with people in it and modelling the air flows with temperature (T), CO₂ (C) and Relative Humidity (R)

Set the overall diffusivity of temperature (T) (But also do the same for C (k_C) and R (k_R)): $k_T = \alpha_s k_{Ts} + (1 - \alpha_s) k_{Tf}$ where α_s is the volume fraction of solid (person, train, seat), k_{Tf} is the Petrov-Galerkin diffusion and $k_{Ts}=0$ is the diffusivity in the solid.

The boundary condition of temperature T on a person can be applied by defining the nodes surrounding a person or the head (if that is where most of the heat transfer occurs) then in those nodes s_p (=1 next to head =0 else) define the temperature source as:

$s_T = \beta_T (T_{skin} - T)$ where T_{skin} is the skin surface temperature of the head. A typical temperature of a persons skin is $T_{skin}=34^\circ\text{C}$ and surface heat transfer coefficient $h_{suf}=10\text{W/m}^2\text{ K}$ (say) in which the heat transfer boundary condition is: $k_T(\partial T / \partial n) = h_{suf}(T - T_{skin})$. Now β_T can be defined: $\beta_T = h_{suf}/\Delta x$ in which Δx is the node width normal to the boundary. We can also linearize s_T about a constant room temperature say of 22°C and thus: $s_T=8s_p (h_{suf}/\Delta x)$.

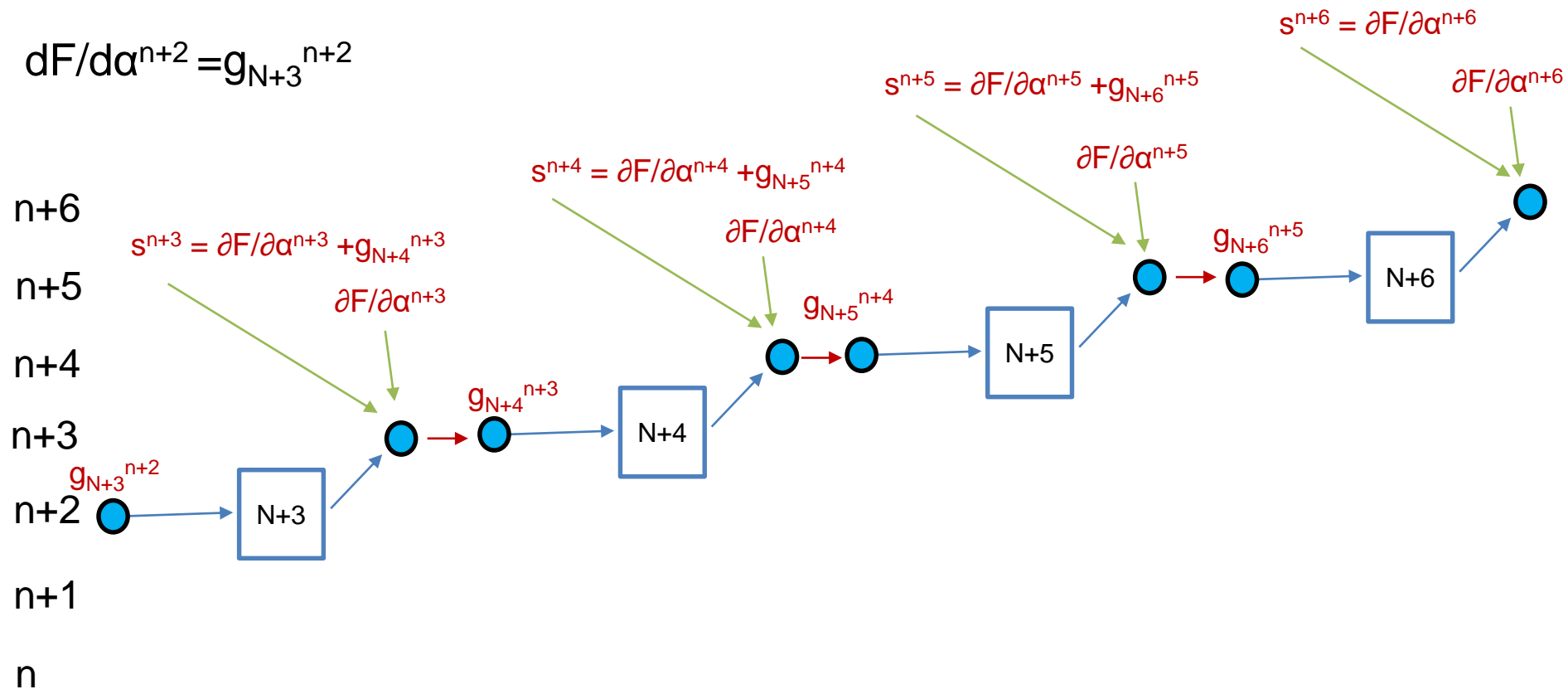
At the mouth outlet (breathing in) and inlet (breathing out) set $\mathbf{u}=\mathbf{u}_m$, $T=T_m$, $R=R_m$, $C=C_m$ boundary conditions but only apply to nodes along mouth boundary. We may also have a time varying \mathbf{u}_m which might oscillate with a sine wave to represent inflowing and outflowing gas.

**Forming
(i) sensitivities,
(ii) data assimilation,
(iii) uncertainty quantification,
(iii) control
(iv) and optimisation
using AI-HFM & AI-Physics modelling**

Two time level stepping method: F is the data mismatch functional in data assimilation
 s^{n+3} is the source that's used in the backpropagation algorithm for neural network N+3
 g_{N+3}^{n+2} is the gradient contribution from neural network N+3 with a source s^{n+3}

The final sensitivities are:

$$dF/d\alpha^{n+2} = g_{N+3}^{n+2}$$



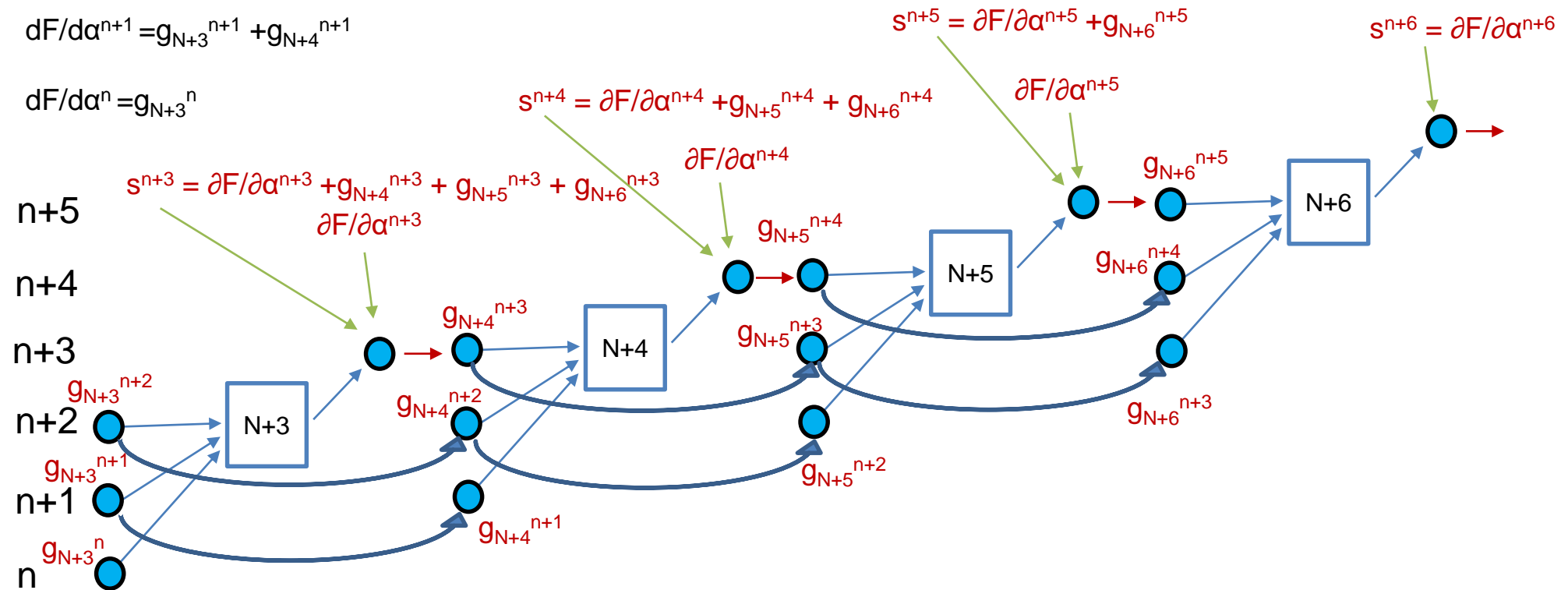
Multi time level stepping method: F is the data mismatch functional in data assimilation
 s^{n+3} is the source that's used in the backpropagation algorithm for neural network N+3
 g_{N+3}^{n+2} is the gradient contribution from neural network N+3 with a source s^{n+3}

The final sensitivities are:

$$dF/d\alpha^{n+2} = g_{N+3}^{n+2} + g_{N+4}^{n+2} + g_{N+5}^{n+2}$$

$$dF/d\alpha^{n+1} = g_{N+3}^{n+1} + g_{N+4}^{n+1}$$

$$dF/d\alpha^n = g_{N+3}^n$$



Data Assimilation and Control using Adversarial Autoencoders (AAE) with sensor outputs:

Suppose \hat{s}_i^n are the desired values at the sensors (i^{th} sensor and n^{th} time level). \hat{s}_i^n could be the values of the measurements at the sensors for the data assimilation (DA) or for control the desired value of the variable e.g. $\hat{s}_i^n = 21$ Deg C for temperature comfort of the room or $\hat{s}_i^n = 400$ for CO₂ – the background CO₂ level or $\hat{s}_i^n = 0$ for viral load and for controls $c_i^n = 0$ could be the desired air velocity of a Dyson fan (desired to minimize energy consumption) and $\hat{c}_i^n = \text{background temperature of the Dyson fan}$ again to minimize its energy use. Everything we have said about the sensor values s_i^n also applies to the controls c_i^n .

Relaxation of the AAE sensor or control inputs

One can decide that a desired value for control or in DA is more or less important with a relaxation coefficient β say, with $\beta \in [0,100]$ in which $\beta = 0$ corresponds to no importance and in which case one uses the value that the time stepping method predicts \tilde{s}_i^n , say, otherwise one uses the value:

$$s_i^n = \beta \hat{s}_i^n + (1 - \beta) \tilde{s}_i^n$$

(\hat{s}_i^n desired value and \tilde{s}_i^n the best prediction e.g. from s_i^{n-1} or from the output of the AAE).

Notice that $\beta=1$ corresponds to a 'standard' weighting and $\beta>1$ puts more importance on achieving the desired output \hat{s}_i^n . Similarly for the controls c_i^n .

Adding the error Δs_i^n in the AAE output-difference:

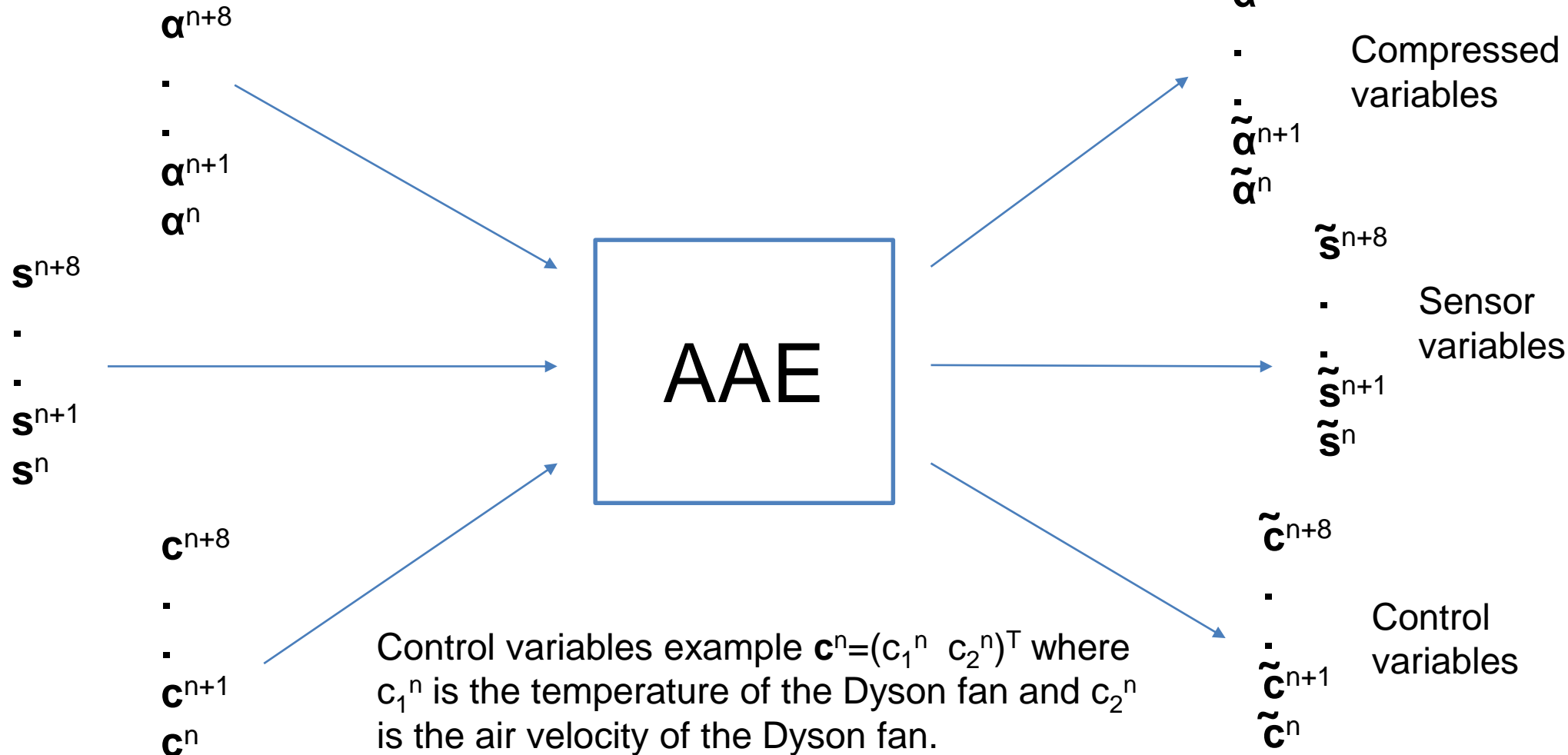
$\Delta s_i^n = \tilde{s}_i^n - \hat{s}_i^n$ in which s_i^n is the AAE output.

Keeping on accumulating the difference:

$$\Delta\Delta s_i^n \rightarrow \Delta\Delta s_i^n + \Delta s_i^n$$

Starting from zero (0.0) and add that into the input. Similarly for the controls c_i^n .

Adversarial Autoencoder (AAE) for time-stepping, data assimilation, uncertainty quantification, optimization and control:



AAE sensitivities with multi time level stepping – $(.)^l$ corresponds to the l^{th} AAE iteration
– 3 AAE iterations below

The final sensitivities are:

$$g_{N+3}^{n+2} = dF/d\alpha^{n+2} = (g_{N+3}^{n+3})^1 + (g_{N+3}^{n+2})^1 + (g_{N+3}^{n+2})^2 + (g_{N+3}^{n+2})^3$$

$$g_{N+3}^{n+1} = dF/d\alpha^{n+1} = (g_{N+3}^{n+1})^1 + (g_{N+3}^{n+1})^2 + (g_{N+3}^{n+1})^3$$

$$g_{N+3}^n = dF/d\alpha^n = (g_{N+3}^n)^1 + (g_{N+3}^n)^2 + (g_{N+3}^n)^3$$

AAE same as multi-level time stepping

$n+3$

$n+2$

$n+1$

n

AAE iterations below

